ANL/ES-CEN-1014
d
FE-1780-3

ANL/ES-CEN-1014
and
FE-1780-3

A DEVELOPMENT PROGRAM ON PRESSURIZED FLUIDIZED-BED COMBUSTION

Quarterly Report
October–December 1975

by

G. J. Vogel, P. T. Cunningham, J. Fischer,
B. R. Hubble, I. Johnson, S. H. Lee, J. F. Lenc,
J. Montagna, S. Siegel, R. B. Snyder,
S. Saxena, G. Smith, W. M. Swift, G. Teats,
W. I. Wilson, and A. A. Jonke

ARGONNE NATIONAL LABORATORY, ARGONNE, ILLINOIS

Operated for the U. S. ENERGY RESEARCH
AND DEVELOPMENT ADMINISTRATION
under Contract W-31-109-Eng-38

DISCLAIMER

The facilities of Argonne National Laboratory are owned by the United States Government. Under the terms of a contract (W-31-109-Eng-38) between the U. S. Energy Research and Development Administration, Argonne Universities Association and The University of Chicago, the University employs the staff and operates the Laboratory in accordance with policies and programs formulated, approved and reviewed by the Association.

MEMBERS OF ARGONNE UNIVERSITIES ASSOCIATION

The University of Arizona
Carnegie-Mellon University
Case Western Reserve University
The University of Chicago
University of Cincinnati
Illinois Institute of Technology
University of Illinois
Indiana University
Iowa State University
The University of Iowa
Kansas State University
The University of Kansas
Loyola University
Marquette University
Michigan State University
The University of Michigan
University of Minnesota
University of Missouri
Northwestern University
University of Notre Dame
The Ohio State University
Ohio University
The Pennsylvania State University
Purdue University
Saint Louis University
Southern Illinois University
The University of Texas at Austin
Washington University
Wayne State University
The University of Wisconsin

Printed in the United States of America
Available from
National Technical Information Service
U. S. Department of Commerce
5285 Port Royal Road
Springfield, Virginia 22161
Price: Printed Copy $5.00; Microfiche $2.25

ANL/ES-CEN-1014
and
FE-1780-3
Coal Conversion and Utilization—
Direct Combustion of Coal
(UC-90e)

ARGONNE NATIONAL LABORATORY
9700 South Cass Avenue
Argonne, Illinois 60439

A DEVELOPMENT PROGRAM ON PRESSURIZED FLUIDIZED-BED COMBUSTION

Quarterly Report
October—December 1975

by

G. J. Vogel, P. T. Cunningham, J. Fischer,
B. R. Hubble, I. Johnson, S. H. Lee, J. F. Lenc,
J. Montagna, S. Siegel, R. B. Snyder,
S. Saxena,* G. Smith, W. M. Swift, G. Teats,
W. I. Wilson, and A. A. Jonke

Chemical Engineering Division

Prepared for the
U. S. Energy Research and Development Administration
under Contract No. 14-32-0001-1780

and the

U. S. Environmental Protection Agency
under Agreement IAG-D5-E681

*University of Illinois - Chicago Circle

BIBLIOGRAPHIC DATA SHEET	1. Report No. ANL/ES-CEN-1014	2.	3. Recipient's Accession No. FE-1780-3
4. Title and Subtitle: A Development Program on Pressurized Fluidized-Bed Combustion			5. Report Date: January 1976 6.
7. Author(s): G. J. Vogel *et al.*			8. Performing Organization Rept. No. ANL/ES-CEN-1014
9. Performing Organization Name and Address: Argonne National Laboratory, 9700 South Cass Avenue, Argonne, Illinois 60439			10. Project/Task/Work Unit No. 11. Contract/Grant No. 14-32-0001-1780 (ERDA) IAG-D5-E681 (EPA)
12. Sponsoring Organization Name and Address: U. S. Energy Research and Development Administration and the Environmental Protection Agency			13. Type of Report & Period Covered QUARTERLY October 1 - Dec. 31, 1975 14.
15. Supplementary Notes			

16. Abstracts: A development program on pressurized fluidized-bed combustion is being carried out in a bench-scale pilot plant capable of operating at 10-atm pressure. The concept involves burning fuels such as coal in a fluidized bed of particulate lime additive that reacts with the sulfur compounds formed during combustion to reduce air pollution. Nitrogen oxide emissions are also reduced at the combustion temperatures used, which are lower than those used in a conventional coal combustor. The $CaSO_4$ produced in the combustor is regenerated to CaO that is recycled to the combustor for removal of sulfur compounds.

This report presents information on: hot testing of the new bench-scale regeneration system, TGA experiments on sulfation and regeneration rates of supported additives and on cyclic sulfation regeneration experiments, petrographic change occurring during half-calcination of dolomite, laboratory-scale experiments on the reaction of calcium sulfide with calcium sulfate, coal combustion reactions, and quality of fluidization and minimum fluidization velocity studies.

17. Key Words and Document Analysis. 17a. Descriptors

Air Pollution
Fluidized-Bed Processing
Sulfur Oxides
Dolomite
Fossil Fuel
Combustion
Coal
Calcium Sulfates
Additives
Sulfur
Calcium Oxides
Calcium Carbonate
Flue Gas
Aluminum Oxide
Roasting
Calcium Sulfide
Lignite
Sorbents
Ashes
X-ray Diffraction
Desulfurization
Particle Shape
Particle Size
Flue Dust
Fly Ash
Particle Size Distribution
Fragmentation
Agglomeration
Hydrogen
Methane

17b. Identifiers/Open-Ended Terms

Air Pollution Control
Stationary Sources
Fluidized-Bed Combustion
Supported Additives
Additive Regeneration
Fluidization Velocity

17c. COSATI Field/Group 13B

18. Availability Statement	19. Security Class (This Report) UNCLASSIFIED	21. No. of Pages
	20. Security Class (This Page) UNCLASSIFIED	22. Price

TABLE OF CONTENTS

LIST OF FIGURES

LIST OF TABLES

A DEVELOPMENT PROGRAM ON PRESSURIZED FLUIDIZED-BED COMBUSTION

Quarterly Report

October—December 1975

by

G. J. Vogel, P. T. Cunningham, J. Fischer, B. R. Hubble
I. Johnson, S. H. Lee, J. F. Lenc, J. Montagna,
S. Siegel, R. B. Snyder, S. Saxena, G. Smith,
W. M. Swift, G. Teats, W. I. Wilson, and A. A. Jonke

ABSTRACT

A development program on pressurized fluidized-bed combustion is being carried out in a bench-scale pilot plant capable of operating at 10-atm pressure. The concept involves burning fuels such as coal in a fluidized bed of particulate lime additive that reacts with the sulfur compounds formed during combustion to reduce air pollution. Nitrogen oxide emissions are also reduced at the combustion temperatures used, which are lower than those used in a conventional coal combustor. The $CaSO_4$ produced in the combustor is regenerated to CaO that is recycled to the combustor for removal of sulfur compounds.

This report presents information on: hot testing of the new bench-scale regeneration system, TGA experiments on sulfation and regeneration rates of supported additives and on cyclic sulfation regeneration experiments, petrographic change occuring during half-calcination of dolomite, laboratory-scale experiments on the reaction of caclium sulfide with calcium sulfate, coal combustion reactions, and quality of fluidization and minimum fluidization velocity studies.

SUMMARY

One-Step Regeneration of Additive, Bench-Scale Unit

The effect of process variables on regeneration in the one-step regeneration method is being studied, using sulfated additive produced by the combustion process. In the one-step method, the $CaSO_4$ contained in the sulfated additive is reductively decomposed to CaO at 1100°C (2000°F). Reducing gases have been obtained by adding CH_4 to the fluidized bed in the regenerator or, more recently, by combusting coal in the bed.

Regeneration Using *In Situ* Combustion of CH_4

Additional information on the earlier reported FAC-series of one-step regeneration experiments is presented below.

The formation of CaS during the one-step reductive decomposition of $CaSO_4$ to CaO and SO_2 was evaluated in the regenerated samples taken at steady state in the FAC-experiments. Sulfide ($S^=$) levels of $\leq$0.1% were obtained in all experiments performed at low reducing gas concentrations (3% reducing gas in the effluent), and sulfide levels of 0.3 and 0.7% were obtained in experiments performed at high reducing gas concentrations (15% reducing gas in the effluent). This disagrees with thermodynamic predictions of the equilibrium concentrations of CaS and $CaSO_4$. At the reducing conditions of the effluent from these experiments, it was predicted that only CaS should exist at equilibrium. The very low actual CaS concentrations found in the steady-state regenerated samples were attributed to the formation of two zones (oxidizing at the bottom of the fluidized bed and reducing at the top) in the regeneration reactor.

Total sulfur regeneration calculations were made from the chemical analyses of the regenerated samples; sulfur regeneration values were generally 10-15% higher than those calculated from flue-gas analyses.

Most of the sulfur and calcium balances ranged from 90 to 110%, which is an acceptable variation.

The extent of decrepitation during these regeneration experiments was evaluated by two methods. First, the calcium value of the particle samples collected from the flue-gas system for the duration of each experiment was evaluated. It was found that 5 to 15% of the total feed (calcium basis) was elutriated and that these elutriated particles were basically smaller than the smallest sulfated particles fed to the regenerator. Secondly, plots were made of the calcium weight ratios of re regenerated additive product to sulfated additive fed, as a function of particle diameter. For all experiments considered, a decrease in the number of larger particles (>800 μm) and an increase in the number of medium size particles (>300 μm and >800 μm) were found.

Agglomeration of sulfated additive has occurred during regeneration experiments. Both agglomerated and nonagglomerated samples removed from the bed after dolomite and limestone regeneration experiments were analyzed by X-ray diffraction. It was found that compounds of calcium-magnesium silicates had formed during the agglomeration (melting) process. In DTA (differential thermal analysis) experiments, sulfated dolomite (the feed to the regenerator) melted at 1200°C in atmospheres of nitrogen and air. The X-ray diffraction analysis of the DTA samples revealed the possible formation of a calcium-silicate compound, but no calcium-magnesium-silicate trace was found. So far, it appears that melting of $CaSO_4$ is the first step in the agglomeration process and that the formation of calcium-magnesium-silicate compound is incidental and not responsible for agglomeration.

Regeneration Using *In Situ* Combustion of Coal

In high-temperature tests being performed to test the operability of the new regeneration system, the reducing gas has been obtained by partial combustion of Arkwright coal. The bed temperature was varied between 1040 and 1100°C. The total reducing gas concentration (maximum) in the

effluent gas was 3%. Following the changes recently made in the regenerator (increase of diameter from 3 to 4.3 in. and removal of the internal overflow pipe), the control of bed temperature was good and the operability of the regeneration system was much improved.

After completion of these high temperature operability tests, an experiment was made with coal at the same experimental conditions used in an earlier regeneration experiment which was made with methane. The experimental conditions were: temperature of 1040°C, pressure of 0.84 kg/cm^3 (gauge) (12 psig), fluidizing gas velocity of 0.91 m/sec (3 ft/sec), and a solids residence time of ∿30 min. In the previous experiments using combustion of methane, the total reducing gas concentration in the effluent was ∿4%; in this experiment with coal, it was ∿2%. In the coal combustion regeneration experiment, the SO_2 concentration in the wet effluent gas was 2.4% and the particle regeneration was 64%; in comparison, in the CH_4 experiment the SO_2 concentration in the wet effluent gas was 1.3% and particle regeneration was 38%.

Development of Supported Additives

A method of preparing synthetic additives containing various concentrations of CaO in α-Al_2O_3 is given.

In sulfation studies, the sulfation rate of pellets containing 6.6% CaO in α-Al_2O_3 and heat-treated at 1100°C before sulfation was found to be 1.5 times lower than for additives heat-treated at 800°C. Water concentrations in the feed gas had no effect on the sulfation rate. A mathematical equation was developed that predicts the sulfation kinetics.

Chemical analysis data on previously sulfated 6.6% CaO additives show that 80-100% calcium utilization occurs at measured reaction temperatures above 850°C, regardless of the concentration of SO_2 in the synthetic combustion mixture.

Finally synthetic additives containing CaO concentrations ranging from 2 to 16.5% were studied for their ability to capture SO_2. The sulfation rate decreased with increasing CaO concentration when measured as a fraction of the maximum possible sulfation; however, the amount of SO_2 captured for a given residence time was usually higher for higher CaO concentrations.

The regeneration rate for the sulfated synthetic additive was determined as a function of temperature. A mathematical equation was developed that predicts the regeneration rate as a function of reducing gas concentration and temperature. The activation energy was found to be -14.9 kcal/mol. The reaction product was dependent upon the regeneration temperature; above 1050°C, the product was CaO while below 900°C it was CaS. Between 900 and 1050°C, the product was a mixture of CaO and CaS with CaO concentration increasing with temperature.

A cyclic sulfation-regeneration experiment (5 cycles) was performed on the 6.6% CaO in α-Al_2O_3 additive that had been heat-treated at 1100°C. The rates of sulfation and regeneration were the same in each cycle.

Sulfur Emission Control Chemistry

Petrographic Changes Occurring in the Half-Calcination of Dolomite No. 1337

The half-calcination process of dolomite involves the reaction:

$$\underset{\text{dolomite}}{CaCO_3 \cdot MgCO_3} + \text{heat} \rightarrow \underset{\text{calcite}}{CaCO_3} + MgO + CO_2 \qquad (1)$$

Rock particles of dolomite, when heated under a partial CO_2 pressure, are transformed into particles containing microscopic crystals of calcite and submicron crystals of MgO. These half-calcined particles may be used for the sorptive removal of SO_2 in coal-fired furnances.

In order to study the nature of the changes which occur duing the half-calcination process, dolomite No. 1337 samples were heated under various conditions in a TGA to yield a series of samples containing various amounts of calcite. Polished sections of the treated samples were examined in reflected polarized light and compared with those of untreated dolomite.

The examination of samples by petrographic methods has yielded some significant results. It has been shown that dolomite crystals are transformed to calcite along grain boundaries, as well as within dolomite crystals. This suggests that greater efficiencies in the half-calcination process may be achieved by selecting finer-grained starting material from the quarry if this is practical. The results also suggest that, since sulfation is a surface-controlled process, partially transformed half-calcined samples might be more readily sulfated along avenues of fine-grained calcite than through a tight interlocking network of larger calcite cyrstals in completely transformed samples. The validity of this suggestion will be tested by experiment.

Regeneration by the $CaSO_4$-CaS Reaction

Initial results from the study of the following solid-solid reaction indicated that it is a potentially feasible candidate as a regeneration scheme:

$$3[CaSO_4 \cdot MgO] + [CaS \cdot MgO] \rightarrow 4[CaO \cdot MgO] + 4SO \qquad (2)$$

In this report, results of the first kinetic experiments of reaction 2, where the starting material is prepared by partial reduction of sulfated dolomite, are presented. In addition, preliminary results are presented on a second method of carrying out reaction 2, *i.e.*, by performing the solid-solid and reduction reactions simultaneously.

Reaction of Calcium Sulfate with Calcium Sulfide, Vacuum Roasting

In additional work to determine if solid-solid reaction 2 is practiable for regenerating sulfated additive, a mixture of sulfated dolomite and calcium sulfide was roasted under vacuum. Preliminary results indicate that the rate of reaction may be higher with the vacuum-roasting technique than that at atmospheric pressure with SO_2 removed by use of a nitrogen purge.

Coal Combustion Reactions

The Determination of Inorganic Constituents in the Effluent Gas from Coal Combustion

Some chemical elements carried by combustion gas are known to cause severe metal corrosion. The purpose of this study is to determine quantitatively which elements are present in the hot combustion gas of coal, either in volatile or particulate form, and to differentiate between volatile and particulate species. Identification of the compound form and amount of particulate species, as well as detemrination of the amount and form of condensable species, are of interest.

The design and preliminary safety review of the laboratory-scale batch unit combustor to be used in these studies was held on July 3, 1975. In accordance with recommendations of the design/safety review committee, several revisions on the design of the combustor have been made. The revisions involve changes in the design to reduce or eliminate thermal and mechanical stresses in the wall of the combustor body.

The specifications for fabrication of the combustor have been revised as recommended by the design/safety review committee. The design of the combustor is considered to be adequately safe upon modification as recommended by the safety review committee.

Systematic Study of the Volatility of Trace Elements in Coal

Knowledge of the vaporization characteristics of trace elements in coal and the rate of their volatilization is important for combined-cycle turbine operation. The objective of this study is to obtain data on the volatility of these elements under practical coal combustion and gasification conditions.

The first series of perliminary experiments has been completed. In these experiments, ash samples produced at an average temperature of 340°C were each heated in a tubular furnace to a temperature between 540°C and 990°C and held for 24 hr at the selected temperature in an air flow of 0.6 scfh. The ash residue was then analyzed for the trace elements of interest by atomic absorption.

The sample after heating shows an increased weight loss with increased heating temperature. The weight loss curve flattens at about 850°C. Above 900°C, the weight loss curve shows an upturn, indicating a further weight loss in this temperature range.

Some elemental analyses for this series of experiments have been obtained. The results indicate that the major fraction of the elements which have been investigated are retained in the ash up to 990°C. To obtain the desired volatility data, ash samples must be heated to high temperatures.

Bench-Scale, Pressurized-Fluid-Bed Combustion Experiments

The ANL, 6-in.-dia, pressurized-fluidized-bed combustor was operated. Reported here are (1) additional results of four combustion experiments (using Arkwright coal and Tymochtee dolomite) to measure the effects of coal

and additive particle size on combustor response variables, (2) the results of two replicate experiments investigating the sulfur-retention capability of lignite ash that has a high calcium content, (3) the results of a replicate experiment duplicating the operating conditions of previously reported VAR-series experiments, and (4) a brief explanation of operating problems and required maintenance.

Combustion efficiencies ranged from 89 to 93% were determined for the four combustion experiments investigating the effects of coal and additive particle size. No consistent effect, however, of particle size of coal or additive on combustion efficiency was indicated. Utilization of additive material for the same experiments ranged from 51 to 78%. Utilization is shown to increase with decreasing additive particle size.

Glenharold lignite was combusted in a fluidized bed of alumina in two replicate experiments to test the sulfur retention capability of the high-calcium lignite coal. Sulfur retentions were calculated from flue-gas data to be 86 to 89% for the two experiments. Sulfur retention was 85% in a previously reported experiment in which the lignite was combusted in a bed of dolomite under similar operating conditions.

A replicate of a VAR-series experiment was also made to check the operation of the combustor and analytical instrumentation and to verify the reliability of comparing current experiments and past experiments. Except for a discrepancy in the level of NO in the flue gas, the results of the experiment agree very well with the previously performed experiments.

An operating problem experienced during startup of a test was a temperature excursion in the combustor which damaged several of the internal metal service lines. Approximately two and one-half weeks of operating time were lost while repairs were made. During a subsequent startup, an external cooling coil (flexible connection) began leaking badly, forcing termination of the experiment. Several days of operation were lost while repairs were made.

Separation of Combustion and Regeneration Systems

The pressurized, fluidized-bed combustor and the regenerator originally utilized several components in common so that is was not possible to operate the two units simultaneously. Modifications of both systems were undertaken to permit concurrent investigations of the combustion process and the regeneration process.

Modifications to the regeneration system equipment were completed, and experiments in the new system were initiated. Alterations to the combustion system equipment were completed earlier (report FE-1780-2), and experiments in the combustion system were resumed. Thus, the task of separating the two systems has been completed and will not be discussed in future reports.

Quality of Fluidization and Minimum Fluidization Velocity Studies

The results of two different series (A and B) of fluidization experiments are described. The superficial fluidizing air velocities at which fluidization first occurs (with only part of the bed fluidized) are reported,

together with the extrapolated values of air velocity for total fluidization (the bed completely fluidized). The quality of fluidization and segregation of particles in a fluidized bed are discussed.

Data from these experiments show that partial segregation of the bed occurred if the ratio of the diameter of the largest particle to the diameter of the samllest particle exceeded at least 16. As a result, the prediction of minimum fluidization velocity for the entire bed becomes complicated, making precise prediction uncertain. A procedure is suggested for the prediction of minimum fluidization velocity of the entire bed.

INTRODUCTION

In this program, funded by the Energy Research and Development Administration and the Environmental Protection Agency, fluidized-bed combustion is being studied as a method of removing from the gas phase nearly all atmospheric pollutants (sulfur and nitrogen compounds) generated during the combustion of fossil fuels. The concept involves burning of fuels such as coal in a fluidized bed of particulate lime solids that react with the sulfur compound formed during coal combustion. In another step, the sulfated lime is regenerated for reuse in the combustor.

This quarterly report presents information on: hot testing of the new bench-scale regeneration system, TGA experiments on sulfation and regeneration rates of supported additives and on cyclic sulfation-regeneration experiments, petrographic change occurring during half-calcination of dolomite, laboratory-scale experiments on the reaction of calcium sulfate, coal combustion reactions, and quality of fluidization and minimum fluidization velocity studies.

ONE-STEP REGENERATION OF ADDITIVE BENCH-SCALE UNIT

Regeneration Using *In Situ* Combustion of Methane

The FAC-series of regeneration experiments was performed using the *in situ* combustion of methane to evaluate the effects of temperature, residence time, height of fluidized bed, and total reducing gas conditions on the regeneration of CaO in sulfated Tymochtee dolomite. Earlier results which were based only on flue-gas analyses have been reported and discussed.[1] To aid in the discussion of additional results obtained by chemical analysis of particulate product samples, the experimental conditions and the results based on flue gas analyses from the FAC-series are re-presented in Table 1.

Sample was initiated when over 90% of the fluidized bed had been replaced while the regenerator was at the design experimental conditions. Steady-state samples were each composed of the overflow product taken over a 30-min period. The particulate product samples were analyzed for total sulfur, sulfide, and calcium (Table 2). The accuracy of the analytical techniques used for these analyses ranged from 5-10%.

To ensure that a steady-state sample was representative of the product at steady state, all samples taken in FAC-1 (including a sample of the final bed) were analyzed for sulfur, sulfide, and calcium. The steady-state sample contained 3.3% total sulfur, 0.1% sulfide, and 29.8% calcium. The final bed contained 3.0% total sulfur, <0.1% sulfide, and 28.2 calcium, which is in good agreement with the compositions of the steady-state sample. The final beds from other FAC-experiments were also analyzed, and the agreement with the steady-state sample was within the analtyical accuracy.

Presence of CaS. The formation of CaS is detrimental to the one-step reductive decomposition of $CaSO_4$. The effects of the four variables

Table 1. Design Experimental Conditions and Sulfur Regeneration Results for the FAC-Series

Pressure, psig: 12
Additive: sulfated Tymochtee dolomite (10.2% S)

Exp.	Temp (°C)	Design Conditions: Additive Feed Rate (lb/hr)	Residence Time (min)	Bed Height (ft)	Total Reducing Gas in Effluent[a] (vol %)	Fluidizing Velocity (ft/sec)	Measured SO_2 in Effluent[b] (% wet)/(% dry)	Sulfur Regeneration (%)
FAC-1	1040	6	30	1.5	3	2.2	3.0 / 4.0	65
FAC-1R1	1040	6	30	1.5	3	2.4	2.6 / 3.6	61
FAC-1R2	1040	6	30	1.5	3	2.5	2.3 / 2.9	57
FAC-2	1095	6	30	1.5	15	Experiment could not be completed		
FAC-3	1040	10	18	1.5	15	2.6	4.1 / 5.7	62
FAC-4	1095	10	18	1.5	3	2.5	5.3 / 7.3	73
FAC-5	1040	10	30	2.5	15	2.7	3.5 / 4.4	54
FAC-9A	1040	6	30	1.5	3	3.0	1.3 / 1.5	38
FAC-7	1040	10	30	2.5	3	2.5	2.7 / 3.3	40
FAC-8	1010	6	30	1.5	3	2.3	0.65/ 0.78	14
FAC-9	1040	6	30	1.5	3	2.5	1.3 / 1.7	55

[a] The actual reducing gas concentrations were within 15% of the design levels.

[b] Determined by infrared SO_2 analysis of the dry flue gas.

Table 2. Chemical Analysis of Regenerated Product, Calculated Material Balances, and Regeneration Results from the FAC-Series.

Exp.	Temp (C°)	Chemical Analysis of Regenerated Samples taken at Steady State: Total Sulfur (%)	Sulfide (%)	Calcium (%)	Material Balances: Sulfur (%)	Calcium (%)	Elutriated[a] Calcium / Feed Calcium x100 (%)	Sulfur Regeneration (%)[b] / (%)[c]
FAC-1	1040	3.3	0.1	29.8	94	109	5	65 / 76
FAC-1R1	1040	3.73	<0.1	23.7	99	109	15	61 / 72
FAC-1R2	1040	5.08	<0.1	26.2	106	113	13	57 / 58
FAC-2	1095		5.2		This experiment could not be completed			
FAC-3	1040	2.89	0.3	30.2	91	102	12	62 / 79
FAC-4	1095	1.53	<0.1	30.0	88	83	9	73 / 89
FAC-5	1040	2.79	<0.7	29	Production rate was not measured			54 / 79
FAC-9A	1040	7.34	0.1	26.8	-	-	-	38 / 40
FAC-7	1040	7.41	< 0.1	25.3	109	110	15	40 / 36
FAC-8	1010	8.38	< 0.1	23.1	71	72	14	14 / 21
FAC-9	1040	2.74	<0.1	29.1	95	91	11	55 / 55

[a] Only particles larger than 15 μm were monitored.

[b] Based on flue gas analysis.

[c] Based on chemical analysis of particulate dolomite samples.

in the FAC-experiments on sulfide formation were found to be generally negligible. Very small amounts of sulfide (<0.1%) were found in the steady state products from all experiments with low reducing gas conditions (*i.e.*, with ∿3% total reducing gas in the effluent). At higher total reducing gas conditions (∿15% in the effluent), the formation of CaS was enhanced. In experiments FAC-3 and FAC-5, which were both performed at ∿15% total reducing gas conditions, sulfide concentrations in the products were 0.3 and 0.7%, respectively. The total sulfur contents of the products from these two experiments were 2.9 and 2.8%, respectively.

These experimental sulfide concentrations are much lower than that predicted for the equilibrium equation below at the experimental flue-gas conditions of these experiments.

$$1/4CaSO_4 + CO \rightleftarrows 1/4CaS + CO_2 \quad \frac{1}{k_p} = \frac{P_{CO}}{P_{CO_2}} \tag{1}$$

At 1040°C, the maximum partial pressure ratio of CO to CO_2 (P_{CO}/P_{CO_2}) for which CaS and $CaSO_4$ coexist is ∿0.017. At higher partial pressure ratios, only CaS should exist at equilibrium.[2] The experimental values of partial pressure ratios of CO to CO_2 in the effluent for the FAC-experiments were all above 0.02. On this basis, higher sulfide concentrations might be expected. However, these experimental results are not surprising considering that (1) the additive in the fluidized-bed reactor is not at equilibrium and (2) the conditions in the fluidized bed are not reducing throughout. Since the combustion fuel (CH_4) was injected at several locations between 6 and 10 in. above the gas distributor, the fluidized bed was highly oxidizing at the bottom and reducing at the top. The additive was continually circulated between the oxidizing and reducing zones. In the reducing zone of the reactor, $CaSO_4$ was reduced to CaS by reaction 1 and to CaO mainly by the reductive decomposition reaction with CO and other reductants (H_2 and CH_4).

$$CaSO_4 + CO \rightarrow CaO + SO_2 + CO_2 \tag{2}$$

The gaseous products of these reactions left the reactor with the effluent. The solid reactants and products in the reducing zone circulated into the oxidizing zone, where the CaS was converted to $CaSO_4$ by the following reaction.

$$1/2\ CaS + O_2 \rightarrow 1/2\ CaSO_4 \tag{3}$$

This can explain the low concentrations of CaS found in all regenerated Tymochtee dolomite products of the FAC-experiments. The existence of two reacting zones in the *in situ* combustion of fuel (CH_4 or coal) will prove to be a very important factor in the development of a one-step reductive regeneration process for sulfated additives.

The high concentrations of CaS (5.2%) in the product formed during approach to the conditions for FAC-2 (when the temperature was being increased from 1060°C to 1100°C at 15% total reducing-gas concentration) is being considered in relation to the role CaS might have played in the agglomeration of the bed material in that experiment.

Total Sulfur Regeneration. Sulfur regeneration has been calculated from the chemical analyses of the steady-state products. It is based on the sulfur to calcium ratio in the steady-state products before and after regeneration. These calculated regeneration ratios for the FAC-experiments are compared with the previously reported ratios based on flue-gas analyses and are given in Table 2. The sulfur regeneration values obtained by chemical analysis of the particulate regenerated products were generally 10-15% higher than the previously reported values.

The difference in the two methods of calculating sulfur regeneration is illustrated by discussing the results of two experiments. Experiments FAC-3 and FAC-5 were both performed at 1040°C (∿1900°F) with a sulfated-additive feed rate of 10 lb/hr, ∿15% total reducing gas in the effluent, fluidized-bed heights of 1.5 and 2.5 ft, respectively, and residence times of 18 and 30 min, respectively. In these two experiments, it was found that increasing the fluidized-bed height at a constant mass feed rate (thereby increasing the residence time from 18 to 30 min) did not increase sulfur regeneration, which was 79% based on chemical analyses of particulate samples. Sulfur regenerations of 62% and 54% were obtained for FAC-3 and FAC-5, respectively, by flue-gas anlaysis. Sulfur regeneration based on flue-gas analysis is the ratio of the total amount of sulfur released into the effluent-gas stream to that contained in the sulfated-dolomite feed. The sulfur regeneration values based on flue-gas analyses each includes the sulfur released in regeneration of the elutriated additive, which was regenerated to a lesser extent than the product solids. In FAC-3, elutriated solids contained ∿9% total sulfur, in comparison with 2.9% sulfur in the regenerated product from the bed. Based on the calcium balances given in Table 2, 5 to 15% of the dolomite feed was elutriated during regeneration. If the elutriated additive underwent negligible regeneration, the true sulfur regeneration of the product alone would be ∿10% higher than the values calculated from the flue-gas analysis.

The newly calculated sulfur regeneration values from the chemical analysis of the regenerated products are more representative of the sulfur-retaining capability of the regenerated additive.

Material Balances. Material balances for sulfur and calcium were obtained for the FAC-experiments. The balances were not performed for the entire experiments, as was the case for previously reported mass balances on other experiments. Instead, the balances were made over a 30-min steady-state period.

Because the experimental system did not contain a final filtration system, particles smaller than ∿15 μm escaped from the system unmonitored. The total mass rate of these fines was measured only in FAC-5, in which the flue gas exiting from the last cyclone was passed through a sintered-metal filter. A pad of ∿0.3 cm built up on the filter, ensuring good particle collection efficiency for the fine particles. A mass collection rate of 4.6 g/min was obtained in this sintered-metal filter, in comparison with 8.3 g/min captured in the normal regenerator system particle collection devices. The particle distribution for the FAC-5 samples of fines was obtained with a Coulter counter particle analyzer and is given in Fig. 1. None of the calculated mass balances contained the contribution from these fines and thus are biased low.

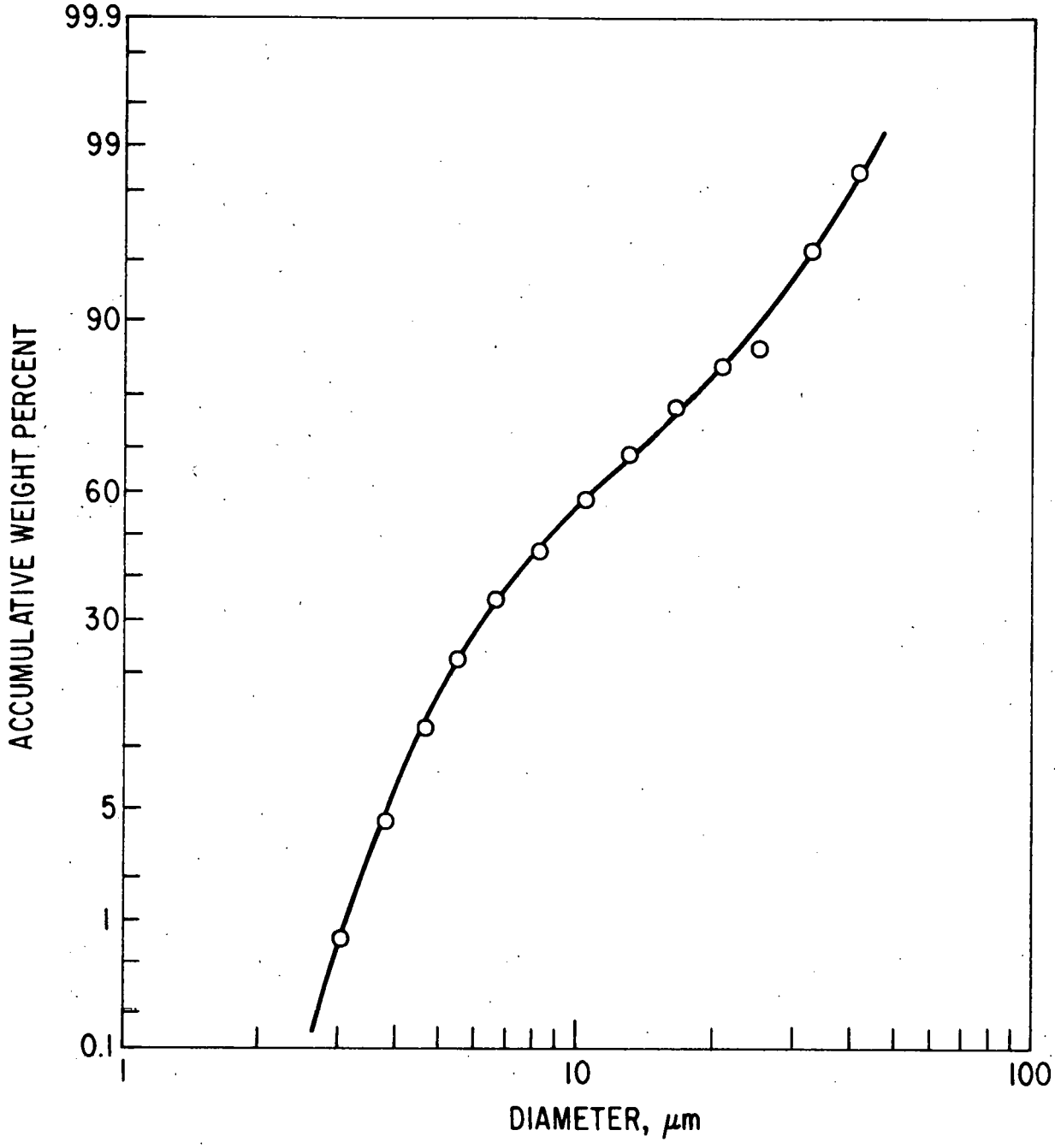

Fig. 1. Particle Size Distribution of the Fines for FAC-5.

The calcium balances ranged from 72% in FAC-8 to 113% in FAC-1R2. These balances were based on the mass rates and chemical analyses of the feed, product, and elutriated solids. The calcium analyses are reliable within ±5%. Errors greater than ∿5% are due mainly to unreliability of the measurements of the mass rates.

The sulfur balances were based on the flue-gas flow rates, the concentrations of sulfur (as SO_2 only) in the flue gas, and the rates and chemical analyses of the solid streams. The sulfur balances ranged from 71% in FAC-8 to 109% in FAC-7. Acceptable material balances should range from 90 to 110%; most of the sulfur balances were acceptable. The lowest sulfur and calcium balances that were obtained (FAC-8) were probably caused by incomplete removal of the 30-min steady-state sample from the receiver. Thus the rate was probably low. (The pre-steady-state removal rate was ∿50% larger than the calculated steady-state rate.) Generally, sulfur and calcium balances agreed within 10%.

Elutriation and Decrepitation of Additive. The extent of decrepitation of additive during regeneration is a major concern in the development of one-step reductive regeneration. Molecular rearrangements within the additive due to regeneration reactions could have a detrimental effect on the physical integrity of the additive. An evaluation was made of regenerated product losses due to decrepitation during regeneration at the different experimental conditions used in the FAC-experiments. Possible decrepitation of the additive when fed to the bed by pneumatic transport was not isolated from these results. Table 2 shows the calcium elutriated from the bed as a percentage of feed calcium for each experiment. This is an indication of the fraction of additive lost during regeneration because of decrepitation and consequent elutriation.

The calcium in the elutraited particles ranged from 5 to 15% of the calcium in the bed. As discussed earlier, elutriated fines smaller than 15 μm were not measured during most FAC-experiments. An increase as large as 50% in the amount of the elutriated calcium could have been obtained by including these fines. Therefore, the true losses could range between 10 and 20%. Sizing data showed that the sulfated feed dolomite samples were all nominally -45 +45 mesh, and the flue-gas particle samples were all nominally -45 mesh (<350 μm). Therefore, the elutriated particles were decrepitation fragments of the larger feed particles.

Two methods for characterizing the particle size distribution of the decrepitated particles have been utilized. In the first method, the accumulative size distribution, *i.e.*, the accumulative weight of particles as a function of the particle size, was obtained by screening and weighing the screened fractions of samples from the feed to the regenerator, the particle trap, and the cyclone in the flue-gas stream. The calcium content in these samples were determined by chemical analysis. A knowledge of the calcium content is necessary because the weight of a particle fed to the regenerator changes during regeneration and therefore all data comparisons of feed samples to flue-gas samples must be based on calcium content of the samples. The accumulative mass distribution for the regenerator feed sample in experiment FAC-1 is plotted in Fig. 2. Data points for the other curves which show the relative quantity of the feed that has decrepitated were obtained by applying the following formula to each

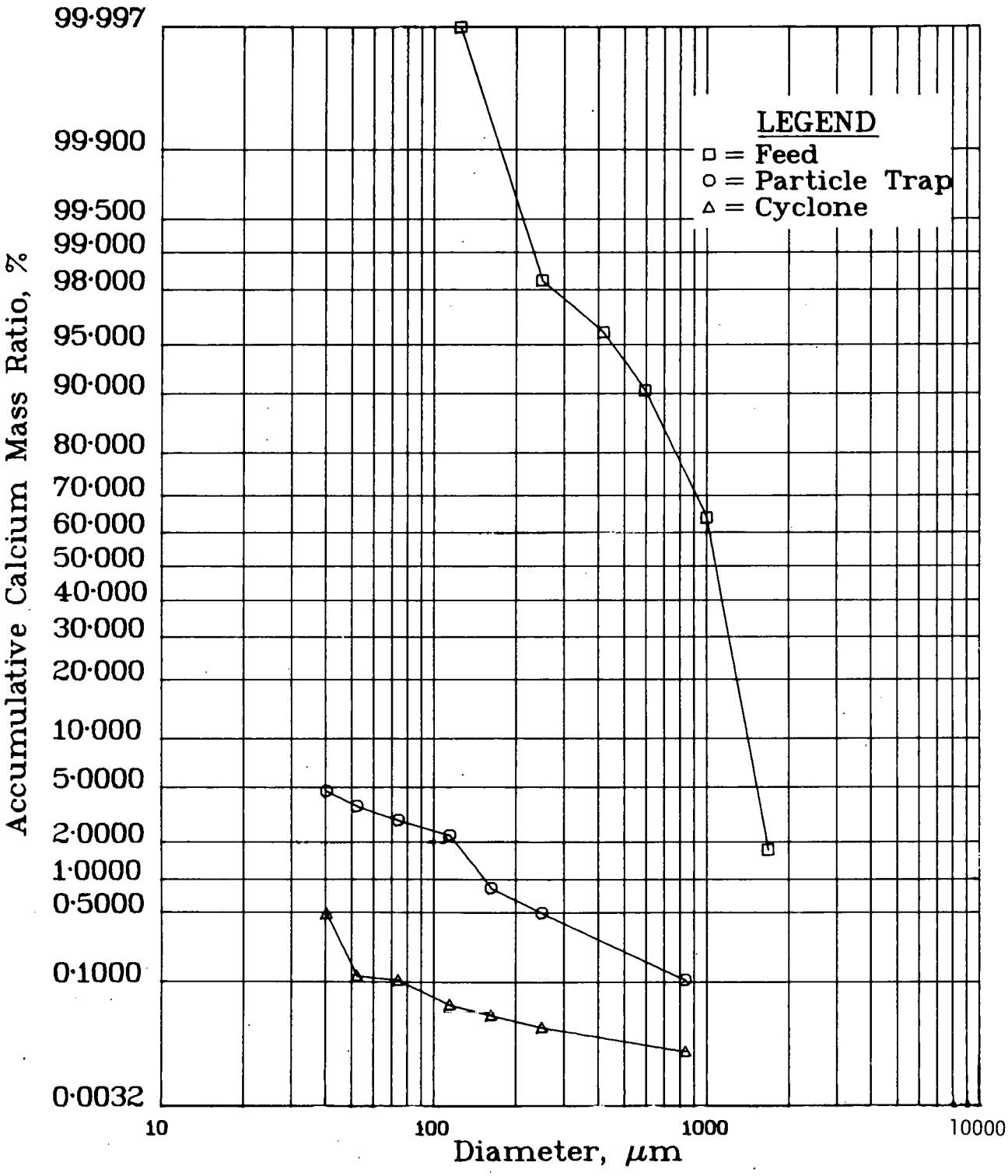

Fig. 2. Individual Sample Accumulative Mass Particle Size Distributions and Their Fractional Relation to the Feed for FAC-1

diameter (D) fraction:

$$\text{Accumulative Mass Ratio} = 100 \frac{AM_{sample}}{AM_{feed}}$$

where

AM_{sample} = accumulative mass of calcium for particles of diameter larger than and equal to D

AM_{feed} = total accumulative calcium in feed

Calculated data for the particle trap and cyclone samples for the FAC-1 experiment are plotted in Fig. 2. The data show, for example, that 5.3% of the calcium mass of the additive was elutriated, 48% of it was captured in the particle trap and 0.5% in the cyclone.

Since most of these elutriated particles were decrepitated fragments of the feed sulfated dolomite, the extent of decrepitation in FAC-1 was ∿5.0%. Similar data have been plotted in Fig. 3 for FAC-7.

A second and more direct approach to the evaluation of decrepitation was also pursued. The mass ratios (the ratios of the calcium contents of the product to the feed additive) as a function of particle diameter were plotted (see Fig. 4, lower plot) for experiment FAC-1 data. Also, the fractional distributions of the sulfated feed and regenerated product were plotted (see Fig. 4, upper plot). Since a high mass balance (109%) was obtained for this experiment (Table 2), the curve for the product to feed calcium mass ratio is shifted upward at all particle diameters. Above 900 μm, decrepitation was responsible for a decrease in the additive particle population during regeneration. Since the total mass value of the 1600 μm particle fraction the feed was small, the 80% decrease in this fraction was of no quantitative consequence. However, the 10% decrease in the 1000-μm particle fraction was meaningful because this fraction contained ∿60% of the feed. As a result of decrepitation, a particle population shift from those large diameter fractions to smaller particle fractions occurred. A 40% increase of 600-μm particles was also meaningful because this fraction constituted 25% of the feed. The 70% increase in the 430-μm fraction was less meaningful because this fraction constituted only 5% of the feed.

The product-to-feed mass ratios were also plotted for FAC-7 (Fig. 5), which was performed at the same residence time and reducing-gas conditions as FAC-1 but with a fluidized-bed height of 2.5 ft (76 cm) instead of 1.5 ft (46 cm). The characteristics of the decrepitation curves for FAC-1 and -7 were very similar. However, the extent of decrepitation was greater in FAC-7. More smaller particles were formed in FAC-7, as is evident from the shift to smaller particle diameters (see Fig. 5). More particles smaller than 250 μm were collected from the flue gas of FAC-7 than from that of FAC-1, (11% vs 4%) as shown in Figs. 2 and 3. The formation of more fines in FAC-7 was probably attributable to greater attrition during regeneration in the deeper fluidized bed.

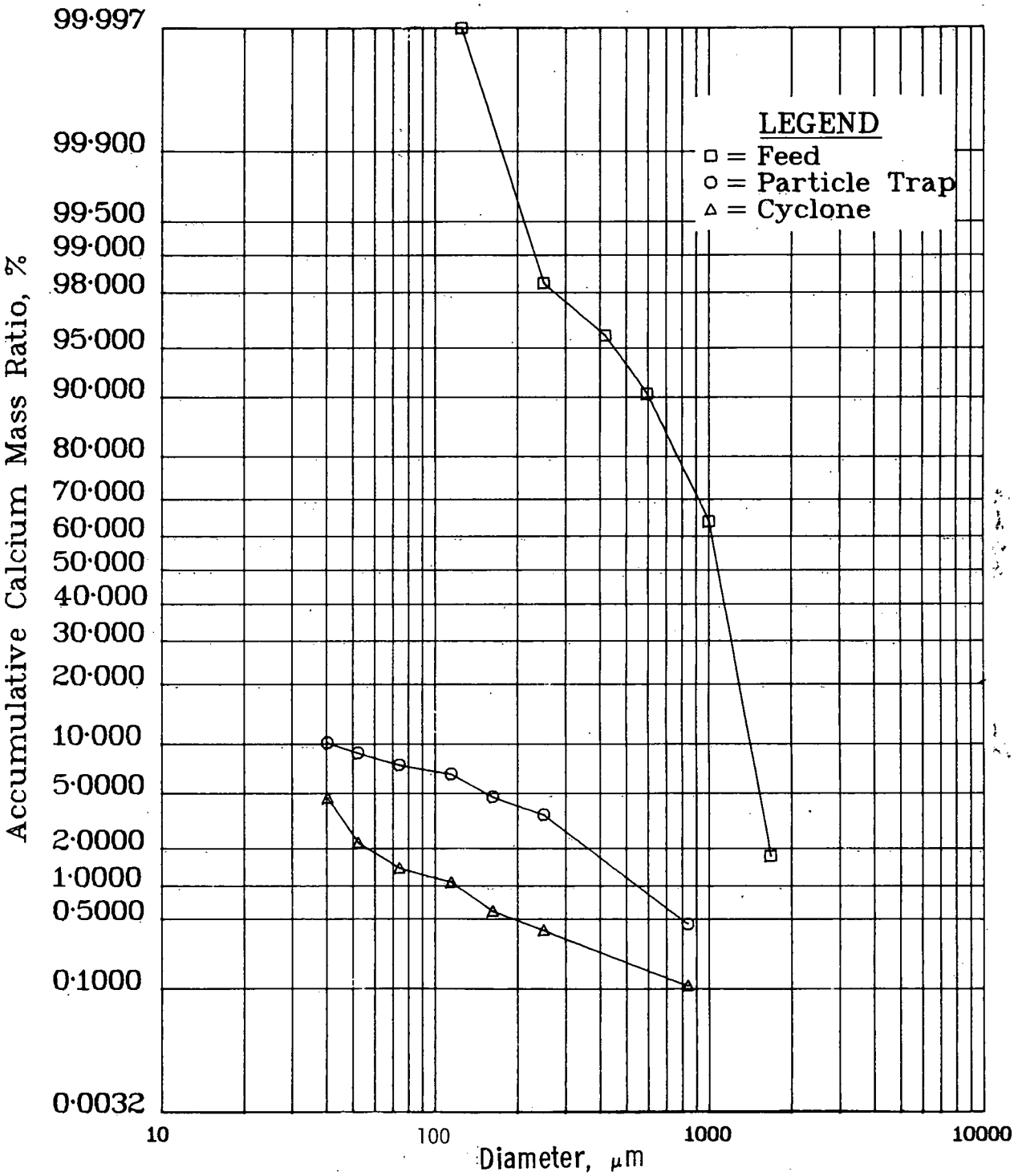

Fig. 3. Individual Sample Accumulative Mass Particle Size Distributions and Their Fractional Relation to the Feed for FAC-7

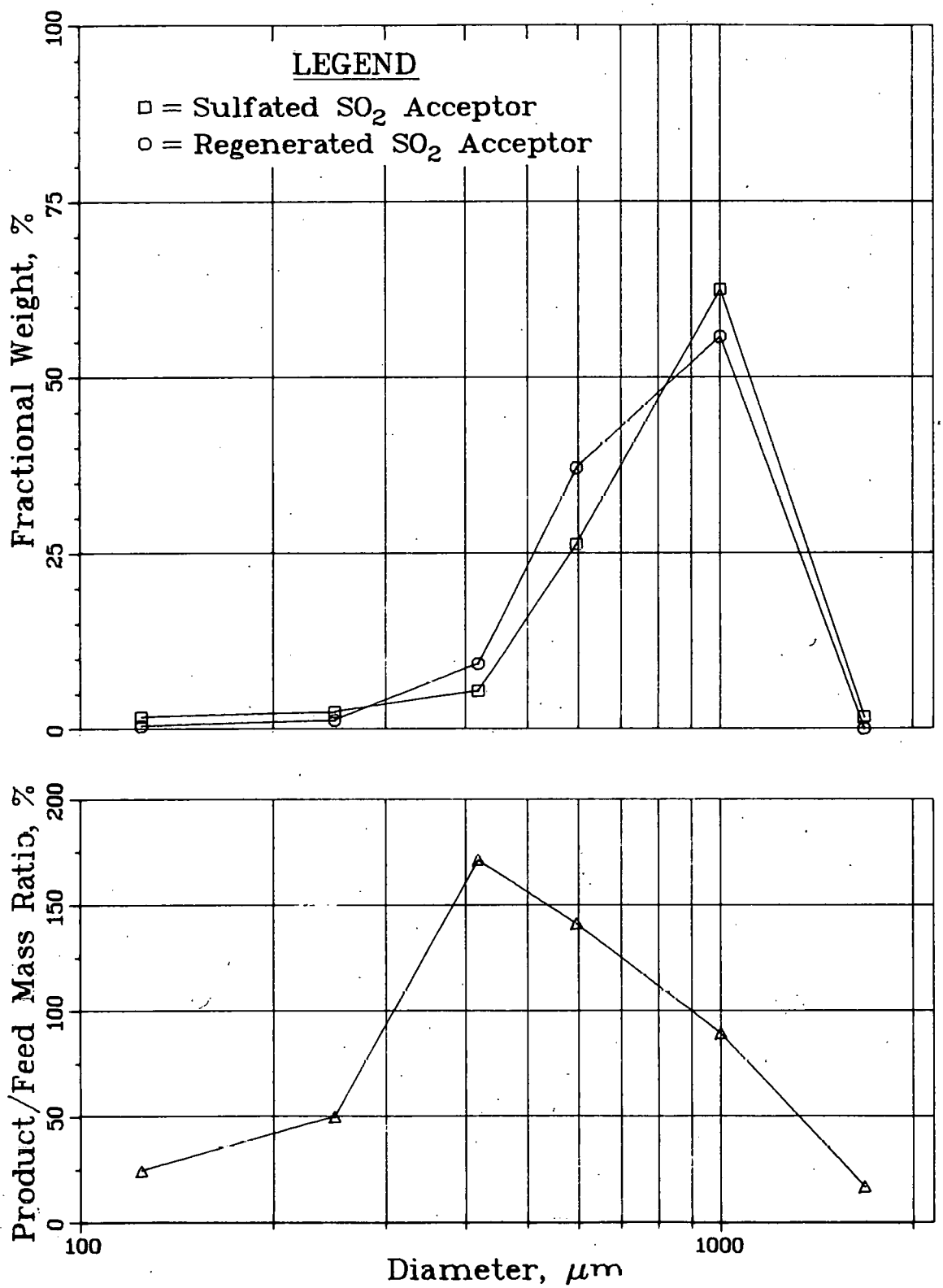

Fig. 4. Fractional Feed and Product Distributions with Decrepitation Characterized by the Fractional Product to Feed Mass Ratios versus Particle Diameters for FAC-1

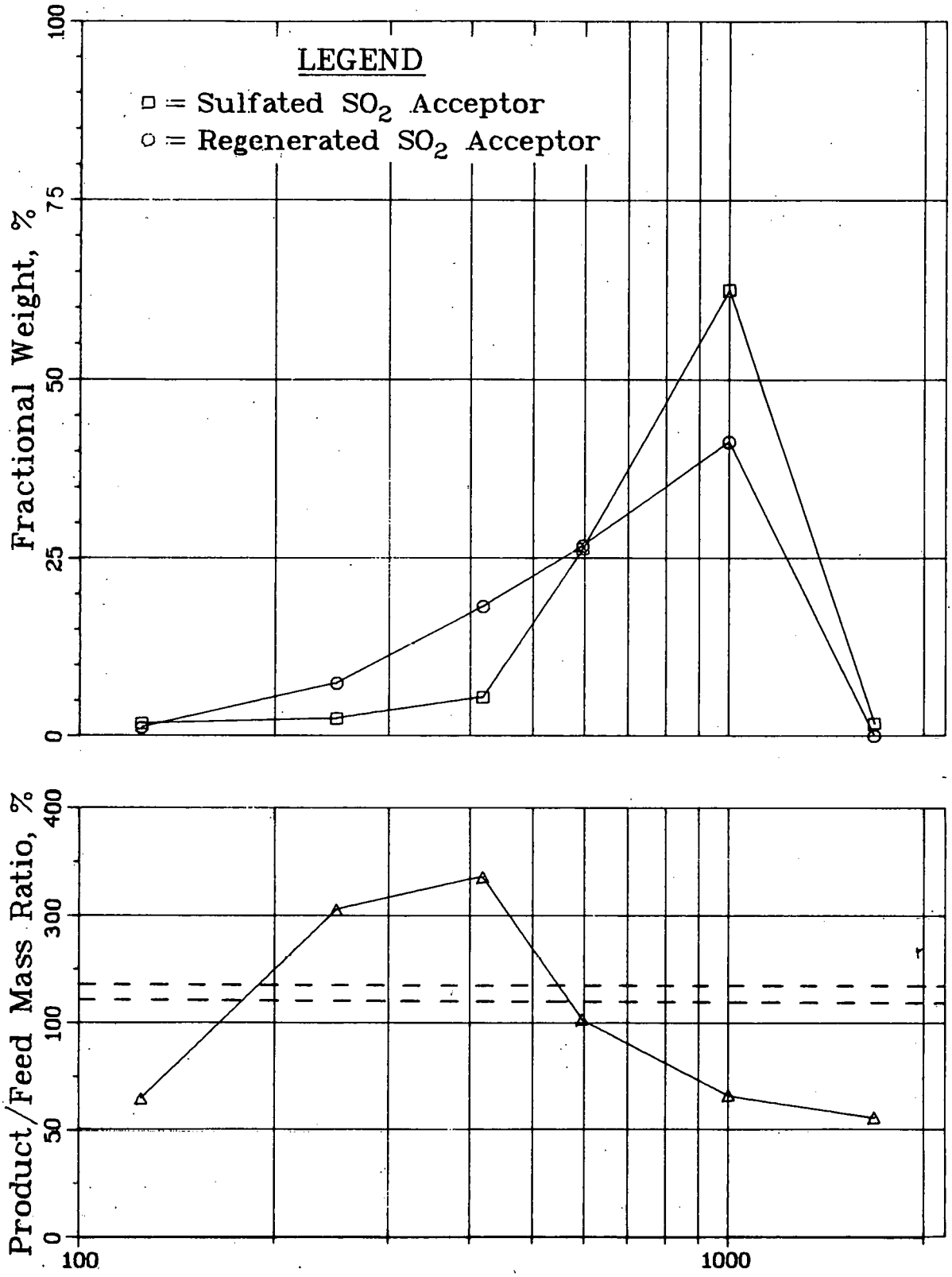

Fig. 5. Fractional Feed and Product Distributions with Decrepitation Characterized by the Fractional Product to Feed Mass Ratios vs Particle Diameters for FAC-7

Experiment FAC-4 was the only experiment in this series performed at ∿1100°C (2000°F). The product-to-feed mass ratios for FAC-4 are plotted in Fig. 6. As in previous plots, the larger particles decrepitated and the number of smaller particles (in the 430-μm fraction) increased. In comparison with FAC-1, which was performed at 1040°C and a residence time of 30 min instead of 18 min, a greater number of large particles decrepitated and the population shift was towards smaller particles in FAC-4. Based on the particle size analysis and the calcium mass balance for FAC-4 and -1, the extent of decrepitation was greater at 1100°C than at 1040°C.

Generally, all plots of product-to-feed calcium ratio as a function of fractional particle diameter showed a decrease in the number of larger particles (≥800 μm) and an increase in the number of medium size particles (>300 and <800 μm).

Agglomeration of Sulfated Additive During One-Step Regeneration Experiments. During one-step regeneration experiments in the bench-scale regenerator, localized temperature excursions have caused partial agglomeration of the sulfated additive. Because agglomerates of additive in the fluidized bed interfere with the fluidization process, a better understanding of the causes and the mechanisms of agglomeration of sulfated additive is necessary in the development of the regeneration process. Even where large-scale agglomeration does not occur, the initial stages of the agglomeration process (softening of the outer particle shell) can lead to loss of the natural additive stone porosity. This hampers the sulfation and desulfation processes of the additive in subsequent cycles, as has been reported by Wheelock and Boylan.[3]

Dolomite, sulfated dolomite, and nonaglgomerated and agglomerated product from the regenerator were analyzed by X-ray diffraction (Table 3). In unsulfated Tymochtee dolomite, traces of α-quartz were found as expected, since the dolomite contains ∿2% SiO_2. Sulfated Tymochtee dolomite contained the expected components, including traces of α-quartz and weak traces of other phases (possible merwinite, $Ca_3Mg(SiO_4)_2$). The regenerated Tymochtee dolomite from FAC-4 which was not agglomerated contained mostly CaO and MgO with traces of α-quartz, $CaSO_4$ and weak traces of other phases (possibly merwinite). During a regeneration experiment (FAC-2), partial agglomeration of the sulfated additive occurred. The loosely bound particles around the agglomerate were found to contain the same major constituents and the same minor constituents of $CaSO_4$ and α-quartz as were found in the regenerated sample from FAC-4. In addition, traces of $CaMg(SiO_3)_2$ were found. In the core of the agglomerated sample, the additive particles were fused together and contained $Ca_3Mg(SiO_4)_2$ (merwinite) as a medium constituent and CaO as a medium rather than major constituent.

Samples of Pope, Evans and Robbins (PER) sulfated Greer limestone were also analyzed by X-ray diffraction. An agglomerate of PER limestone taken from a regeneration experiment (Coal Test No. 3) was analyzed at two locations in the agglomerate. The loosely bound limestone particles contained $Ca_3Mg(SiO_4)_2$ as a minor constituent. The fused limestone particles contained $Ca_3Mg(SiO_4)_2$ as a major constituent. Again, as the additive softened, the formation of the calcium-magnesium-silicate compound progressed.

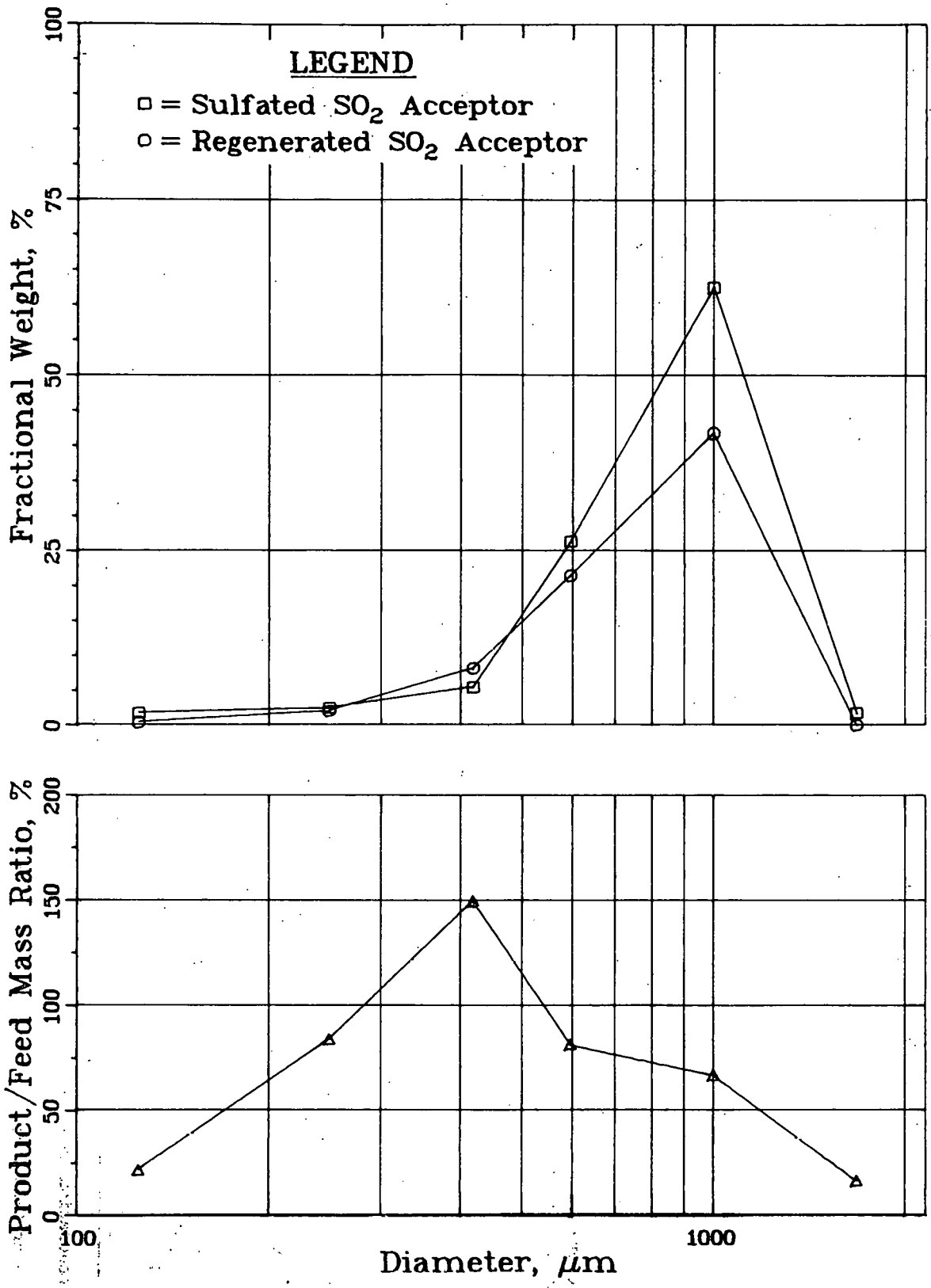

Fig. 6. Fractional Feed and Product Distributions with Decrepitation Characterized by the Fractional Product to Feed Mass Ratios vs Particle Diameters for FAC-4

Table 3. Qualitative Chemical Compositions of Various Regenerated and Unregenerated Samples of Additive.

Analysis Method: X-ray Diffraction

Material	Source	Pertinent Constituents		
		Major	Medium	Minor
Regenerated[a] Tymochtee dolomite from FAC-2	fused particles from regenerator bed	MgO	CaO and Possible $Ca_3Mg(SiO_4)_2$	$CaSO_4$
Regenerated[a] Tymochtee dolomite from FAC-2	loosely bound particles from regenerator bed	MgO, CaO		Possible $CaSO_4$, α-quartz, and $CaMg(SiO_3)_2$
Regenerated[a] Tymochtee dolomite from FAC-4	unbound regenerated additive from regenerator bed	CaO, MgO		α-quartz; possible $CaSO_4$, $CaMg(CO_4)$, $Ca(OH)_2$, and other phases.
Sulfated Tymochtee dolomite	Combustor Product	$CaSO_4$, $CaCO_3$		CaO, possible α-quartz and other phases
Tymochtee dolomite		$CaMg(CO_3)_2$		α-quartz and possible $Al_2Si_2O_5(OH)_4 \cdot 2H_2O$
Regenerated[b] PER-limestone[c] from Coal Test No. 3	fused particles from regenerator bed	MgO and probable $Ca_3Mg(SiO_4)_2$		possible $CaSO_4$, $MgAl_2O_4$; very minor: possible CaO
Regenerated[b] PER-limestone from Coal Test No. 3	loosely bound particles from regenerator bed	$CaSO_4$, MgO		possible $Ca_3Mg(SiO_4)_2$

[a] Regeneration temperature was ~1100°C.

[b] Regeneration temperature was 1040°C.

[c] Pope, Evans, and Robbins.

On the basis of X-ray diffraction analysis described, it appears that during the agglomeration process (probably during the softening) calcium, magnesium, and quartz combine and form calcium-magnesium-silicate compounds. Larger fused additive samples will be analyzed to further identify and characterize these compounds. The melting point of this class of materials is ∿1250°C. Formation of these calcium-magnesium-silicate compounds seems to be incidental to and not responsible for the agglomeration process. This was partially confirmed by data obtained from preliminary DTA experiments.

Differential thermal analyses were performed on unsulfated and sulfated Tymochtee dolomite in different gas environments. The X-ray diffraction analyses of the samples taken from the DTA experiments are given in Table 4. Only one reaction was observed from ambient to 1300°C in unsulfated dolomite in either air or nitrogen. It occurred at 550-850°C; this was the calcination reaction. The sulfated dolomite (which contained a small amount of carbonate) calcined at 600-750°C, melted at 1200°C in both air and nitrogen. This is lower than the melting point of any of the major constituents of sulfated dolomite. In addition to the weight loss attributed to calcination, a weight loss was noted as the temperautre of the sulfated samples was raised above 1100°C. This might have been due to decomposition of $CaSO_4$. During cooling, an exothermic reaction(solidification) occurred at 1150°C. X-ray diffraction analysis of these samples showed that $CaSO_4$ and MgO were the major and CaO the minor constituents. $CaSO_4$ was present as large crystals indicative of post-melting instead of the small crystals that are normally present in sulfated dolomite. Also, in both of these samples, calcium silicate was formed as a possible minor constituent, instead of the calcium-magnesium-silicate compounds found in the agglomerated dolomite samples.

Because the DTA samples were small, ∿30 mg, the samples may not have been totally representative of nonhomogeneous Tymochtee dolomite. Larger samples will be used in future experiments, which will be performed on another DTA apparatus.

The last of these DTA experiments was performed with sulfated dolomite in a reducing atmosphere (100% H_2). The calcination weight loss at 600-700°C was followed by further weight loss, which continued to ∿1000°C. This weight loss was probably due to the reduction of $CaSO_4$ to CaS, as confirmed by X-ray diffraction analysis of the final product. This product contained CaS and MgO as the major constituents. No melting was observed up to 1300°C.

Regeneration Using *In Situ* Combustion of Coal

Cold tests of the bench-scale regeneration system were recently completed, and hot testing is under way. Test CS-3 was performed using coal to supply heat and the reductants with a bed temperature ranging from 1043°C to 1077°C (1910-1970°F) and a sulfated additive feed rate ranging from 2.7 to 5.4 kg/hr (∿7-12 lb/hr). During one segment of this test, 5.2 kg/hr of sulfated Tymochtee dolomite (11.1 wt % S) was fed into the bed, which was at a temperature of 1063°C (1945°F). The coal (Arkwright) feed rate was 4 lb/hr. The total reducing gas (H_2, CO, and CH_4) concentration in the dry effluent was 2.8%. It was assumed that

Table 4. Qualitative Chemical Composition (obtained by X-Ray Diffraction Analysis) of Samples Taken from DTA Experiments.[a]

Material	Reaction Atmosphere During DTA Experiment	Pertinent Constituents		
		Major	Medium	Minor
Tymochtee dolomite	N_2	MgO	CaO	$Ca(OH)_2$, possible $CaCO_3$ and other weak phases.
Tymochtee dolomite	Air	CaO, MgO		very minor: possible $CaAl_2O_4$ or $NaCa_4Al_2O_3$
Sulfated Tymochtee dolomite	N_2	MgO $CaSO_4$ (very crystalline)		CaO, possible calcium silicate
Sulfated Tymochtee dolomite	Air	MgO, $CaSO_4$ (very crystalline)		CaO, possible calcium silicate
Sulfated Tymochtee dolomite	H_2	CaS, MgO		

[a] Final DTA furnace temperature was 1300°C.

the sulfur from all of the fed coal was liberated as SO_2. In calculating regeneration, this amount was subtracted from the total SO_2 in the effluent. Based on the quantities of SO_2 and H_2S in the effluent, an additive regeneration of ∿71% was calculated. A sample of regenerated material from this segment of CS-3 was analyzed for total sulfur and sulfide. It was found that the regenerated Tymochtee dolomite contained 1.8 wt % sulfur (the sulfated dolomite feed contained 11.1 wt % S) and <0.1 wt % sulfide. Since CS-3 was a shakedown test, the results as reported are considered preliminary.

Hot testing of the regeneration system has shown that good temperature control can be maintained in the modified regenerator. The bed temperature was varied between 1040°C and 1100°C, and total reducing gas concentrations up to 3% in the effluent were obtained.

A regeneration experiment was performed (CS-5) to compare the regeneration results obtained (1) in an earlier experiment in which CH_4 was combusted *in situ* (FAC-9A, Table 1) and (2) in this experiment with *in situ* combustion of Arkwright coal. Both experiments were performed with a fluidizing gas veloicty of 0.91 m/sec (∿3 ft/sec), a solids residence

time of ∿30 min in the reactor, a bed temperature of 1040°C, and a fluidized-bed height of 46 cm (18 in.). The total reducing gas concentration in the effluent was ∿4% in FAC-9A and ∿2% in CS-5. The experimental conditions and the results for FAC-9A and CS-5 are given on Table 5. In FAC-9A, the SO_2 concentration in the wet effluent gas was 1.3% and the particle regeneration (based on the quantity of SO_2 in the effluent) was 38%. In experiment CS-5, the SO_2 concentration in the wet effluent gas gas was 2.4% and particle regeneration (based on SO_2 plus H_2S) was 64%. The H_2S for FAC-9A was not included because the H_2S concentration was not continuously measured in that experiment.

In CS-5, the H_2S constituted 1.8% of the total sulfur in the effluent gas, and the sulfur released by the combustion of coal* constituted 11% of the total sulfur released into the effluent gas. An appropriate adjustment was made for sulfur in the coal in calculating the product particle regeneration. The chemical composition of the regenerated product from CS-5 will be reported upon completion of the analysis.

Table 5. Experimental Conditions and Regeneration Results for FAC-9A and CS-5.

Fluidizing Gas Velocity: 0.91 m/sec (3 ft/sec)
System Pressure: 0.84 kg/cm^2 (12 psig)
Bed Temperature: 1040°C
Nominal Particle Residence Time: 30 min
Bed height: 46 cm
Additive: Sulfated Tymochtee Dolomite
(a) 10.2 wt % S (FAC-9A)
(b) 11.1 wt % S (CS-5)

Experiment No.	Regenerator Diameter (cm)	Combustion Fuel	Additive Feed Rate (kg/hr)	Total Reducing Gas Concentration (%)	Measured S (as SO_2 and/or H_2S) in the Wet Effluent Gas (vol %)	Particle Regeneration (%)
FAC-9A	7.6	CH_4	2.7	4	1.3[a]	38
CS-5	10.8	Arkwright Coal	5.0	2	2.4[b]	64

[a] Only SO_2 was monitored continuously.

[b] H_2S and SO_2 were monitored continuously.

*Carbon analysis was not completed, and it was assumed that all sulfur in the coal fed to the regenerator was released.

Based on the flue-gas analysis, the extent of regeneration in CS-5 was greater than in FAC-9A. These experiments differed in only two basic aspects: first, the kind of combustion fuel (CH_4 in FAC-9A and coal in CA-5) and second, the bed diameter. It is not believed at this time that the differences in regeneration were due to differences in the fuel. The diameter of the fluidized bed was 7.6 cm in FAC-9A and 10.8 cm in CS-5. The larger diameter in CS-5 improved the length to diameter ratio (L/D = 4.2 in CS-5 and 6.1 in FAC-9A) of the fluidized bed. This, in turn, probably improved the quality of fluidization in CS-5. The quality of fluidization might play an important role since the regeneration reactions are relatively fast and good solid-gas contact is important.

DEVELOPMENT OF SUPPORTED ADDITIVES

A research program is under way to investigate the utility of synthetic supported additives for the reduction of the SO_2 content of the combustion gas in the fluidized-bed coal combustor. It is proposed that these supported additives would be used in place of limestone or dolomite. In the current studies, calcium oxide supported on α-alumina is under investigation. Results are reported on the process used to prepare the supported additive and on the kinetics of the sulfation and regeneration reactions. The results of cyclic sulfation-regeneration experiments are also reported.

Preparation of Synthetic Additive

A method of preparing CaO in α-Al_2O_3 support at various CaO concentrations has been developed and is described below.

The pellets of the alumina support are placed in an aqueous calcium nitrate solution, refluxed for 8 hr, and then cooled to 25°C for 4 hr. The pellets are removed from the solution and slowly heated to the heat-treating temperature of either 800 or 1100°C, where they are held for one hour. Heating is allowed to proceed very slowly around 100°C, 132°C, and 561°C since the evolution of H_2O and the decomposition of $Ca(NO_3)_2 \cdot 4H_2O$ to CaO occur at those temperatues. Figure 7 shows the percent CaO in α-Al_2O_3 support for various concentrations of $Ca(NO_3)_2 \cdot 4H_2O$ in aqueous solutions.

Sulfation Studies

From chemical analysis results, the calcium utilization during sulfation of pellets containing 6.6% CaO in α-Al_2O_3 is presented. The sulfation kinetics of 1100°C heat-treated pellets containing 6.6 in α-Al_2O_3 was determined and was compared with the rate for the 800°C heat-treated pellets. Also, the effect on the sulfation rate of water in the gas was determined. A mathematical equation was developed that predicts the rate of sulfation. Finally, the rate of sulfation was determined for synthetic additives containing various concentrations of calcium oxide.

Calcium Utilization. Wet chemical analyses for calcium and sulfur have been performed on sulfated 6.6% CaO in α-Al_2O_3 pellets. These results, along with TGA weight change data obtained during sulfation experiments, helped determine the extent of sulfation of the sorbent under different

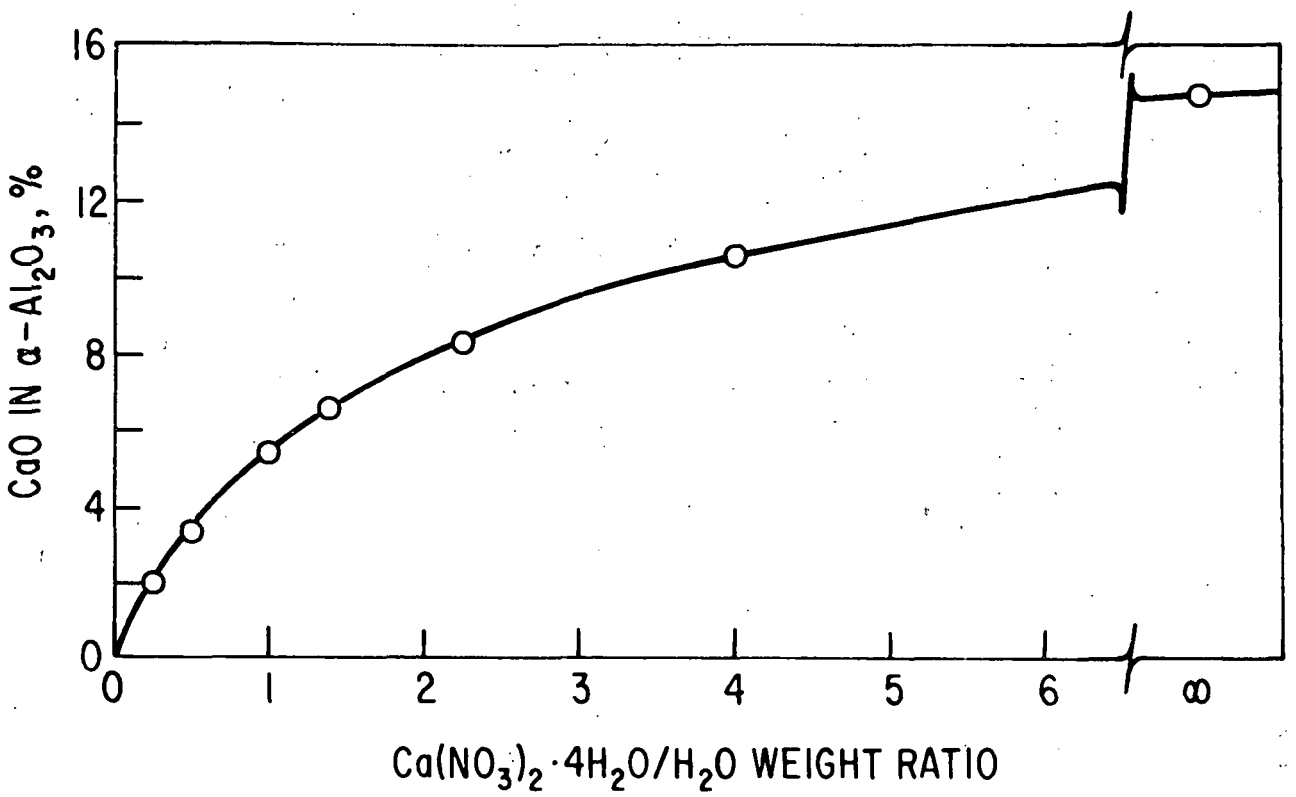

Fig. 7. CaO Concentration in α-Al_2O_3 as a Function of Preparation Solution Concentration.

conditions. Table 6 compares the percent calcium utilization (percent sulfation) computed from the chemical analyses with the utilization estimated from the weight change which occurred during sulfation. The percent sulfation (or calcium utilization) based on chemical analyses, is shown in column 2; the average calcium concentration is 4.27%, which is below the value of 4.71% Ca (6.6% CaO) which had been estimated from the gain in weight of the pellets after loading with CaO. Column 4 gives the percent calcium utilizations calculated from the weight changes which occurred due to CaO converting to $CaSO_4$. Column 5 presents the percent deviation between the two methods of calculating the percent calcium utilization. Fair agreement (a variance of 6.1%) was found between the two methods of calculating the percent calcium utilization. The variance was 4.6 when Run 40 was excluded from the calculations. The 80-90% calcium utilization at 900°C is only slightly dependent upon SO_2 concentration. This result contrasts with the experimental TGA results for dolomite, which indicated that the percent utilization is strongly dependent upon the SO_2 concentration.

The percent calcium utilization at 750 and 800°C were 63 and 72%, respectively, which values are somewhat lower than the 80 to 100% conversions found in the 850 to 1050°C temperature range.

Sulfation Rates for Pellets Heat-Treated at 800 and 1100°C. Pellets that had been heat-treated (H.T.) to 800°C and to 1100°C were sulfated

Table 6. Calcium and Sulfur Content of Sulfated 6.6% CaO in α-Al_2O_3 Sorbent

1 Run	2 Ca Conc, Chem. Analysis (wt %)	3 Sulfation, Computed from Chem. Analysis (%)	4 Sulfation Computed from Wt Change (%)	5 Deviation, Col. 3 vs Col. 4 (%)	6 Operating Conditions	
W51	4.22	82.3	82.4	0.0%	0.05% SO_2	900°C
W50	4.39	91.4	91.2	-0.2%	0.1% SO_2	900°C
W49	4.29	86.5	88.4	+2.1%	0.2% SO_2	900°C
W23	4.27	98.2	94.1	-4.1%	0.3% SO_2	900°C
W23 (repeat)	4.06	94.2	98.9	+5.0%	0.3% SO_2	900°C
W39	4.26	75.4	82.3	+9.2%	1% SO_2	900°C
W40	4.19	88.3	100.6	+13.9%	3% SO_2	900°C
W90	4.01	67.6	62.6	-7.4%	0.3% SO_2	750°C
W89	4.47	71.3	72.1	+1.1%	0.3% SO_2	800°C
W73	4.07	92.8	93.0	+0.3%	0.3% SO_2	850°C
W23	4.06	94.2	99.0	+5.0%	0.3% SO_2	900°C
W70	4.63	85.3	87.0	+2.0%	0.3% SO_2	950°C
W72	4.52	79.4	75.8	-4.6%	0.3% SO_2	1050°C
Av.	4.27	84.4	85.7	variance 6.1% (4.6%)[a]		

[a]Excluding Run W40.

on the TGA unit at 900°C, using 0.1, 0.3, and 1% SO_2 with 5% O_2. The extent of sulfation of the 800°C and 1100°C. H.T. pellets as a function of time and SO_2 concentration in the gas stream is given in Fig. 8. The sulfation rate for the 800°C H.T. pellets was 1.5 times higher than for the 1100°C H.T. pellets for all SO_2 concentrations in the gas stream. It is speculated that the lower rate for the 1100°C H.T. pellets is due to the formation of more stable aluminate complexes ($CaAl_2O_4$,$CaAl_4O_7$) at 1100°C than at 800°C ($Ca_3Al_{10}O_{18}$,$CaAl_{12}O_{21}$).

Effect of H_2O Concentration in the Feed Gas on Sulfation Rate. Yang *et al.*[4] found a beneficial effect of water vapor on the sulfation rate of dolomite, the concentration of H_2O being immaterial. The rate of sulfation of the pellets at 900°C was determined with reactant gases containing 0.3% SO_2 - 5% O_2 and 0, 0.1, 0.47, and 1.27% H_2O (est). The sulfation rate was independent of the H_2O concentration in the feed gas.

Mathematical Analysis of Sulfation Rate. A mathematicl equation was developed that correlates the rate of sulfation of the 6.6% CaO in α-Al_2O_3 sorbent with CaO concentration in the additive, SO_2 concentration in the feed gas, and temperature. This equation is:

$$\ln \frac{CaO_{t=t}}{CaO_{t=0}} = \frac{-C}{1 + \frac{2.9 \times 10^{-6}}{e^{\frac{-2700}{RT}}}} [SO_2]^{0.7} t \qquad (1)$$

where C = 0.025 for 800°C heat-treated sorbent
C = 0.0172 for 1100°C heat-treated sorbent
t = time, sec
T = temperature, °K
$[SO_2]$ = conc. of SO_2, mol %
[CaO] = conc. of CaO, mol/m^2 of surface area

The reaction was found to be 0.7 order in SO_2, first order in CaO concentration, independent of O_2 concentration when oxygen is present in stoichiometric excess, and independent of H_2O concentration.

The temperature dependence of the reaction was determined by measuring the rate over a temperature range of 750 to 1050°C, using a 0.3% SO_2 -5% O_2 gas mixture. A gas-solid reaction can be either diffusion-controlled or chemical reaction-controlled; for some such reactions, diffusion control occurs at the higher temperatures. In these experiments, the sulfation rate increased with temperature up to 900°C; at higher temperatures, it was independent of temperature. The expression for the overall rate constant, $k_{overall}$, which is shown below, takes into account both diffusion control and chemical reaction control.[5]

When $D_{SO_2} >> k_r$, $k_{overall} = k_r$; when

$k_r >> D_{SO_2}$, $k_{overall} = D_{SO_2}$

$$k_{overall} = \frac{D_{SO_2}/\delta}{1 + \frac{D_{SO_2}}{k_r \delta}} \qquad (2)$$

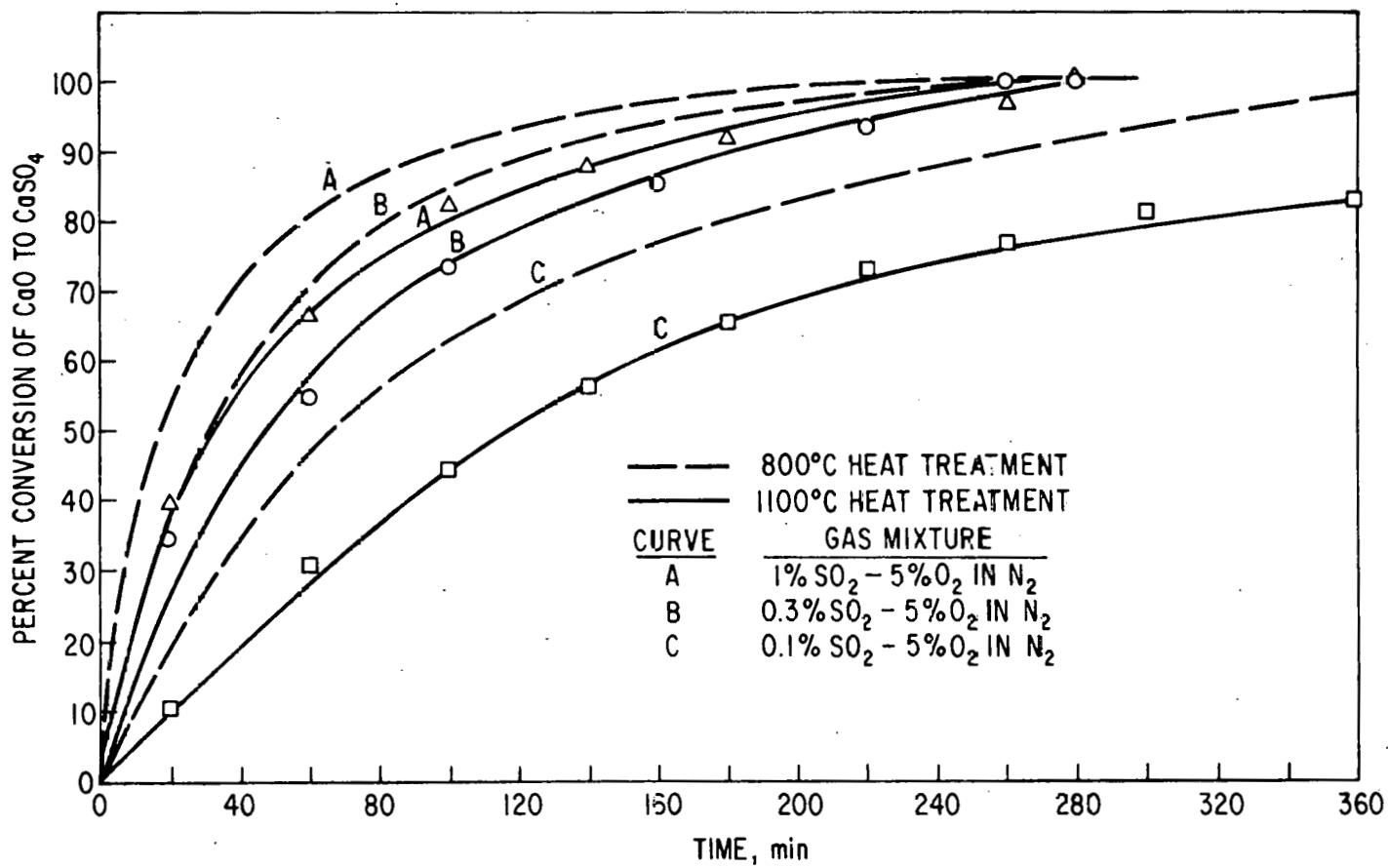

Fig. 8. Effect of Heat-Treatment Temperature on Rate of Sulfation at 900°C.

where $k_{overall}$ = experimentally measured rate constant, sec^{-1}
D_{SO_2} = SO_2 diffusion coefficient, cm^2/sec
δ = diffusion length, cm
k_r = chemical reaction rate constant, sec^{-1}

By use of this equation and the experimentally determined sulfation rates at various temperatures and with the assumption of no activation energy for SO_2 diffusion, Equation 1 was developed.

Figure 9 gives a comparison of calculated (Eq. 1) and experimental rates of sulfation of 6.6% CaO in α-Al_2O_3 at 900°C as a function of SO_2 concentration. The gas also contained 5% O_2, and the remainder was nitrogen. Agreement is good.* Figure 10 shows a comparison of the same data as a function of temperature. Agreement is satisfactory at low conversion; however, at conversions above 50%, the experimental rate is much lower than the predicted rate for temperatures below 900°C.

Figure 11 gives an "activation energy" curve for the experimental and predicted sulfation rates. The temperature dependence of the rate decrease rapidly above 900°C.

Sulfation Rate as a Function of Calcium Loading in Support. In Fig. 12 the percent conversion of CaO to $CaSO_4$ is given as a function of time for 2 to 16.5% CaO in α-Al_2O_3 heat treated at 1100°C. The rate of sulfation, when measured as a fraction of the maximum possible sulfation, decreases with increasing CaO concentration. However, as shown in Table 7, the sorbent

Table 7. Sorbent Weight Gain during Sulfation for Various Calcium Oxide Concentrations.

Sulfation Conditions: Feed Gas, 0.3% SO_2, 5% O_2
Temp, 900°C

	Weight gain, g/kg of additive (1100°C H.T.)								
Hours into Run	2% CaO	3.3% CaO	5.4% CaO	6.6% CaO	8.3% CaO	10.5% CaO	14.8% CaO	16.5% CaO	Tymochtee Dolomite
0.5	18.0	30.2	27.5	34.9	34.4	31.5	32.6	24.3	93.4
1	21.0	38.1	40.6	48.1	51.8	49.3	49.0	43.9	
2	22.5	42.9	53.2	76.7	74.7	77.7	74.0	72.6	161.2
3	23.7	44.6	60.7	84.4	88.6	95.3	94.7	96.0	191.2
4	--	45.4	64.5	88.2	96.7	109.2	112.7	112.0	213.1
5	--	--	67.0	--	100.7	119.4	126.4	126.4	230.0
6	--	--	--	--	102.9	123.6	136.3	140	243.0
Max possible wt gain	28.6	47.1	77.1	94.3	119.0	150	211.4	235.8	546.0

* The various constituents of the feed gas were monitored with rotatmeters and were mixed to give the proper feed gas compositions. Feed gas compositions were verified by a mass spectrometric method, and a gas chromatographic method for this determination was developed by M. Homa of the Analytical Chemistry Laboratory, Chemical Engineering Division.

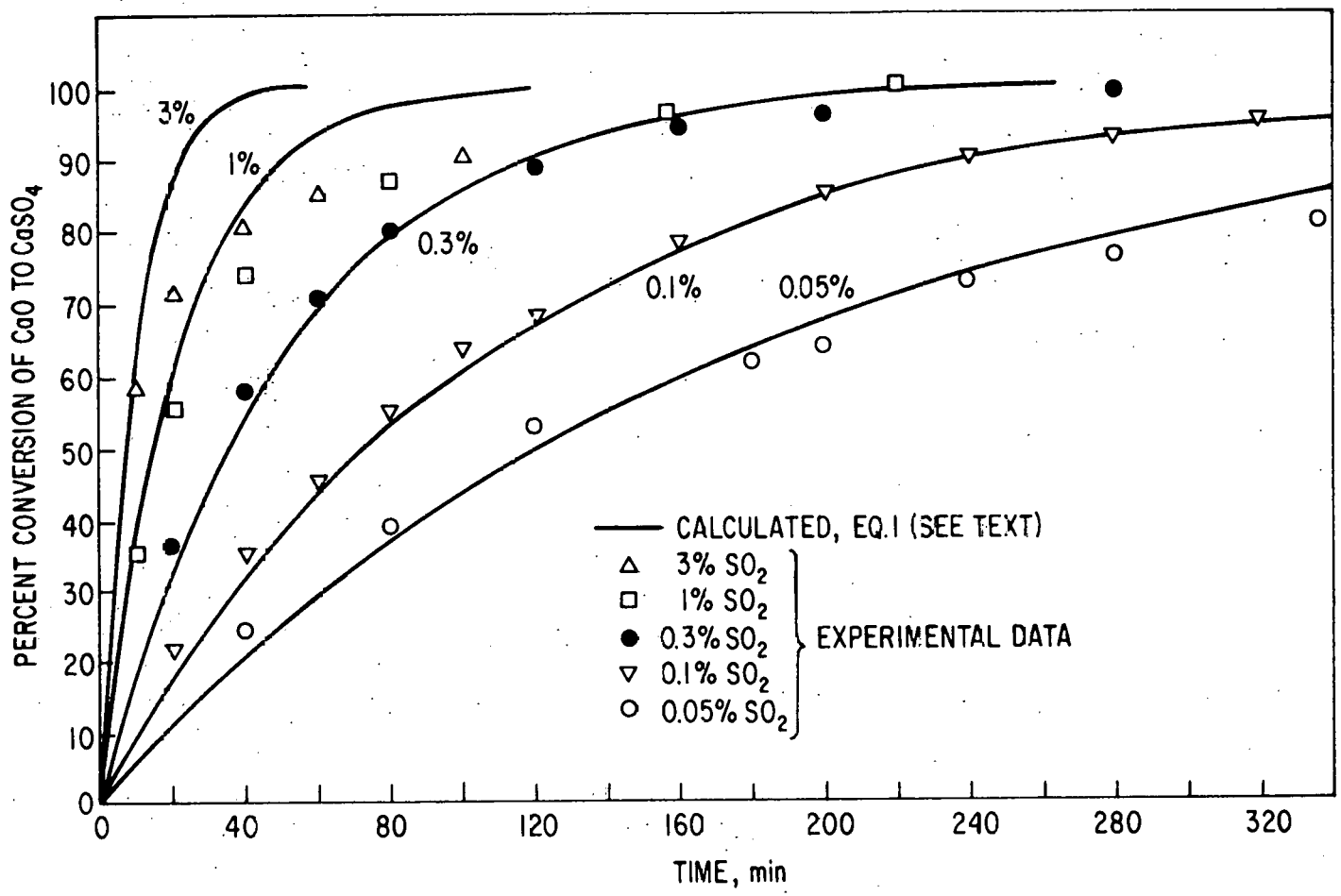

Fig. 9. Comparison of Predicted and Experimental Sulfation Rates of 6.6% CaO in α-Al_2O_3 as a Functicn of SO_2 Concentration.

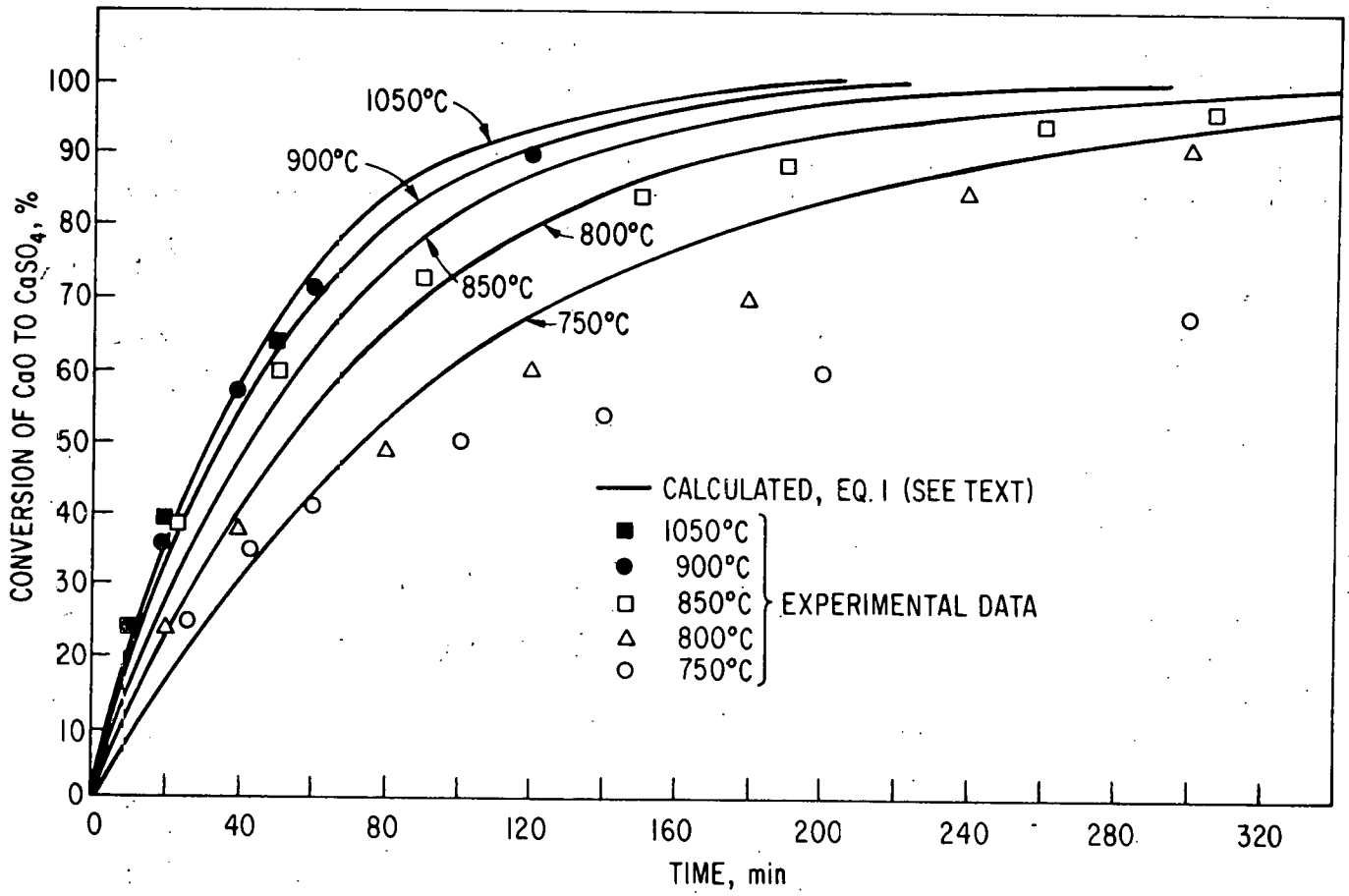

Fig. 10. Comparison of Predicted and Experimental Rates of Sulfation of 6.6% CaO-α-Al_2O_3 with 0.3% SO_2 as a Function of Temperature.

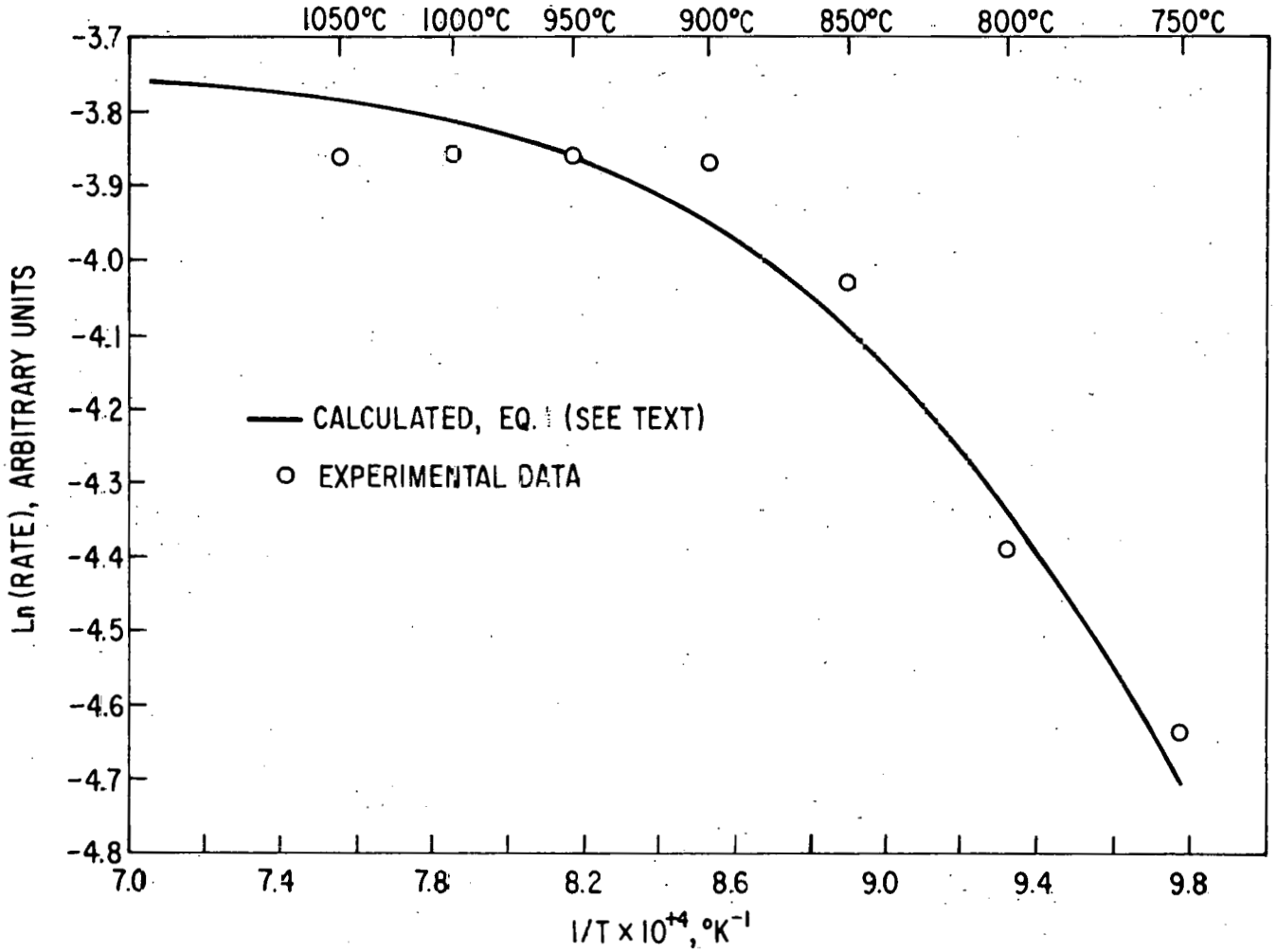

Fig. 11. Comparison of Experimental and Predicted Rates of Sulfation of 6.6% CaO-α-Al_2O_3.

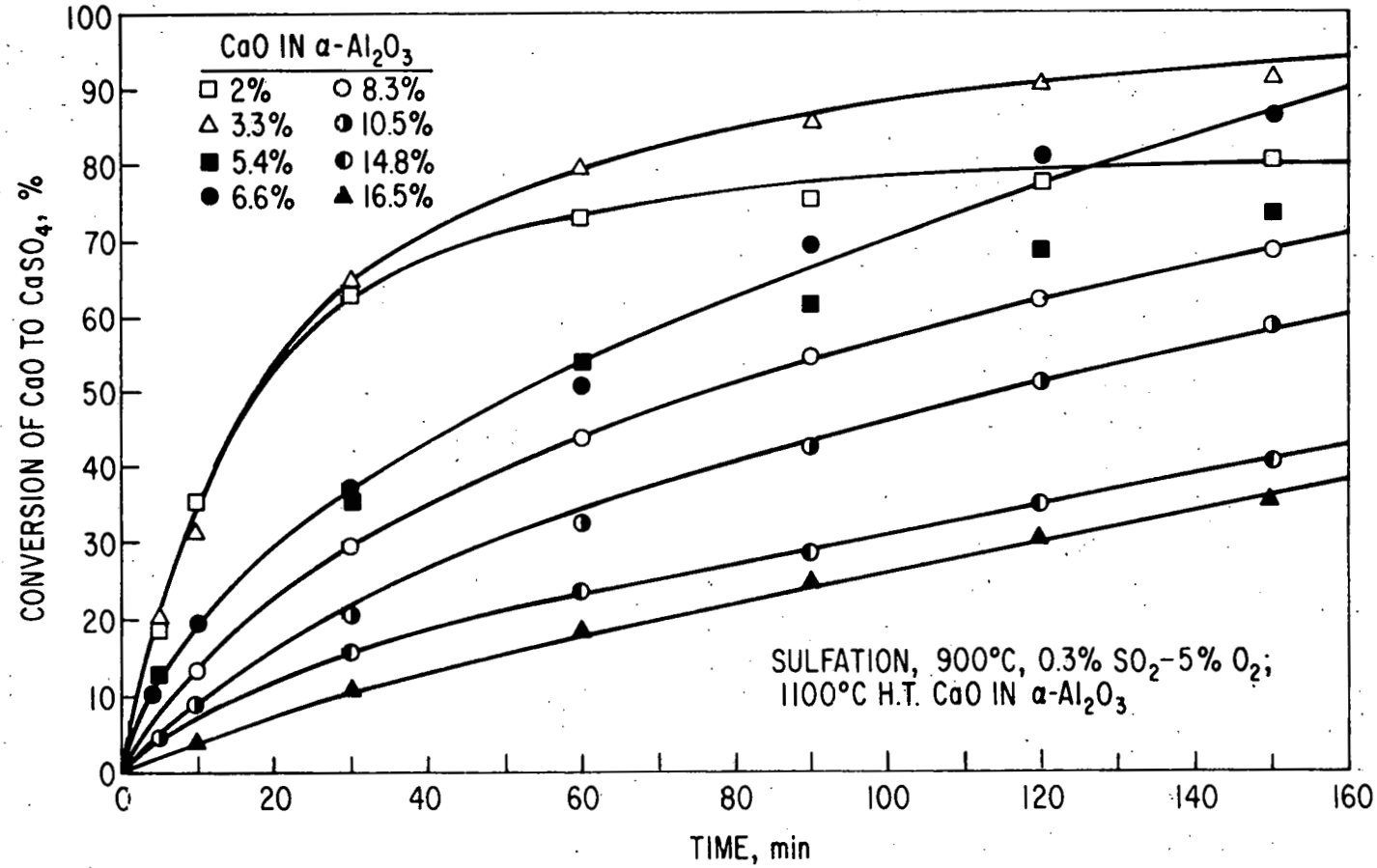

Fig. 12. Sulfation of Supported Sorbents with Various CaO Loadings.

weight gain at any given time during sulfation is usually higher for the supports containing more CaO. The SO_3 weight gain for Tymochtee dolomite is also given for comparison. It captures approximately twice as much SO_2 as does the 16.5% CaO in α-Al_2O_3 sorbent for any given residence time. Figure 13 shows the sorbent weight gain as a function of CaO concentration in α-Al_2O_3 at the end of 1, 3, and 6 hr; this figure is a plot of the data in Table 7.

Regeneration of Supported Additives

The rate of regeneration of the sulfated synthetic sorbent was determined, and an equation was developed that predicts the regeneration kinetics as a function of reducing gas concentration, $CaSO_4$ concentration, and temperature.

Regeneration Rate as a Function of Temperature. Regeneration experiments over a temperature range of 800 to 1200°C, using 1% H_2 in the gas stream, have been completed. The results for 1200, 1100, 1000, and 900°C (Fig. 14) show that the regeneration rate increases with temperature.

The composition of the regeneration reaction product is a function of temperature, as shown in Table 8. X-ray diffraction analyses indicate that

Table 8. Product of the Regeneration Reaction As a Function of Temperature (Obtained by X-ray Diffraction Analyses)

Regeneration Temp (°C)	Product
1200	CaO
1150	CaO
1100	CaO
1050	Mostly CaO-Little CaS
1000	Medium quantities of CaO and CaS
950	Mostly CaS-little CaO
900	Mostly CaS-little CaO
850	CaS
800	CaS

above 1100°C, the only product is CaO, and below 900°C, the entire product is CaS. In the intermediate temperature range of 900 to 1050°C, the product is a mixture of CaO and CaS, with CaO concentration increasing with temperature.

Mathematical Analysis of the Regeneration Kinetics. The experimental regeneration kinetic data were analyzed, using the following equation:

$$\text{regeneration rate} = \frac{d[CaSO_4]}{dt} = -k[R.G.]^x[CaSO_4]^y \exp(-E_a/RT) \qquad (3)$$

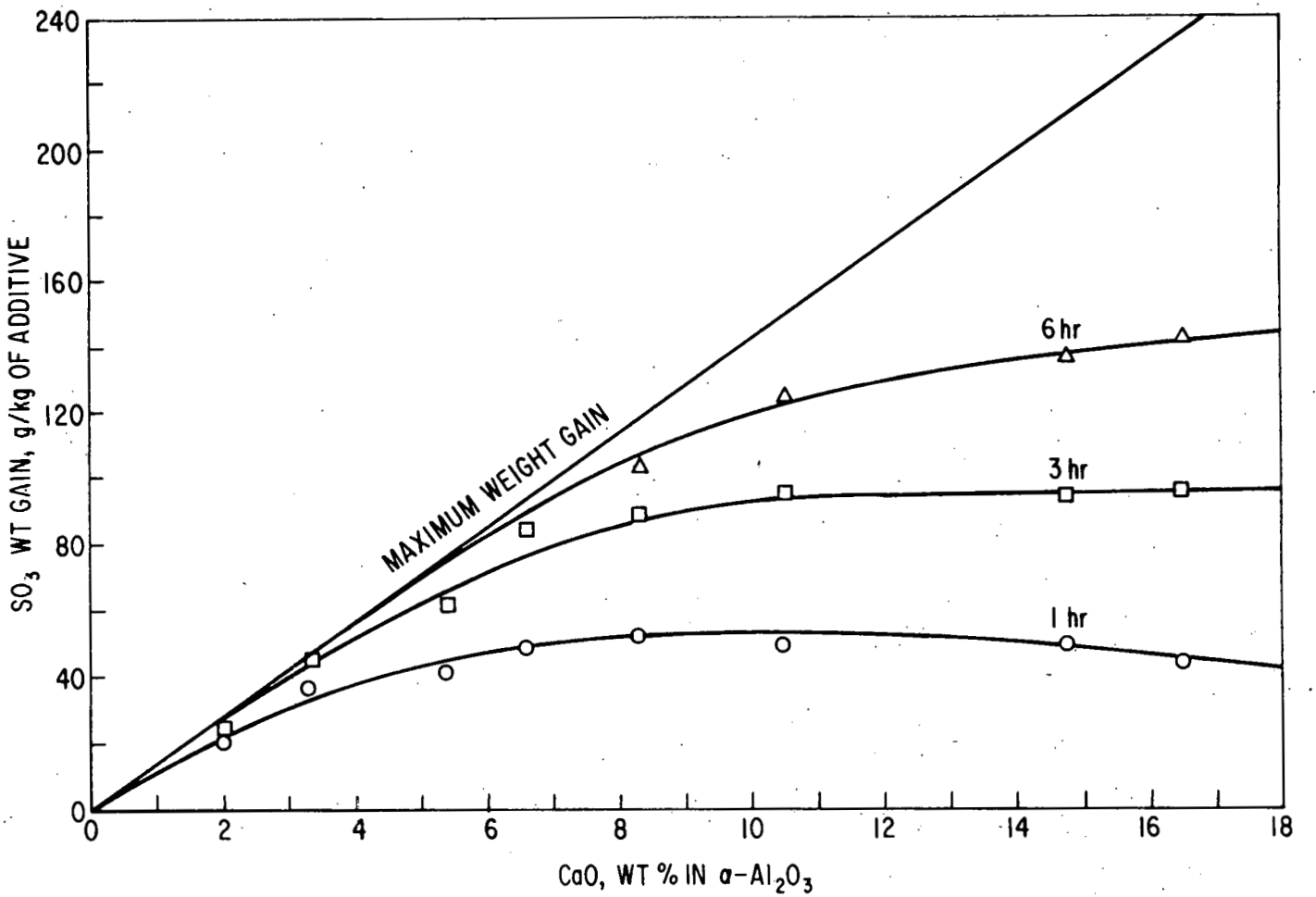

Fig. 13. Sorbent Weight Gain as a Function of Calcium Loading of Sorbent.

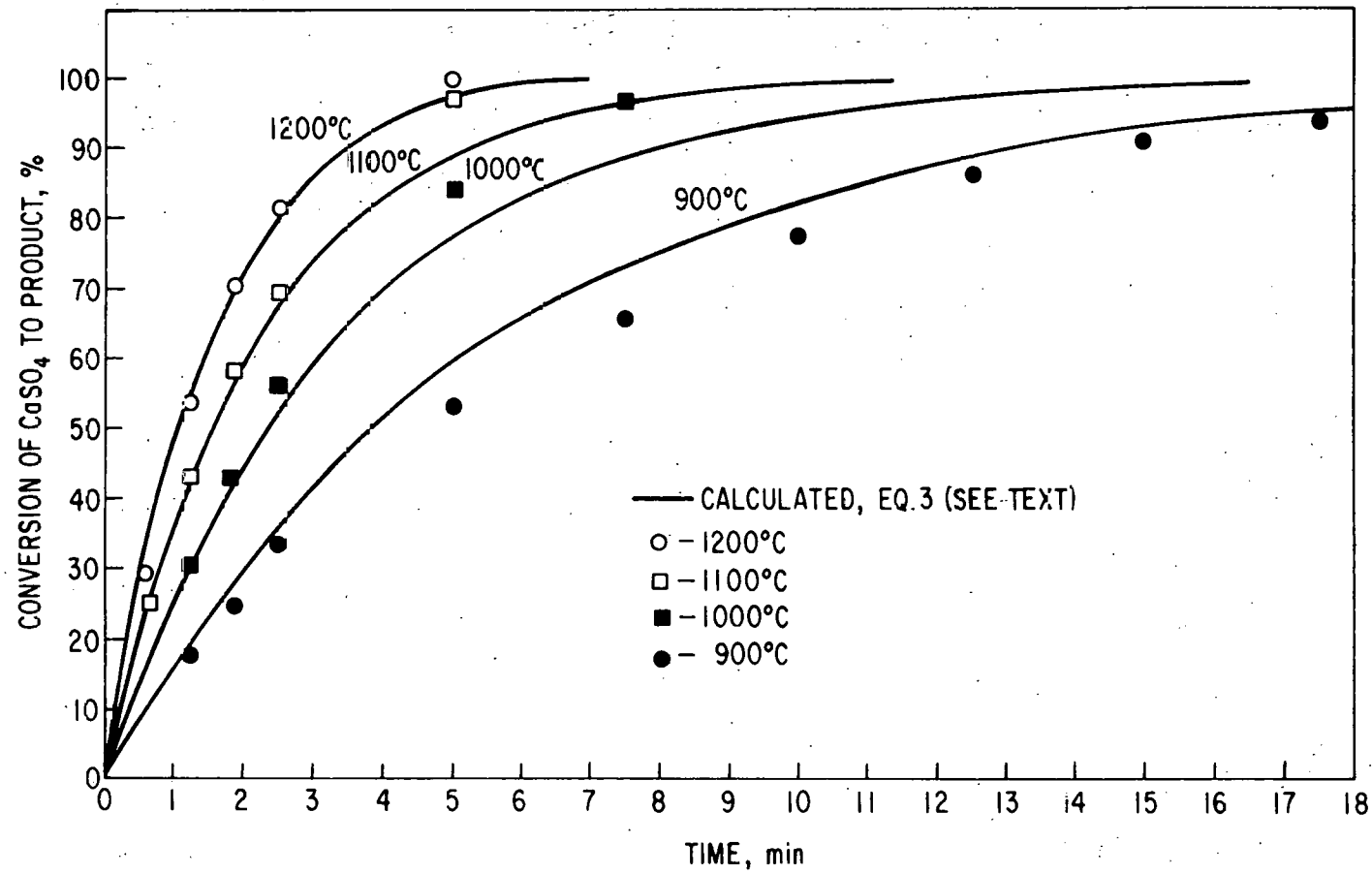

Fig. 14. Regeneration of Sulfated 6.6% CaO-α-Al_2O_3 Pellets Using 1% H_2-N_2

where $[CaSO_4]$ = $CaSO_4$ conc, moles/m^2
$[R.G.]$ = reducing gas conc, moles/m^3
t = time, sec
E_a = activation energy, cal/mole
T = temperatue, °K
R = gas constant
x, y, k = constants

A linear dependence of the log of the experimental regeneration rate as a function of 1/T, [R.G.], and $[CaSO_4]$ was found. Therefore, E_a, k, x, and y could be determined. The results are shown below for each reducing gas:

$$\frac{d[CaSO_4]}{dt} = -3.36 \begin{matrix} H_2 \\ \text{or} \\ CH_4 \end{matrix}^{0.8} [CaSO_4]\exp(-14{,}900/RT \qquad (4)$$

$$\frac{d[CaSO_4]}{dt} = -1.08\,[CO]^{0.8}\,[CaSO_4]\exp(-14{,}900/RT) \qquad (5)$$

The order of the reaction with respect to the reducing concentration is 0.8 for all reducing gases; however, the regeneration rate is three times lower for CO compared to H_2 or CH_4. The activation energy was determined from the experimental data for hydrogen presented above; the activation energy for CO was assumed to be the same. Figures 14, 15, and 16 give a comparison of the experimental and calculated (Eq. 3, 4, and 5) results. (Earlier versions of Fig. 15 and 16 were presented in Reference 6.) The agreement of the experimental and calculated results is good for the regeneration rate as a function of temperature and hydrogen concentration (shown in Figs. 14 and 15, respectively). It should be noted that the activation energy was found to be independent of the product formed. Figure 16 presents the regeneration rate as a function of CO concentration; agreement of experimental and theoretical results was poor only at the lowest CO concentration of 0.1%.

Cyclic Sulfation-Regeneration Studies Using 1100°C H.T. Pellets

The sulfation rate of 800°C H.T. pellets* under cyclic sulfation-regeneration operation was reported earlier.[6] The data showed that the sulfation rate for the second cycle was much lower than for the first cycle. It was speculated that this was due to the formation of different calcium aluminates during regeneration at 1100°C ($3CaO\cdot5Al_2O_3$ and $CaO\cdot6Al_2O_3$ form at 800°C, whereas $CaO\cdot Al_2O_3$ and $CaO\cdot2Al_2O_3$ form at 1100°C). Therefore, in the current work pellets containing 6.6% CaO were heat-treated at 1100°C before undergoing five sulfation-regeneration cycles.

As shown in Fig. 17, the rate of sulfation of the pellets was the same for the five cycles (100% sulfation in each cycle was assumed). In Table 9 the percent calcium utilization during sulfation and percent conversion of $CaSO_4$ in α-Al_2O_3 to CaO during regeneration are given. Based on the assumption that the pellets contain 6.64% CaO, calcium utilization was greater than 96%.

* The final step in impregnating the pellets with calcium oxide is heat-treating the sorbent at a proper temperature to form stable calcium aluminates that react with SO_2 and can be re-formed during regeneration.

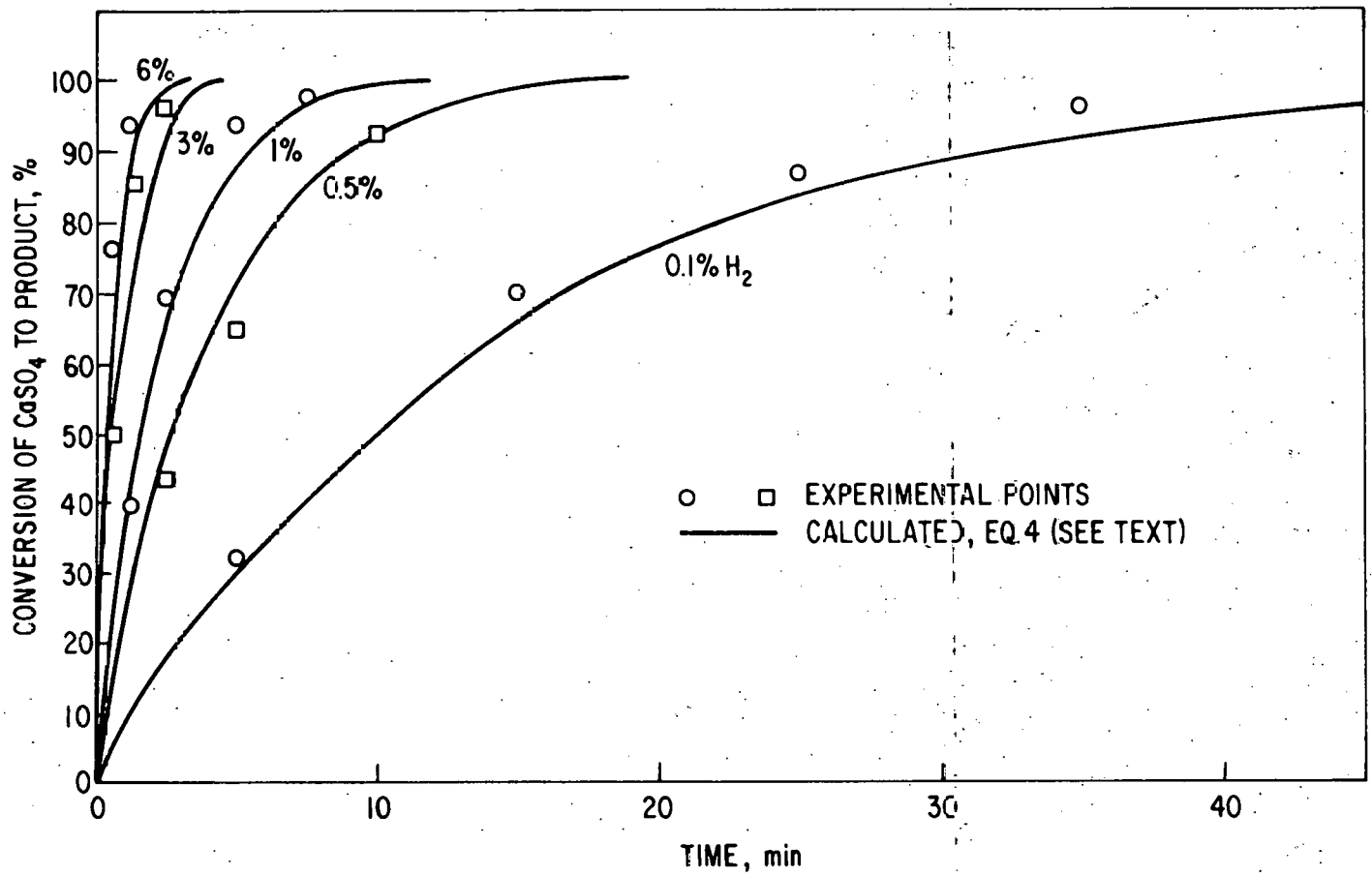

Fig. 15. Regeneration of Sulfated 6.6% CaO-α-Al_2O_3 Pellets Using Hydrogen at 1100°C.

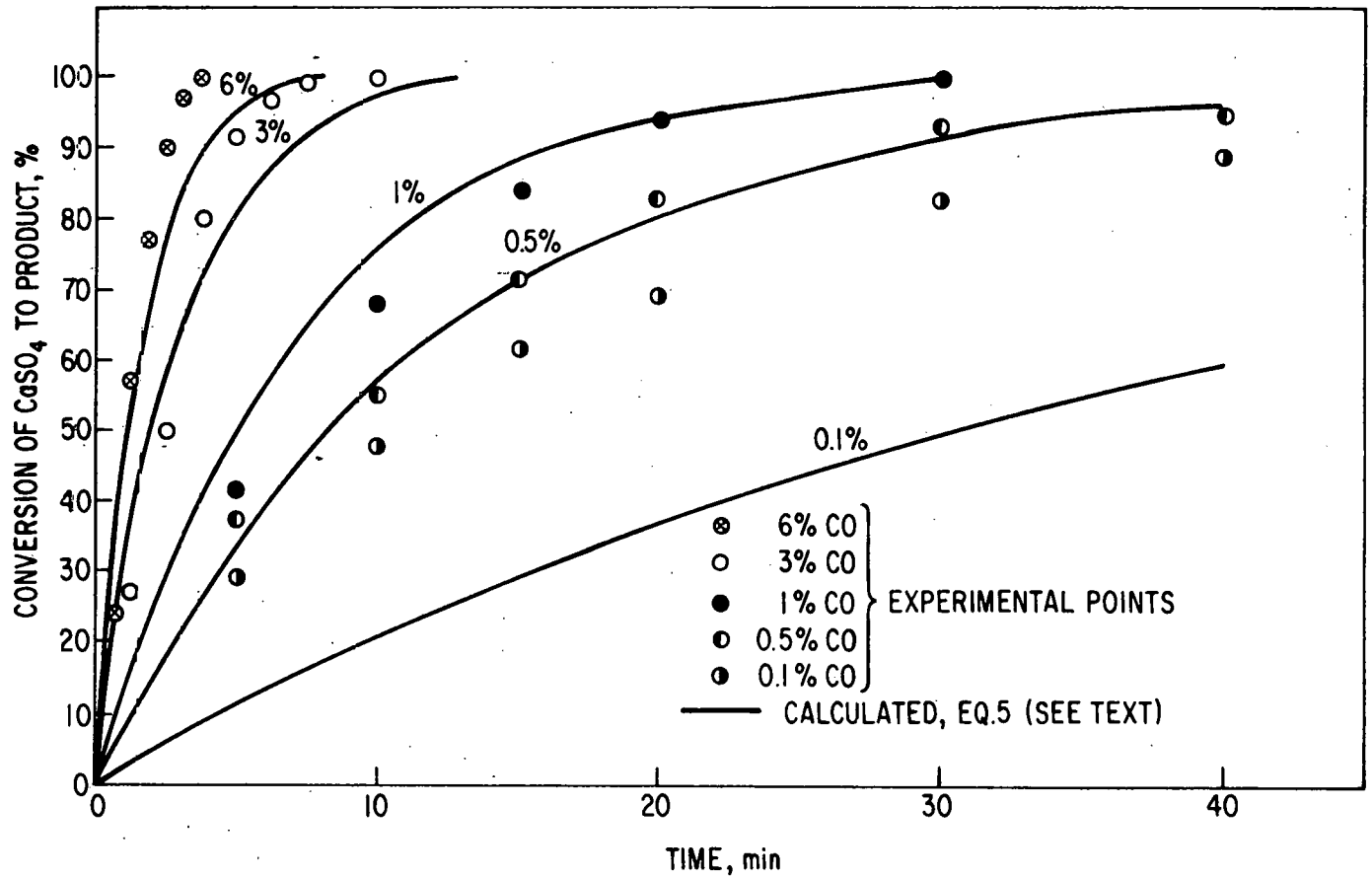

Fig. 16. Regeneration of Sulfated 6.6% CaO-α-Al_2O_3 Pellets, Using Carbon Monoxide at 1100°C.

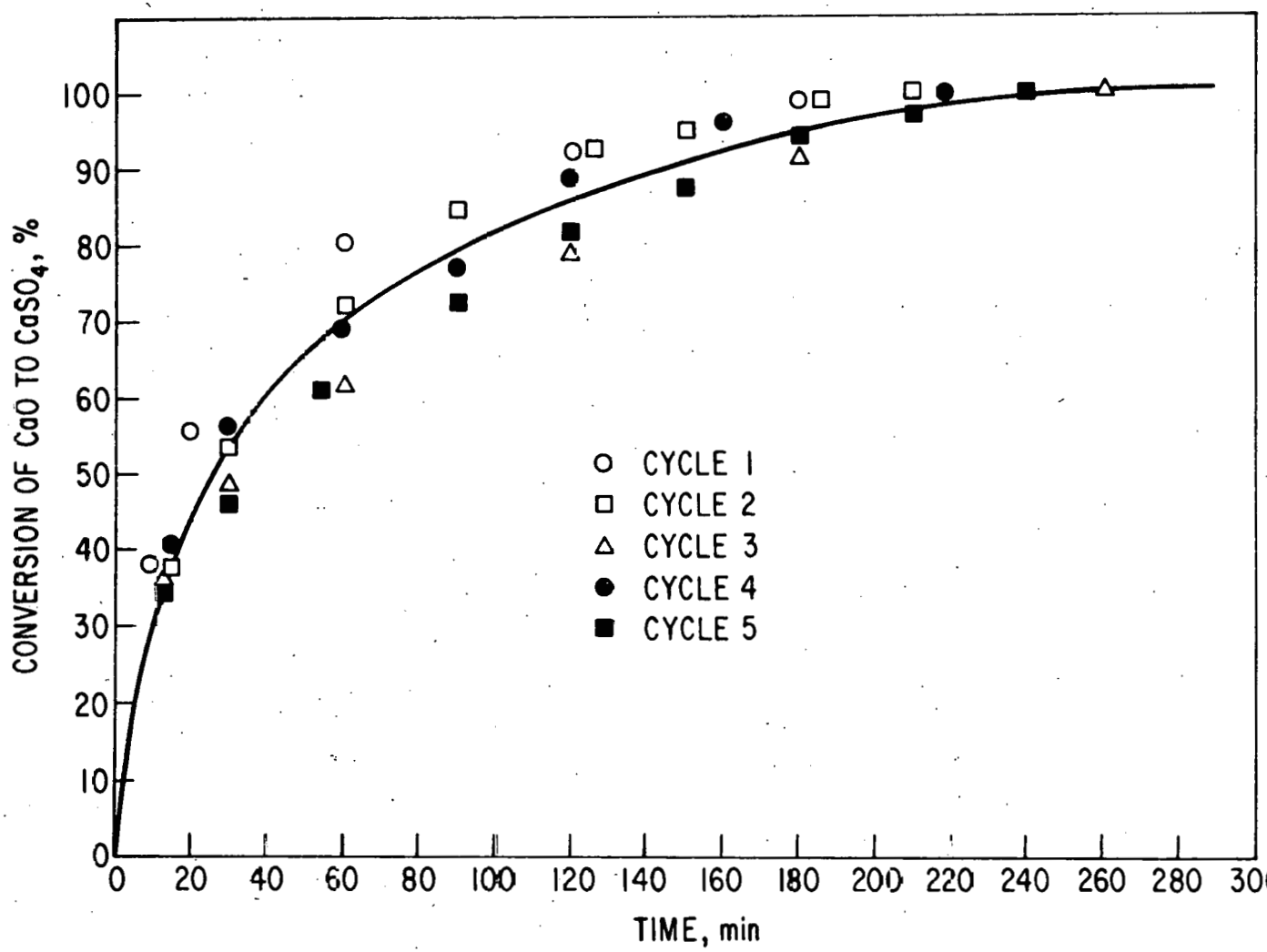

Fig. 17. Cyclic Sulfation of 1100°C Heat-Treated Pellets Using 3% SO_2 - 5% O_2-N_2 at 900°C.

Table 9. Calcium Utilization and Regeneration during Sulfation-Regeneration Cyclic Experiments Using 1100°C H.T. Pellets

Cycle	Sulfation(%)	Regeneration(%)
1	--	--
2	97	97
3	98	97
4	98	99
5	97	96

A minimum of approximately 50 cycles is probably needed to determine if any structural degradation will occur due to the phase changes occurring because of the internal chemical reactions. The purpose of this cyclic test was to show that reproducible and predictable sulfation rates could be obtained when the synthetic additive was heat-treated at 1100°C. This reproducibility, not found for the 800°C heat-treated sorbent, was found for the 1100°C heat-treated sorbent.

SULFUR EMISSION CONTROL CHEMISTRY

Petrographic Changes Occurring in the Half-Calcination of Dolomite No. 1337

The half-calcination process of dolomite involves the reaction:

$$\underset{\text{dolomite}}{CaCO_3 \cdot MgCO_3} + \text{heat} \rightarrow \underset{\text{calcite}}{CaCO_3} + MgO + CO_2 \qquad (1)$$

Rock particles of dolomite, when heated under a partial CO_2 pressure, are transformed into particles containing microscopic crystals of calcite and submicron crystals of MgO. These half-calcined particles may be used for the sorptive removal of SO_2 in coal-fired furnaces.

In order to study the nature of the changes which occur during the half-calcination process, dolomite No. 1337 samples were heated under various conditions in a TGA to yield a series of samples containing various amounts of calcite. The TGA results are summarized in Table 10. Polished sections of the treated samples were examined in reflected polarized light and compared with those of untreated dolomite.

Table 10. Half-Calcination Experiments on Dolomite No. 1337

Sample No.	Treatment	% Calcite Conversion[a] (from TGA results)
HII-32A	100% CO_2, 640°C, 60 hr	50
HII-36A	100% CO , 640°C, 120 hr	75
BRH WIW-2	40% CO_2, 800°C 0.3 hr	100
HII-37A	40% CO_2, 800°C 6 hr	100
HII-37B	40% CO_2, 800°C 26 hr	100

[a]Untreated dolomite = 0%; all dolomite converted to calcite = 100%

Untreated Dolomite. Crystals in any one particle are equigranular and coarse-grained, but the average size varies between 0.04 and 0.3 mm. Grain boundaries are sharp and optical extinction is uniform across each grain. Occasionally, a grain may contain small well-defined occluded grains in different crystal orientation.

HII-32A. Dolomite grain boundaries become slightly diffuse, and the extinction across grains is interrupted by patchy inclusions of irregularly shaped grains in different crystallographic orientation from the surrounding grains. The section is then mildly etched with 0.02N HCl for five seconds. This treatment serves to distinguish calcite from dolomite; dolomite surfaces are unaffected, but calcite surfaces become etched. A comparison of the section before and after etching shows that the onset of calcite formation occurs both along dolomite grain boundaries and within the dolomite grains as patchy areas. There is an excellent correlation in the shapes of the etched areas with those of patchy inclusions observed in polarized light on the unetched

section. Calcite growth may begin from the edge of dolomite grain inward but may also begin within a grain.

HII-36A. This sample, heat treated for 60 hr longer than the previous sample, shows all of the above effects but to a greater degree. Original dolomite grain boundaries are still present but are more diffuse. An etched section under the microscope appears to be 75% converted to calcite, in agreement with the TGA results. MgO is too fine-grained to be visible in reflected light.

BRH-WIW-2. Calcite crystals have grown to 5 μm in diameter and form a mosaic-like texture. Some preferred orientation is present; the direction of the dominant component changes from one area to another. These well-defined areas correspond dimensionally to the grain outlines of the original dolomite crystals, even though each dolomite grain has been completely transformed to many calcite crystallites which assume some unknown, but preferred, orientation from the original dolomite grain. This preferred orientation was also observed in X-ray powder patterns.

As noted above, MgO is too fine-grained to be seen in polished section, but its distribution could materially have an effect on subsequent sulfation reactions since it is more resistant to sulfation than is CaO or $CaCO_3$. It was found, however, by some preliminary SEM studies on this sample, that MgO is uniformly distributed throughout the half-calcined particles. It does not migrate or form at grain boundaries of calcite or at relic grain boundaries of dolomite but is occluded in the calcite structure. These SEM results suggest that MgO will not adversely affect subsequent sulfation reactions.

HII-37A. This sample, like the former, has been completely recrystallized into calcite, but, unlike the previous sample, relic dolomite grain boundaries have been completely obscured by recrystallization into randomly oriented calcite crystals which have an average diameter of 20 μm. The X-ray results confirm this loss in preferred orientation.

HII-37B. The 20 hr additional treatment has had no major effect except that there is a slight indication of enhanced calcite crystal growth.

The examination of the above samples by petrographic methods has yielded some significant results. It has been shown that dolomite crystals are transformed to calcite along grain boundaries, as well as within dolomite crystals. This suggests that greater efficiencies in the half-calcination process may be achieved by selecting finer-grained starting material from the quarry, if this is practical. The results also suggest that since sulfation is a surface-controlled process, partially transformed half-calcined samples might be more readily sulfated along avenues of fine-grained calcite than through a tight interlocking network of larger calcite crystals in completely transformed samples such as HII-37A or HII-37B. The validity of this suggestion will be tested by experiment.

Regeneration by the $CaSO_4$-CaS Reaction

Initial results from the study of the solid-solid reaction

$$3[CaSO_4 \cdot MgO] + [CaS \cdot MgO] \rightarrow 4[CaO \cdot MgO] + 4SO_2 \qquad (2)$$

given in prior reports,[1,6] indicated that reaction 2 is a potentially feasible candidate as a regeneration scheme. Starting material for reaction 2 in these studies was prepared by partial reduction of sulfated dolomite No. 1337. TGA and X-ray diffraction analyses of the composition of sulfated and partially reduced stones (starting material for reaction 2) were shown to be essentially in agreement. This suggested that the progress of reaction 2 can be monitored by both of these techniques during kinetic experiments.

In this report, results of the first kinetic experiments of reaction 2, where the starting material is prepared by partial reduction of sulfated dolomite, are presented. In addition, preliminary results are presented on a second method of carrying out reaction 2, *i.e.*, by performing the solid-solid and reduction reactions simultaneously.

Solid-Solid Reaction Kinetics (Partially Reduced Starting Material). The experimental procedure followed was similar to that used in the earlier study. A large stock supply of sulfated dolomite No. 1337 was prepared by half-calcining the stone and subsequently sulfating at 750°C in a 4% SO_2-5% O_2 simulated flue gas mixture until the weight gain process halted. The percentage of sulfation achieved was determined by performing a reduction experiment on an aliquot of the sulfated stones at 880°C with a 3% H_2 in He mixture. A stock supply of partially reduced stones for use in the kinetic experiments was prepared by a reduction reaction at 880°C, using a 3% H_2 in He mixture. This material was used in all kinetic experiments performed at 945°C under 1-atm partial pressure of helium flowing at a rate of 300 cc/min to remove the SO_2 formed. Each kinetic experiment was performed by placing the starting material in the TGA apparatus, which was at 945°C with the helium purge flowing, and monitoring the weight change process until the experiment was halted. Kinetic runs were performed for reaction times of 1/4, 1/2, 1, 2, 5 1/2, and 18 hr. X-ray diffraction analyses were obtained on aliquots of 30 to 50 stones from material sampled at the end of each kinetic experiment.

The results of these experiments are summariezed in Table 11. The first column identifies the experiment, and the second column gives the sample history. Columns three through seven list the results based on analysis of TGA measurements. The third column lists the percentages of the available material in the sample that have been converted as the result of the history of the samples. The fourth through sixth columns give the composition of the samples as percentages of "maximum weights possible" of CaO, $CaSO_4$, and CaS, respectively ("maximum weight possible" refers to the weight if all the calcium were present as a pure species, *e.g.*, in column 4, the pure substance would be CaO, with no calcium existing in the form of sulfate or sulfide). The seventh column lists calcium species material balances as total percentages of calcium species existing in the stones. The X-ray diffraction results are given in the eighth through eleventh columns, with columns eight through ten listing the percentages of maximum weights possible of CaO, $CaSO_4$, and CaS, respectively, and the last column giving the material balances for the calcium species.

From Table 11, it is apparent that for each experiment, extremely good agreement exists for TGA and X-ray analyses of CaO and $CaSO_4$ concentrations in the material (columns 4 and 8, and columns 5 and 9, respectively). The values are in good agreement, and values from both techniques show a similar

Table 11. Results of $CaSO_4$-CaS Reaction Kinetic Measurements at 945°C where Starting Material was Prepared by Partial Reduction of Sulfated Dolomite

Expt. No.	Sample History	Stone Composition - TGA Results: % Available Material Converted	% Maximum Weight Possible of CaO	% Maximum Weight Possible of $CaSO_4$	% Maximum Weight Possible of CaS	Σ % Ca Species	Stone Composition - X-Ray Results: % Maximum Weight Possible of CaO	% Maximum Weight Possible of $CaSO_4$	% Maximum Weight Possible of CaS	Σ % Ca Species
I	Sulfated 1337 Dolomite	91% of $CaCO_3$ Sulfated	16	84	0	100	17	90	0	107
II	Partially Reduced Stones t = 0	36% of $CaSO_4$ Reduced	16	53	31	100	23	60	20	103
III	0.25 hr Reaction	20% of $CaSO_4$ Converted to CaO	30	43	27	100	29	49	16	94
IV	0.50 hr Reaction	26% of $CaSO_4$ Converted to CaO	34	40	26	100	29	47	8	84
V	1.0 hr Reaction	29% of $CaSO_4$ Converted to CaO	36	38	26	100	31	46	10	87
VI	2.0 hr Reaction	32% of $CaSO_4$ Converted to CaO	38	37	25	100	27	50	7	84
VII	5.5 hr Reaction	40% of $CaSO_4$ Converted to CaO	45	32	23	100	35	38	5	78
VIII	18.0 hr Reaction	38% of $CaSO_4$ Converted to CaO	43	33	24	100	46	30	7	83

trend of change as the reaction proceeds. Similarly to the earlier reported results, the results of the two techniques for the amount of CaS do not agree as well as for the CaO and $CaSO_4$. However, there is agreement for the trend of change as the reaction proceeds.

The chemical kinetics of this reaction are summarized in Fig. 18, where the percentage of CaO in the stones is plotted against reaction time. The percentage of CaO values in this figure are each an average of the values from the TGA and X-ray analyses as listed in Table 11. The CaO content of the stones increased from 20% to 45%. Therefore, the yield of the reaction (amount of CaO formed as a result of reaction) is not as great as that obtained in some earlier reported experiments, where it was shown that yield is dependent on the composition of the starting material. Kinetic experiments are planned in which the composition of the starting material will be varied. The point to be emphasized is that the rate of the solid-solid reaction is surprisingly high, that is, the CaO content increases from 20% to 40% in less than six hours or, stated in another manner, the reaction has reached 80% completion in less than six hours. Such a reaction rate is comparable to sulfation reaction rates where the SO_2 concentration in the simulated flue gas is low.

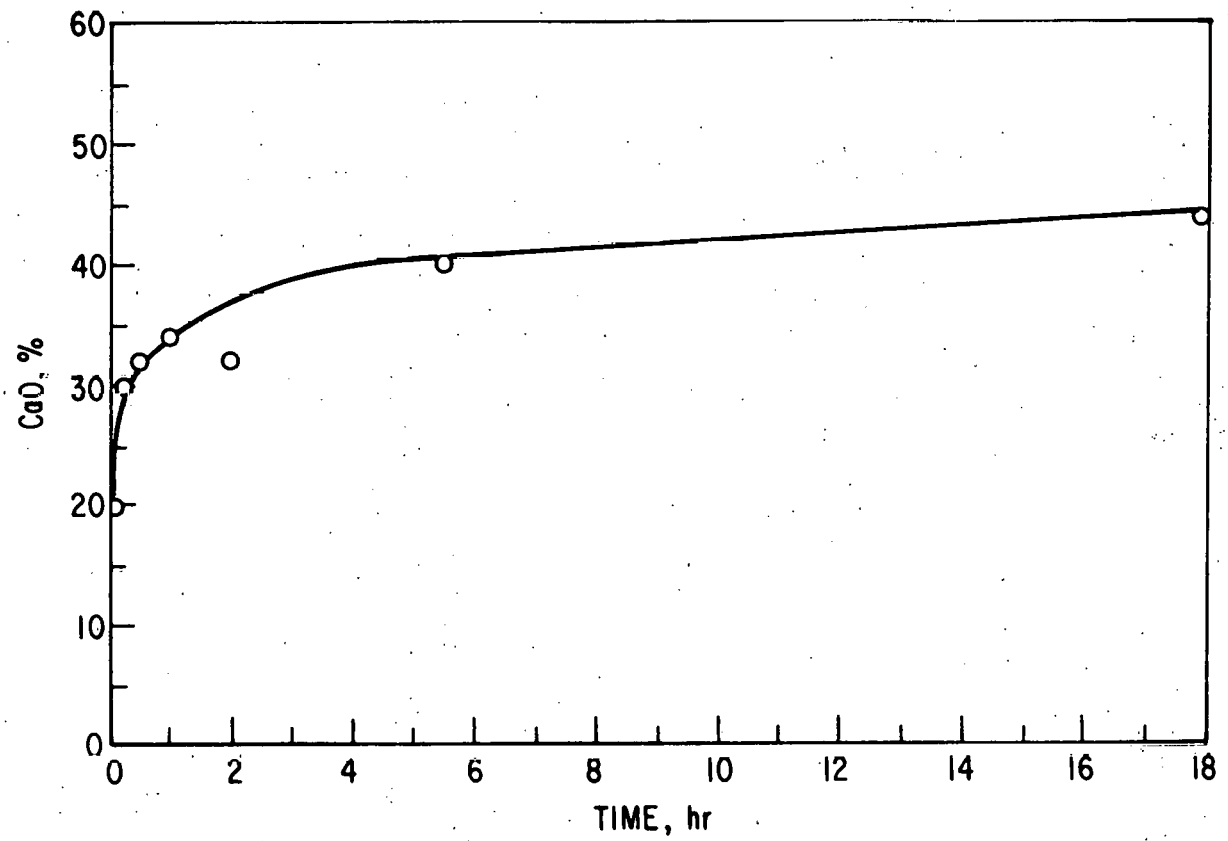

Fig. 18. CaO Content as a Function of Reaction Time.

Solid-Solid Reaction--Simultaneous Reduction Reaction. Three methods may be considered for the study of reaction 2:

(1) The sulfated material can be reduced to the proper starting mole ratio of $3CaSO_4/CaS$ (two-step process), as previously reported.

(2) The sulfated material can be reduced while the $CaSO_4$-CaS reaction is proceeding simultaneously. This method requires the ability to control the conditions for the reduction reaction so that its rate is in balance with the $CaSO_4$-CaS reaction (one-step process).

(3) CaS can be added directly to the sulfated material to obtain the proper stoichiometry for the starting material (two-step process).

Preliminary results are reported here on method 2.

The experimental procedure was as follows: An aliquot of the stock supply of sulfated dolomite No. 1337, described earlier as sample I in Table 11, was placed in the TGA, which was at 950°C and under helium flow, for stabilization. Following this, the flow of H_2 in He gas mixture was started and the weight change was monitored. The composition of the stones at the end of the experiment was determined by X-ray diffraction analysis of aliquots of 30 to 50 stones.

The results of initial experiments indicated that both reactions were occurring simultaneously when a reducing gas mixture containing less than 1% H_2 was used. However, reducing gas mixtures with higher concentrations of hydrogen resulted primarily in the formation of CaS, *i.e.*, the reduction reaction was the dominant process. Yields of CaO as high as 80% (or approximately a 60% increase in CaO content) were obtained in these initial experiments. Therefore, it can be concluded that method 2 is at the least as attractive as method 1 from the stand-point of potential technical application. In addition, it is believed that method 2 offers a means by which information on the reaction mechanism(s) of reaction 2 might be obtained.

Table 12 lists the results of additional recent method 2 experiments, which were performed after calibration of the rotameters used to blend the hydrogen in helium gas mixtures. All experiments were performed at 950°C and were allowed to go to completion. The first column in Table 12 lists the experiment number; the second column, the reducing gas composition; the third, the reducing gas flow rate; and the fourth, the reaction time until the weight ceased to change. Columns five, six, and seven list the stone compositions at the end of the experiments as percentages of maximum weights possible for CaO, $CaSO_4$, and CaS, respectively. The last column lists calcium species material balances as total percentages of calcium species existing in the stones.

These data confirm the results of the initial experiments in illustrating that both reactions occur simultaneously. High yields of CaO are again evident (as large as approximately a 45% increase in CaO content). The reactions proceed until all $CaSO_4$ is consumed. Yields of CaO are similar when 0.10% H_2 or 10% CO is used as a reducing gas.

A number of points related to these results are surprising and difficult to explain. For example, in contrast to the initial experiments, these results suggest that CaO was formed at hydrogen concentrations as high as 2%. In addition, it is difficult to establish a firm relationship between the yield of CaO and the concentration of hydrogen used as a reducing gas. In general it can be stated that the highest CaO yields are associated with the lower hydrogen concentrations. However, Table 12 shows no obvious smooth correlation. Figure 19 is a plot of CaO yield *vs.* logarithm of the hydrogen concentration (moles/cm^3) and might be interpreted to suggest a logarithmic

Table 12. $CaSO_4$-CaS Reaction--Simultaneous Reduction Reaction Experiments

Expt. No.	Reducing Gas Composition	Reducing Gas Flow Rate (cm^3/min)	Reaction Time (hr)	Stone Composition - X-Ray Diffraction Results: % Maximum Weight Possible of CaO	% Maximum Weight Possible of $CaSO_4$	% Maximum Weight Possible of CaS	Σ % Ca Species
I[a]	0	0	0	17	90	0	107
IX	2.0% H_2 in He	300	ca. 2/3	33	0	40	73
X	1.1% H_2 in He	300	ca. 1	29	0	51	80
XI	0.58% H_2 in He	300	ca. 3	32	0	51	83
XII	0.10% H_2 in He	300	ca. 4	49	0	38	87
XIII	0.10% CO in N_2	300	ca. 12	49	0	25	87
XIV	0.04% H_2 in He	300	ca. 7	50	0	23	73
XV	0.01% H_2 in He	300	ca. 21	61	0	17	78
XVI	0.006% H_2 in He	600	ca. 20	54	0	20	74

[a]Starting material for other experiments described in this table.

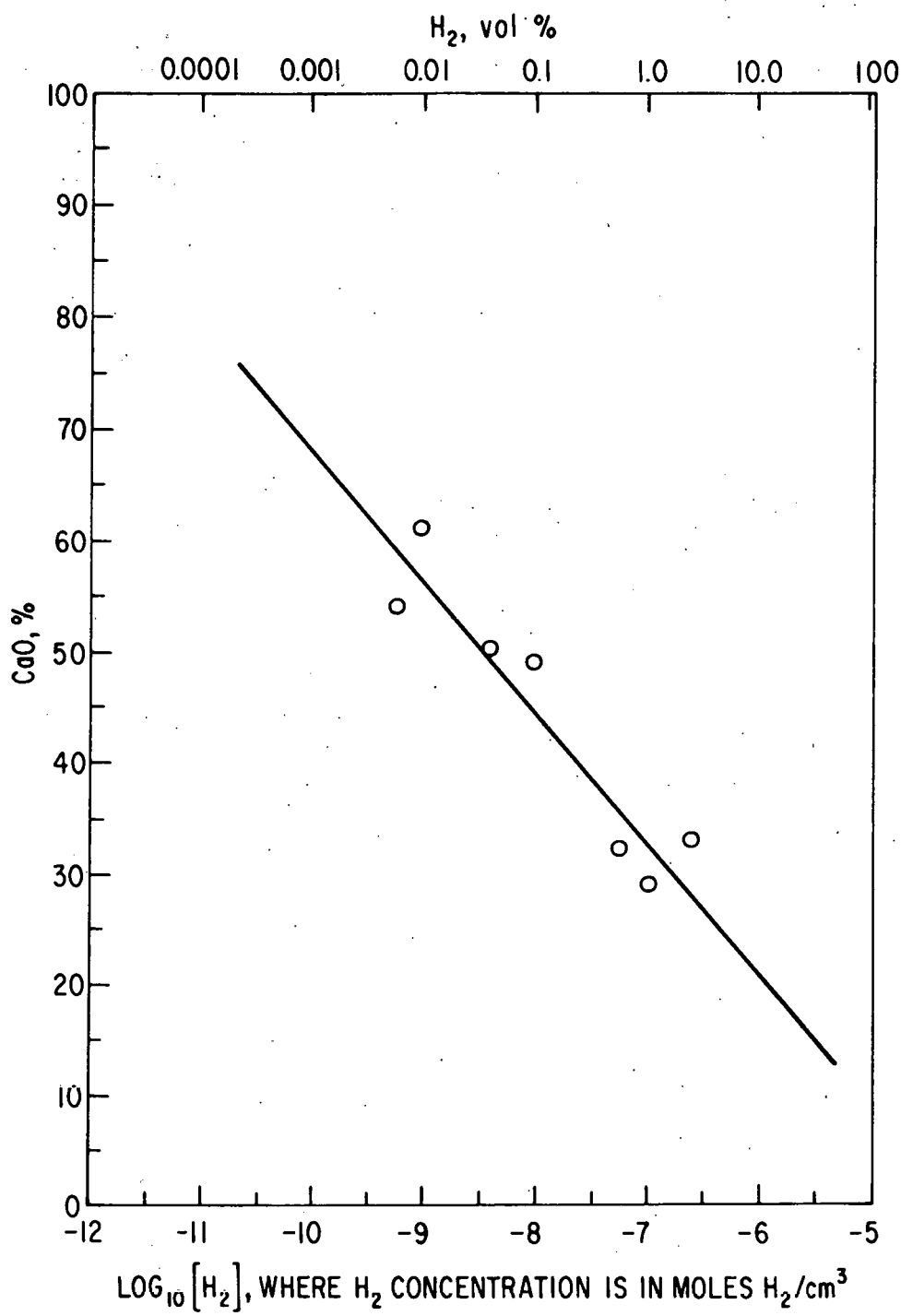

Fig. 19. CaO Content as a Function of Logarithm of Hydrogen Concentration.

relationship. This interpretation is not being made, however, until the results of more experiments become available. These data should be considered preliminary until more experimental data can be obtained.

Further studies are planned to (a) determine if these results are reproducible, (b) perform experiments at 950°C over a wider reducing gas concentration range, and (c) perform simultaneous experiments as a function of reaction temperature. These studies are intended to provide information on questions not answered by the preliminary results reported herein, as well as information on the reaction mechanisms involved.

Reaction of Calcium Sulfate with Calcium Sulfide, Vacuum Roasting

Additional work is being done to determine if the solid-solid reaction, $3CaSO_4 + CaS \rightarrow 4CaO + 4SO_2$, is feasible as a regeneration scheme.

Previous experiments (CAS-1 through CAS-16) tested the extent of the desulfurization of sulfated dolomite under various conditions, using a nitrogen purge stream to remove the SO_2 product. In the most recent investigations, the SO_2 product was removed by vacuum pumping. In two experiments (CAS-17 and CAS-19), fully calcined sulfated dolomite particles (from the VAR-3 combustion experiment performed previously in the ANL 6-in.-dia, fluidized-bed combustor) were reacted with a stoichiometric excess of CaS at 1000°C.

In each experiment, ∿90 g of sulfated dolomite (∿52% $CaSO_4$) and ∿23 g of CaS were mixed and then placed in a boat inside a quartz tube reactor, which was evacuated and then heated to 1000°C. During CAS-17, the initial "vacuum-roasting" experiment, the pressure inside the reactor was allowed to increase to ∿650 torr, and the reactor was then evacuated; there were a total of four pressure buildup and expansion cycles. In the other experiment (CAS-19), the heated reactor was continuously evacuated.

Samples from the two experiments have been submitted for wet chemical analysis to determine the degree of $CaSO_4$ decomposition. An approximation of the extent of reaction, however, can be obtained on the basis of weight-loss data. Table 13 lists the reactants, the raction time and conditions, the weight loss, and an estimate of the SO_2 production and reaction completeness based on weight loss for CAS-17 and CAS-19. To allow comparison, the same parameters are listed for CAS-12, the experiment in which SO_2 was most successfully removed using a nitrogen purge.

Wet-chemical analytical results should provide more definitive information on the extent of regeneration. However, the extent and rate of the reaction may be higher with the vacuum-roasting technique than with the nitrogen purge approach.

Table 13. Reaction of Calcium Sulfate with Calcium Sulfide in Experiments CAS-12, -17, and -19

Reaction Temperature: 1000°C

Exp. No.	Reactants	SO_2 Removal Method	Duration of Reaction, hr	Reactant Wt Loss,[a] g	Based on Wt Loss: SO_2 Produced, millimole	Based on Wt Loss: Reaction Completeness, %
CAS-12	fully calcined sulfated dolomite (89.2 g from VAR-7) (35% $CaSO_4$) and CaS (23.2 g)	N_2 purge	43[b]	18.6	301	88
CAS-17	same as above, except dolomite from VAR-3 (52% $CaSO_4$)	Vacuum pumping, intermittent	2.6	5.3	83	16.7
CAS-19	same as CAS-17	Vacuum pumping, continuous	5	17.5	292	58.6

[a]Weight loss due to elemental sulfur production was found in all cases to be less than 0.4 g.

[b]In 7-hr intervals - not continuous heating.

COAL COMBUSTION REACTIONS

The Determination of Inorganic Constituents in the Effluent Gas from Coal Combustion

Some chemical elements carried by combustion gas are known to cause severe metal corrosion. The objective of this study is to determine quantitatively which elements are present in the hot combustion gas of coal, either in volatile or particulate form, and to differentiate between volatile and particulate species. Identification of the compound form and amount of particulate species and determination of the amount and the form of condensable species are desirable.

The design/preliminary safety review of the laboratory-scale batch fixed-bed combustor was held. The conceptual design of the combustor was presented in a previous report.[1] The purpose of this review was to determine if the design of the fixed-bed combustor will meet safety requirements. At the review meeting, the preliminary detailed design and engineering drawings of the combustor, specifications for fabrication of the combustor, and stress calculations for supporting the safety consideration of the design were presented.

Several constructive recommendations pertaining to design and operational safety were made by the design/preliminary safety review committee. Based on these recommendations, the design has been revised slightly as described in the following sections. Also, information about the maximum allowable stress for 310 stainless steel[7] has been applied to further evaluation of the safety of this design. These data show that the maximum allowable stress for 310 SS at 900°C (1650°F) is at least 400 psi. The value is double the stress value obtained from extrapolation of the stress data given in the ASME Boiler and Pressure Vessel Code and on which the design of this combustor was originally based.

The thermal stresses from heating and from axial thermal gradients at both the intersection of the preheating and combustion sections and the intersection of the filtration and cold trap sections have been considered. The possibility of thermal stresses at both intersections has been removed by the following revisions of the design:

1. At the preheating section, the cooling coils have been entirely removed. Instead, a 1/8-in.-thick Fiberfrax insulation layer will be inserted between the internal heater and the inner wall of the pipe. This insulation layer will decrease heat flow radially. Heat transfer calculations indicate that the wall temperature of the pipe at this section will be only about 260°C (500°F) and that the temperature difference between the inner wall and the outer wall will be about 28°C (50°F). The thermal stresses due to this thermal gradient have been computed and are shown to be insignificant when compared with the maximum allowable stress of the material at that temperature. In addition, since no restraint to thermal expansion is imposed on the pipe at this section, no thermal stresses due to axial thermal gradients are expected.

2. At the cold trap section, the number of turns of cooling coils has been reduced; therefore, there is an $\sim$ 7-in. transitional section between the end of the hot filtration zone and the point where the cooling coils start. Heat transfer calculations show that the

average wall temperature at the point where the cooling coils start will be about 150°C (300°F). The 310 stainless steel is strong enough at this temperature to withstand the thermal stresses caused by a thermal gradient at the wall as large as 50°C (90°F). The thermal gradient will not reach 50°C at this section of the pipe.

3. Two more metal supports have been added to hold both ends of the combustor where heavier loads are located. There are a total of five mechanical supports along this 6 1/2-ft-long combustor. Because there is a rather short span between supports, the mechanical support stresses are negligible in comparison with other types of stresses. For example, the filtration section has the greatest span; therefore, the maximum flexural stress due to a bending moment is expected at this section. Stress calculations indicate that this maximum flexural stress is only in the order of a few pounds per square inch.

The flat head of the cold trap has been redesigned, in accordance with Paragraph UG-34, ASME Code,[8] to ensure good joints between the head and the shell. A working table on which the combustor will be rested has been so designed that the axis of the combustor body is tilted 5° downward towards the gas discharge end; and connections will be so oriented that water will drain out with minimum accumulation.

The design of the combustor has been considered to be adequately safe upon modification as recommended by the review committee.

Two furnaces used for heating the filtration section and alumina combustion boats have been received, as scheduled. The inclined table designed for the combustor has been constructed. Work on setting up water and electricity facilities is continuing. The induction heating unit and the furnaces will be tested as soon as these facilities are ready.

Systematic Study of the Volatility of Trace Elements in Coal

Knowledge of the vaporization characteristics of trace elements in coal and of the rate of their volatilization is important for combined-cycle turbine operation. The purpose of this study is to obtain data on the volatility of these elements under practical coal combustion conditions. This study is also intended to obtain data supporting "The Determination of Inorganic Constituents in the Effluent Gas from Coal Combustion" (above).

Several coals from different locations have been prepared for this volatility study. The proximate analyses of these coals are shown in Table 14. Their ASTM ranks (obtained from 1974 Keystone Coal Industry Manual) are also included.

The first series of preliminary experiments has been completed. The purpose of these experiments is to determine required experimental conditions, such as the ashing time and the range of the ashing temperature, in order to obtain desired volatility data. Some results are presented in this report.

In this series of experiments, ~3-g ash samples were heated in a tubular furnace to a temperature between 540°C and 990°C for 24 hr in an airflow of 0.6 scfh.

Table 14. Proximate Analyses of Coals Chosen for this Study

No.	Source of Coal	% H_2O	% Vol. Mate.	% Ash	% Fixed Carbon	ASTM rank[a]
1	Herrin (No. 6) Coal Montgomery County, Ill.	7.41	35.39	15.41	41.78	Hvcb
2	Herrin (No. 6) Coal Franklin County, Ill.	5.19	34.66	7.41	52.74	Hvcb
3	Harrisburg (No. 5) Coal Saline County, Ill.	4.15	34.41	7.82	53.62	Hvcb
4	Pittsburg Seam Coal Montour #10 Mine Allegheny County, Pa.	1.64	36.44	7.83	54.09	Hvab or Hvbb

[a]Obtained from "1974 Keystone Coal Industry Manual," published by Mining Informational Service, McGraw-Hill, New York.

In this series of experiments ∿3-g ash samples were heated in a tubular furnace to a temperature between 540°C and 990°C for 24 hr in an airflow of 0.6 scfh.

The samples were prepared by ashing -200 mesh Illinois Herrin No. 6 Montgomery County Coal in an airflow of 9 liters/min for 48 hr at an average temperature of 340°C in a muffle furnace. The samples were held in a high-purity (99.7%) recrystallized alumina combustion boat (1 7/8 x 1 7/16 in. x 5/8 in.) during heat treatment. The combustion boat was preheated to 1000°C for several hours before use.

The 340°C ash sample was chosen as a starting material, instead of coal, in this study for the following reasons: (1) when coal is rapidly heated to a high temperature, a violent combustion occurs, resulting in a mechanical loss of sample material. (2) for each experiment, a greater amount of ash residue can be obtained by the use of a 340°C ash sample as a starting material than by the use of coal. Most of the trace elements of interest in coal would remain in the ash obtained at 340°C.[9,10]

In each experiment, the sample was weighed before and after heating to determine the weight loss due to heating. This information is necessary for computing all elemental analyses on the same basis. The weight loss as a function of temperature is given in Table 15 and plotted in Fig. 20. These results clearly indicate that the weight loss increases with increasing heating temperature; the weight loss curve flattens at about 850°C. The weight loss is considered to be due to further oxidation of the residual carbon (5.61%C in 340°C ash), dehydration reactions, and the evolution of CO_2, SO_2, and SO_3, etc. as a result of the decomposition of carbonates and sulfates in the ash. The oxidation of pyrites, which constitute about 23% by weight of the mineral matter of Illinois coals, may also play a role in the weight loss during this period of heating.[10] The upturn of the curve at about 900°C indicates the start of a further weight loss due to the evolution of compounds which have appreciable vapor pressures in this temperature range, such as chlorides, sulfates,[11] and oxides.[12]

Table 15. Effect of Temperature on Weight Loss of 340°C Ash

Experimental Conditions: 0.6 scfh airflow and 24-hr heating time.

Heating Temperature (C°)	Wt of Sample (g)	Wt Loss as a Result of Heating (g)	Weight Loss (%)	Average Wt Loss (%)
542	2.9829	0.2863	9.60	9.62
	2.9963	0.2890	9.64	
640	3.0062	0.3972	13.21	13.22
	2.9961	0.3967	13.24	
740	3.0123	0.4344	14.42	14.34
	3.0380	0.4335	14.27	
340	3.0233	0.4524	14.96	14.91
	3.0179	0.4483	14.85	
940	3.0213	0.4544	15.04	15.13
	3.0124	0.4586	15.22	
990	3.0032	0.4775	15.90	15.91
	3.0007	0.4776	15.92	

[a]This ash was prepared from Illinois Herrin No. 6 coal from Montgomery County.

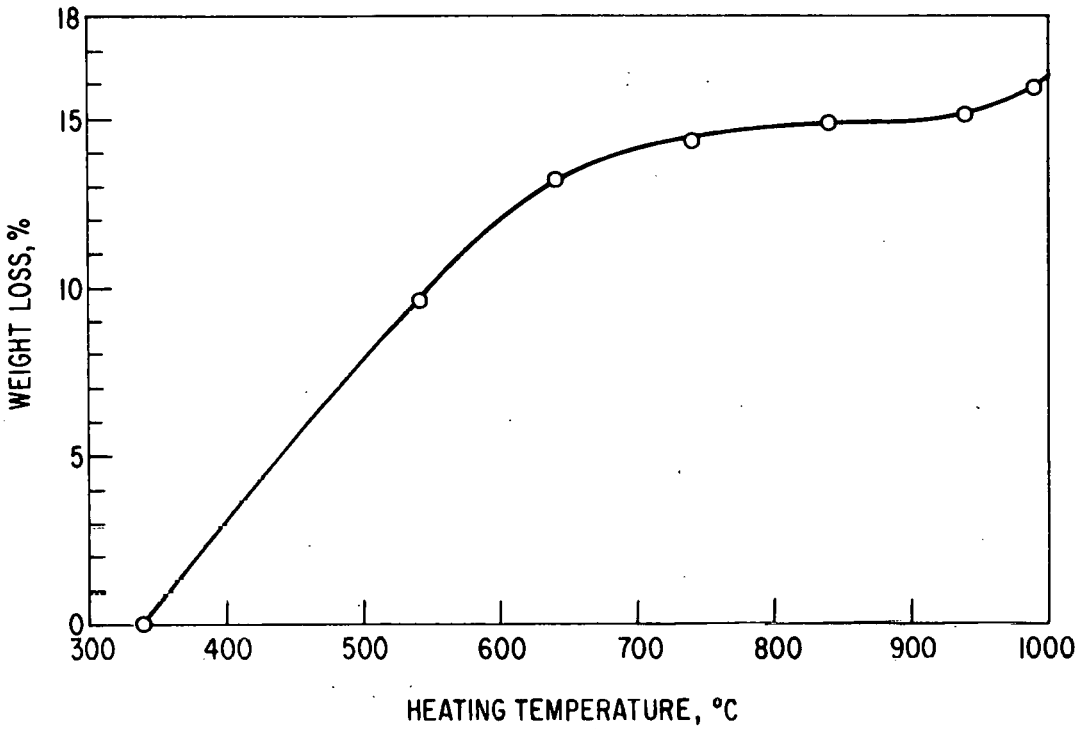

Fig. 20. Effect of Temperature on Weight Loss of 340°C Ash.

Coal Sample: Illinois Herrin No. 6 Coal from Montgomery County
Experimental Conditions: 0.6 scfh airflow; 24-hr heating time

In Table 16 are listed the observed elemental concentrations in residues corrected for the weight losses, *i.e.*, on the basis of the same initial sample weight of the 340°C ash. For the elements Al, Ni, and Mn, there is apparently an unreasonably large jump in concentration for samples obtained above 740°C. This may be related to the three samples heated to 340, 542, and 640°C being analyzed at the same time, and the other four samples (740, 840, 940, and 990°C samples) being analyzed at another time. The reason for the change in concentrations is not known. Further checking is required.

Within the limits of experimental and analytical errors, the results generally indicate that the elements being investigated, except probably Co and V, are retained in the ash up to 990°C. Previous workers[9,10] have reported a similar finding at lower temperature ranges. This general conclusion, therefore, indicates that it will be necessary to heat the ash samples to higher temperatures to obtain volatility data for these elements.

Atomic absorption (AA) is known to be an excellent method for the analysis of trace elements. However, this capability is greatly offset by the disadvantages of tedious sample preparation and its one-element analysis (namely, only one element is analyzed each time). For this study, because of the quantity of samples and the number of elements being investigated, a multi-element analytical method is urgently needed. X-ray fluorescence seems to be a good analytical method insofar as this study is concerned. This method is being developed at the Chemical Engineering Division, ANL. X-ray fluorescence can be used as a major analytical tool and AA as a supplemental analysis method for double-checking of results.

Table 16. Elemental Concentration[a] of High-Temperature Ash Corrected for Weight Losses at the Temperature

		Heating Temperature, (C°)						
		340	542	640	740	840	940	990
ppm	Be	6.5±0.6	6.3±0.6	6.2±0.6	6.2±0.6	6.8±0.7	7.2±0.7	6.3±0.6
	Pb	15±2	26±3	29±3	29±3	54±5	10±1	21±2
	V	210±50	200±50	230±60	150±40	130±30	150±40	130±30
	Cr	90±9	91±9	87±8	100±10	94±9	93±9	170±20
	Co	17.0±0.8	16.9±0.8	17.1±0.9	15.4±0.8	14.0±0.7	14.4±0.7	13.9±0.7
	Ni	52±5	52±5	53±5	62±6	60±6	66±7	100±10
	Cu	130±10	110±10	110±10	120±10	120±10	126±10	130±10
	Zn	540±30	510±30	520±30	460±20	480±20	560±30	560±30
	Mn	500±20	550±30	540±30	680±30	680±30	660±30	670±30
	Hg	<0.01						
	Li	59±3	64±3	62±3	N.C.[b]			
%	Al	4.6±0.2	5.7±0.3	5.4±0.3	8.1±0.4	7.7±0.4	8.1±0.4	8.0±0.4
	Fe	10.5±0.5	10.7±0.6	11.1±0.6	11.2±0.6	11.3±0.6	11.5±0.6	11.5±0.6
	Na	0.74±0.04	0.75±0.04	0.87±0.04	N.C.			
	Mg	0.28±0.01	0.29±0.01	0.33±0.02	N.C.			
	K	1.08±0.05	1.26±0.06	1.21±0.06	N.C.			
	Ca	4.9±0.2	4.3±0.2	4.2±0.2	N.C.			
	Ti	0.6±0.1	0.6±0.1	0.5±0.1	N.C.			
	Cl	N.C.						

[a]Each precision is based on an estimate of the precision of measurement obtainable with standard solutions.

[b]N.C. - to be completed.

BENCH-SCALE, PRESSURIZED-FLUID-BED COMBUSTION EXPERIMENTS

Reported here are (1) additional results of four combustion experiments (using Arkwright coal and Tymochtee dolomite) to measure the effects of coal and additive particle size on combustor response variables, (2) the results of two replicate experiments investigating the sulfur-retention capability of lignite ash that has a high calcium content, (3) the results of a replicate experiment duplicating the operating conditions of previously reported VAR-series experiments, and (4) a brief explanation of operating problems and required maintenance.

Equipment

The major items of the ANL bench-scale equipment are coal and additive feeders, a preheater for the fluidizing gas, a 6-in.-dia fluidized-bed combustor, a 3-in.-dia regenerator, cyclones and filters, and gas sampling and analyzing equipment. The combustor and regenerator are designed for operation at pressures up to 10 atm. The temperatures of the combustor and regenerator are controlled by electrical heaters and cooling coils. The gas-analysis system provides on-line measurement of the flue gas-components SO_2, NO, NO_x, CH_4, CO_2 and O_2 on a continuous basis. The system is thoroughly instrumented and is equipped with an automatic data-logging system.

Combustion Efficiency and Additive Utilization Values for Particle-Size (PSI-Series) Experiments

Preliminary results of four combustion experiments to measure the effects of coal and additive particle size on combustor response variables were presented in a previous report.[6] Sulfur retention was reported to increase with decreasing additive particle size. No effect of additive or coal particle size on NO_x emissions was indicated. Table 17 summarizes the previously reported results and presents additional results on combustion efficiency and additive utilization.

Combustion efficiency for the four experiments ranged from 89 to 93% with no consistent effect of either coal or additive particle size indicated. At the high level of coal particle size, however, the combustion efficiency was considerably lower with the finer size fraction of additive. A finer bed material would be expected to result in a lower residence time of the coal particles in the bed and hence, a lower combustion efficiency. The results are inconclusive on this point, however.

Additive utilizations for bed and bed overflow material (at steady state) are also given in Table 17. As expected, the levels of utilization increase with increased sulfur retention. The measured utilizations (by chemical analysis) are generally lower than the calculated utilizations, indicating that the finer additive particles elutriated in the off-gas are more highly sulfated than the coarser material.

Combustion of Lignite in Fluidized Bed of Alumina

Combustion experiments LIG-2D and LIG-2-R were made to duplicate all operating conditions but one of a previous combustion experiment, LIG-1.

Table 17. Operating Conditions and Results of Combustion Experiments to Measure the Effects of Coal and Additive Particle Size on Combustion Response Variables.

Combustor: ANL, 6-in. dia
Bed Temperature: 840°C (∿1550°F)
Pressure: 810 kPa (8 atm)
Bed Height: 0.9 m (3 ft)
Excess Air: ∿17%
Additive: Tymochtee Dolomite
Coal: Arkwright (2.8 wt % Sulfur)

Exp No.	Mass Mean Particle Diameter (μm)		Gas Velocity (m/sec)	Ca/S Mole Ratio	Response Variables				
	Coal	Dolomite			Sulfur Retention (%)	Combustion Efficiency (%)	Additive Utilization[a] (%)		NO_x level in Flue Gas (ppm)
PSI-1R	640	740	0.94	1.3	90	94	58	(65)[b]	160
PSI-2	640	370	0.85	1.4	92	89	71	(58)	170
PSI-3	150	370	0.73	1.3	93	93	65	(66)	180
PSI-4	150	740	0.82	1.4	89	92	54	(58)	210

[a] Bed and overflow additive at steady state. Utilization (%) = [(wt % S)(40/32) (100)]/(wt % Ca)

[b] Values in parentheses are calculated utilizations in percent.

Calculated utilization (%) = [1/(Ca/S Mole Ratio)][sulfur retention (%) + combustion efficiency (%) - 100%]

Combustion in LIG-1 had been carried out in a fluidized bed by Tomochtee dolomite with a 1.1 Ca/S mole feed ratio, whereas LIG-2D and LIG-2-R were carried out in a fluidized bed of alumina. It has been proposed that sulfur is retained in the ash when lignite is burned, even at combustion temperatures as high as 1200°C (2000°F), due to the relatively high calcium content of most lignite coals.[13] If the coal calcium content were to be included in the Ca/S mole ratio for experiment LIG-1, the effective Ca/S mole ratio would be 3.0. Sulfur retention for LIG-1 was 85%, which corresponds to a sulfur dioxide emission of ∿0.2 lb $SO_2/10^6$ Btu.[14]

Operating conditions and results for experiments LIG-2D and LIG-2-R are given in Table 18. Bed temperature and flue-gas analysis data for the two

Table 18. Operating Conditions and Flue Gas Analysis for Combustion Experiments LIG-2D and LIG-2-R

Combustor: ANL, 6-in. dia
Bed Temp: 840°C (∿1550°F)
Pressure: 810 kPa (8 atm)
Bed Height: 0.9m (3 ft)
Excess Air: ∿1/%
Coal: Glenharold lignite (0.56 wt % S)
Bed: 30 mesh alumina

Exp. No.	Coal Feed Rate (kg/hr)	Gas Velocity (m/sec)	Flue Gas Analysis SO_2 (ppm)	NO (ppm)	NO_x (ppm)	CO (ppm)	CO_2 (%)	O_2 (%)	Sulfur Retention[a] (%)
LIG-2D	24.2	0.91	80	90	150	80	19	3.1	89
LIG-2-R	24.5	1.00	102	140	170	35	b	3.8	86

[a] Based on flue-gas analysis.

[b] Not available.

experiments are plotted in Figs. 21 and 22. Sulfur retentions (calculated on basis of flue-gas analysis) for experiments LIG-2D and LIG-2-R were 89 and 86%, respectively. These values compare extremely well with the value of 85% calculated for experiment LIG-1 made with an additive bed. These experiments confirm the premise that sulfur is retained by the ash during the combustion of lignite.

Replicate of VAR-Series Experiment

An additional replicate (VAR-6-3R) of one of the VAR-series experiments (VAR-6) was made to check the operation of the combustor and analytical instrumentation and verify the reliability of comparing current experiments with experiments performed previously. Operating conditions for experiment VAR-6-3R duplicated the operating conditions of replicate experiments VAR-6, VAR-6-R, and VAR-6-2R, the results of which have been reported previously.[13] Operating conditions and results for the four experiments are given in Table 19. Bed temperature and flue-gas composition curves for experiment VAR-6-3R are given in Fig. 23.

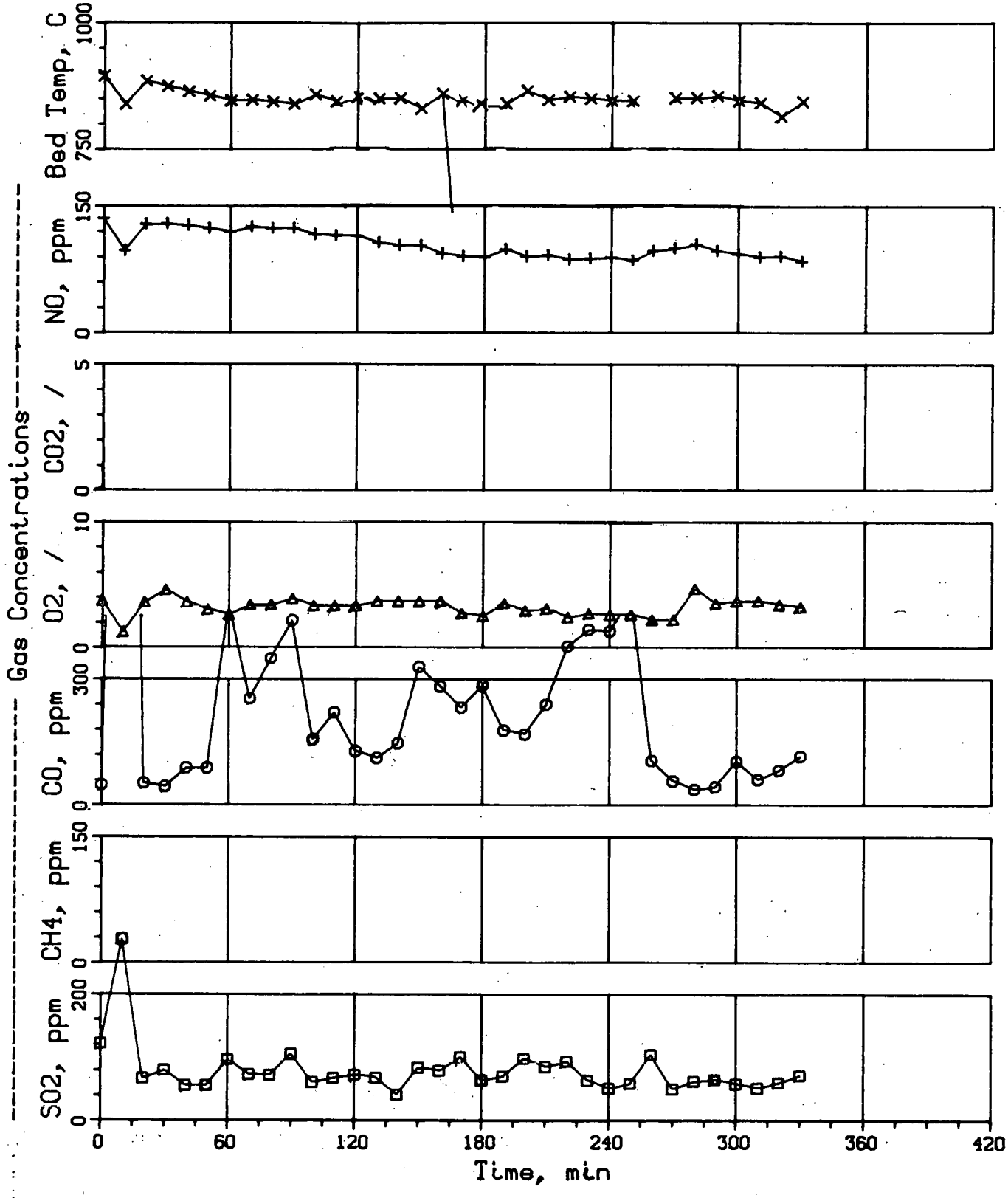

Fig. 21. Bed Temperature and Flue-Gas Composition, Experiment LIG-2D

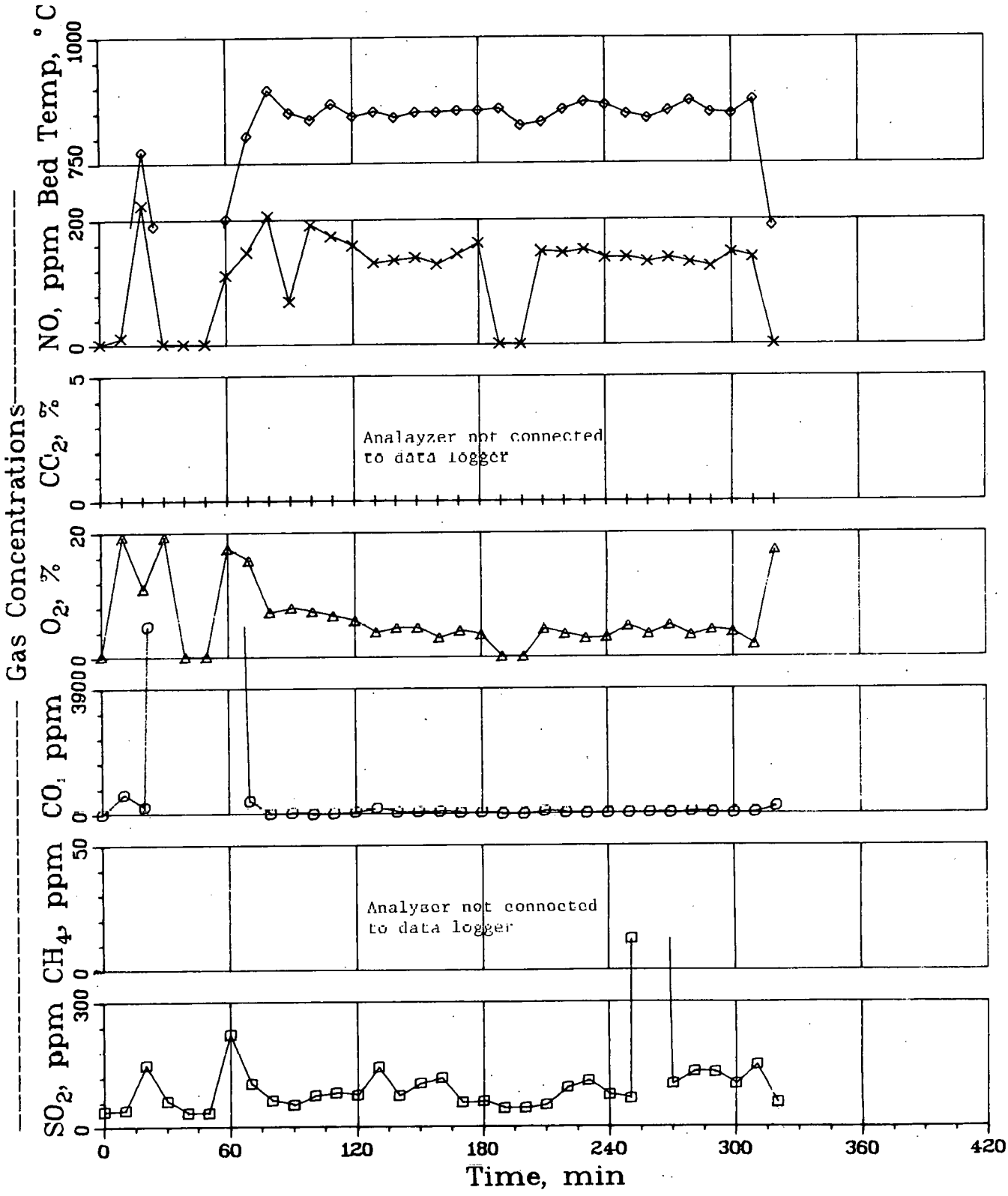

Fig. 22. Bed Temperature and Flue-Gas Composition, Experiment LIG-2R

Table 19. Operating Conditions and Flue-Gas Compositions for VAR-6 Replicate Experiments

Combustor: ANL, 6-in. dia
Bed Temperature: 840°C (1544°F)
Pressure: 810 kPa (8 atm)
Bed Height: 0.9 m (3 ft)
Excess Air: ∿17%
Additive: Tymochtee Dolomite
Coal: Arkwright (2.8 wt % Sulfur)

Exp. No.	Feed Rates (kg/hr) Coal	Dolomite	Ca/S Mole Ratio	Gas Velocity (m/sec)	Flue-Gas Compositions SO_2 (ppm)	O_2 (%)	CO_2 (%)	NO (ppm)	CO (ppm)
VAR-6	13.5	4.7	2.0	1.10	170	3.0	18	190	32
VAR-6-R	13.3	4.8	2.0	1.10	210	2.9	18	180	33
VAR-6-2R	13.3	4.7	2.0	1.07	190	3.0	18	160	33
VAR-6-3R	13.4	4.9	2.1	0.97	170	3.2	18	135	20

The results of experiment VAR-6-3R are very encouraging. With the exception of the concentration of NO in the flue gas, the results of VAR-6-3R agree very well with the previously performed experiments in the VAR-series. Solid samples are currently being analyzed and will also be used to compare past and current operation of the combustor. This reproducibility of results helps to establish the VAR-series of experiments as a basis for comparison for future experiments in the ANL, 6-in.-dia combustor.

Combustor Maintenance

During startup of a test run, a temperature excursion in the ANL 6-in.-dia combustor was experienced which severely damaged several of the thermocouple wells, feed lines, and overflow lines. As a result, the distributor section was removed from the combustor and all lines penetrating the distributor were replaced. The combustor was out of service for a period of two and one-half weeks. Cause of the excursion was determined to be an excessive accumulation of carbon in the bed during startup and prior to ignition, resulting in highly reducing conditions, hot spots, and bed agglomeration.

During a subsequent startup, an external cooling coil began leaking (in a flexible section), forcing termination of the experiment. Several days of operation were lost as a new flexible section was installed.

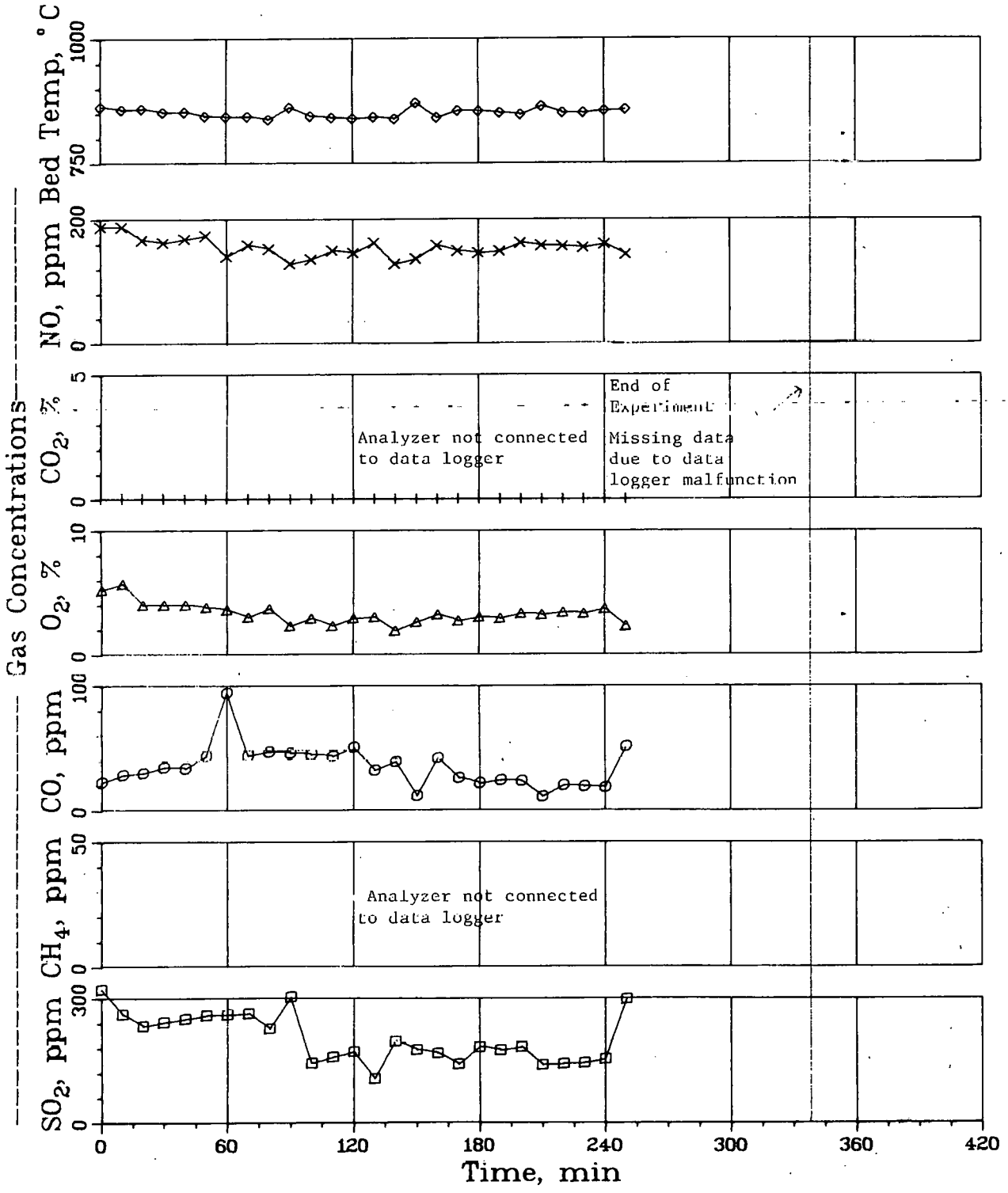

Fig. 23. Bed Temperature and Flue-Gas Composition, Experiment VAR-6-3R

SEPARATION OF COMBUSTION AND REGENERATION SYSTEMS

The pressurized, fluidized-bed combustor and the regenerator originally utilized several components in common. Due to the dual function of these components, the two units could not be operated simultaneously. The equipment common to both units included the inlet and outlet surge tanks, the gas preheater, the additive solids-feeder, the off-gas system (cyclones, filters, pressure-control valve, etc.), and the off-gas analysis system.

Modifications of the two systems and installation of additional equipment were undertaken to physically separate the combustor from the regenerator and to provide each unit with its own auxiliary equipment. The purpose of the modifications is to permit concurrent investigations of the combustion process and the regeneration process, thereby increasing research capabilities relating to both processes.

Alterations to the combustion system equipment were completed earlier (report FE-1780-2), and the combustor was returned to service. During the past quarter, the necessary regeneration system modifications were completed and experiments in the new regeneration system were initiated. Thus, the task of separating the two systems has been completed and will not be discussed in future reports.

The major components of the new regeneration system are shown schematically in Fig. 24. The only major component which has not been received as yet is the gas preheater. For initial regeneration experiments, a resistance-heated section of the fluidizing-gas inlet line is being used in lieu of the gas preheater.

The regenerator vessel was rebuilt and modified. The inside diameter of the reactor was increased from 7.62 cm (3.0 in.) to 10.8 cm (4.25 in.), and the internal product-overflow pipe (formerly used to control the fluidized-bed height) was replaced with an external (to the fluidized bed) overflow pipe. Coal and the sulfated additive are fed separately for independent control of feed rate to a common pneumatic transport line which conveys the solid feed materials into the bottom of the reactor.

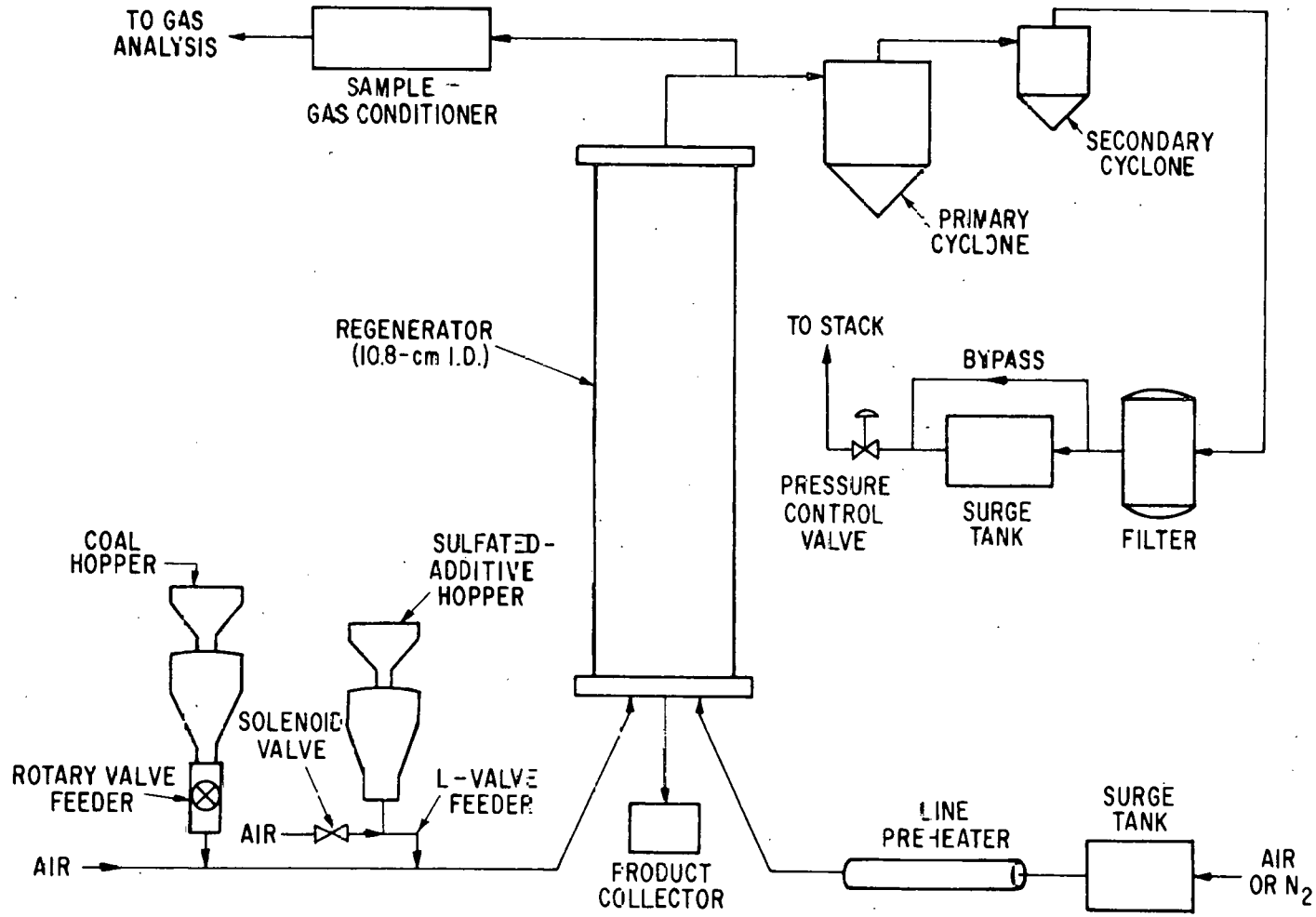

Fig. 24. Schematic Diagram of New Regeneration System.

QUALITY OF FLUIDIZATION AND MINIMUM FLUIDIZATION STUDIES

Introduction

Recently, we reported[15] the minimum fluidization velocities for a fluidized bed of partially sulfated dolomite particles of a size distribution in the range of about 1410-88 μm as a function of temperature (70-800°F) and pressure (26-121 psia). Additional similar experiments have not been completed on a fresh unsulfated dolomite bed with a particle size range of about 2000-88 μm (series A) or about 2000-44 μm (series B); the results are reported here.

These experiments are being done to gain a better understanding of the quality of fluidization and to correlate minimum fluidization velocities with (1) particle size distributions of the solids making up the bed, (2) bed temperature, and (3) reactor pressure. The results of these experiments, which consisted of the measurement of pressure drops across the bed and across the density probes as a function of fluidizing air velocity (u) for each condition of bed temperature (T) and combustor pressure (P), have been interpreted to determine the minimum fluidization velocities of the partially fluidized bed (u_{mf}), the height of the bed at minimum fluidization of the partial bed (L_{mf}) and the degree of segregation in the fluidized bed (S). The measure of the last quantity is taken as the weight fraction of the bed not fluidized. An approximate procedure is also proposed for determining the minimum fluidization velocity for the entire bed from measurements of the pressure drop across the bed as a function of the fluidizing velocity.

Equipment and Procedure

The combustor consist of a 6-in.-dia, schedule 40 pipe (Type 316SS), approximately 11 ft long. In these experiments, the reactor was charged with a known amount of dolomite and then operated in a batch fashion. The pressure drop across the bed was measured with two probes located 5/8 in. and 114 in. above the distributor plate. The two density probes were separated by a distance of 5.75 in.; the lower probe was located 10 in. above the gas distributor plate. The two differential pressure signals were recorded using a Taylor pneumatic transmitter-recorder system. The different components immersed in the bed occupied about 15 percent of the combustor cross section. A Hewlett-Packard 2010C data acquisition system was used to record the temperatue and pressure.

Minimum Fluidization Velocity of a Segregated Bed

A series of six runs (A4 through A8) was performed on a sample of dolomite of the size range given in Part (a) of Table 20. The particle size distribution and the computed average particle diameters from the following relation, before and after the series of runs were completed, are listed in Table 20:

$$\bar{d}_p = \frac{1}{\Sigma_i (x/d_p)_i} \qquad (1)$$

Here, x is the weight fraction of particles in a small size range i of mean diameter d_p, and $\bar{d}_p$ is the average particle diameter for the entire size range.

Table 20. Particle Size Distribution of Fresh Unsulfated Dolomite Before and After the Runs of Series A

Part(a): Runs A4 through A8

US Sieve No.	Size Range (mm)	Weight Fraction in Size Range	
		Before	After
+10	>2.00	0.0024	0.0000
-10 +12	2.00 - 1.68	0.0805	0.0409
-12 +14	1.68 - 1.41	0.2776	0.2060
-14 +25	1.41 - 0.71	0.6256	0.6940
-25 +35	0.71 - 0.50	0.0066	0.0318
-35 +170	0.50 - 0.088	0.0072	0.0266
-170	<0.088	0.0000	0.0007
	Average Particle Diameter (μm)	1177	1047

Part(b): Run A9

US Sieve No.	Size Range (mm)	Weight Fraction in Size Range
		After the Run
+10	>2.00	0.0005
-10 +12	2.00 - 1.68	0.0582
-12 +14	1.68 - 1.41	0.2508
-14 +25	1.41 - 0.71	0.6594
-25 +35	0.71 - 0.50	0.0196
-35 +170	0.50 - 0.088	0.0109
-170	<0.088	0.0005
	Average Particle Diameter (μm)	1122

At the beginning of series A, 8.093 kg of dolomite was charged to the combustor; 7.403 kg was recovered after the series was completed. Thus, about 9% of the feed was elutriated. The computed average particle diameter from the analysis of the final bed is about 89% of the computed average diameter of the initial bed particles.

In these experiments, the pressure drop across the bed, ΔP, increased as the fluidizing-air velocity was increased, until a value of the air velocity was reached where the pressure drop remained constant with increasing fluidizing-air velocity. At this ΔP, the bed was partially fluidized. The fluidizing-air velocity at which ΔP becomes constant is referred to as the minimum fluidization velocity for the partial bed and is denoted by u_{mf}. As the fluidizing-air velocity was further increased, the pressure drop again increased and more and more of the bed was fluidized. At some value of the fluidizing air velocity, the pressure drop again became constant and did not change with further increases in the air velocity. At this stage, the entire bed was fluidized and the fluidization factor, Q, defined as the ratio of the pressure drop across the bed to the weight of the bed per unit area, was unity. The fluidizing-air velocity at which $\Delta P = (W/A)$ and consequently the fluidization factor is unity is referred to here as the minimum fluidization velocity for the total bed and is denoted by u'_{mf}. Figure 25 shows (qualitatively) pressure drop across the bed, ΔP, with increasing fluidizing air velocity, as well as the minimum fluidization velocities u_{mf} and u'_{mf}.

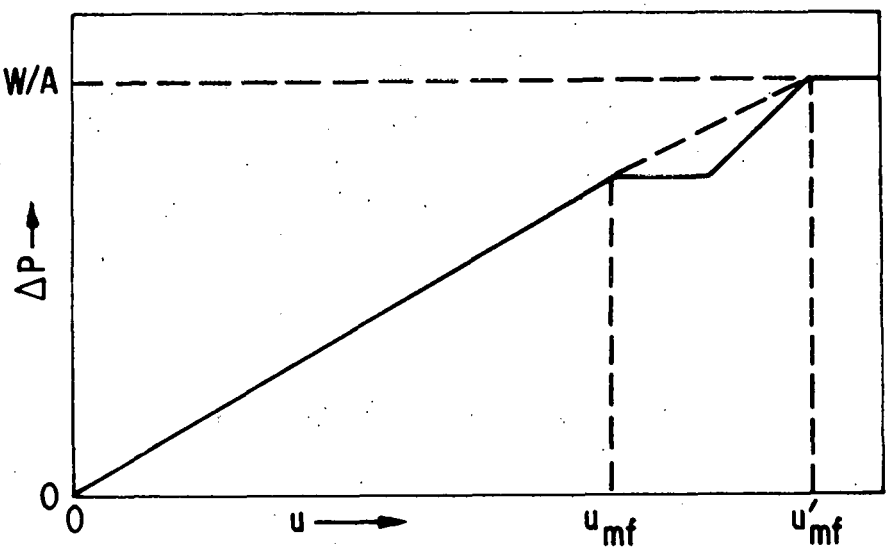

Fig. 25. Qualitative Dependence of the Pressure Drop Across the Bed, ΔP, on the Fluidizing Gas Velocity.

The value of ΔP when the fluidization factor, Q, is unity and the entire bed is fluidized will be denoted by ΔP_{mfeb}. Similarly, the pressure drop value corresponding to the partial fluidization of the bed is indicated by ΔP_{mfpb}. The degree of segregation, S, may be computed from the following relation:

$$S = \frac{(\Delta P_{mfeb} - \Delta P_{mfpb})}{\Delta P_{mfeb}} \qquad (2)$$

Alternatively, S may be defined in terms of the weight of bed fluidized, W′, and the total weight of the bed, W, such that

$$S = \frac{(W - W')}{W} \tag{2a}$$

and

$$Q = \Delta P/(W/A) \tag{3}$$

Q and S are interrelated, such that

$$Q = 1 - S \tag{3a}$$

For an entirely fluidized bed, the fluidization factor is unity and the degree of segregation is zero.

The experiments to be described substantiate the procedure depicted in Fig. 25 for determining u'_{mf}. It was found that the linear plot is a good guide for determing u'_{mf} at which $\Delta P = W/A$. The pressure drop remains constant for a range of u values beyond u_{mf}, but after a certain value is reached, more and more of the bed is fluidized and ΔP rises with u at a higher rate than its initial rise in the range $u < u_{mf}$. The experiments suggest that the occurrence of the partial fluidization of the bed at $u = u_{mf}$ only influences the pattern of approach to the fluidization of the entire bed in the region $u_{mf} < u < u'_{mf}$. The final state when the entire bed is fluidized is that which would be obtained by extrapolating the rate of rise of the ΔP versus u plot in the range $u < u_{mf}$. We suggest this as the basis of a procedure for predicting minumum fluidization velocities for beds for which the degree of segregation is not high, that is to say, up to about 0.3 (*i.e.*, with Q about 0.7 or larger).

In the above mentioned series of six runs, the pressure drop for the final bed was about 0.65 psi; this value was used in calculating the minimum fluidization velocity for the total bed, u'_{mf}. This ΔP is the expected value for each experiment if the bed is completely fluidized, *i.e.*, if the fluidization factor (Q) is unity and the degree of segregation (S) is zero. The pressure drop, ΔP, at which fluidization was initially observed with the bed partially fluidized is indicated in Table 21 for each run. The ΔP varies from 0.55 to 0.60 psi. The temperatures and pressures for each of the six runs are given in columns two and three of Table 21. The computed values of the bed height at minimum fluidization, L_{mf}, from the measured pressure drops across the bed and the density probes are given in column four. Column five lists the minimum fluidization velocities for the partial bed, u_{mf}, each of which is the value at the intersection of a line representing linear fall of pressure drop across the bed as the fluidizing air velocity is decreased and a line representing the constant pressure drop at high flow rates.

A single run, A9, was performed with a dolomite feed of a similar size range as in the above runs; 8.097 kg of the bed was charged to the reactor,

Table 21. Series A: Experimental Values of u_{mf} and L_{mf} at Various Temperatures and Pressures

Equipment: ANL 6-in.-dia reactor

Bed Charge: Unsulfated fresh dolomite

Run No.	Temp (°F)	Pressure (psia)	L_{mf} (in.)	u_{mf} (ft/sec)	ΔP (psi)	Q	u'_{mf} (ft/sec)
A4	65	127±0	20.3	1.26	0.60	0.92	1.36
A5	65	97±1	18.2	1.26	0.60	0.92	1.37
A6	65	73±10	18.2	1.38	0.60	0.92	1.49
A6'	740±60	24±5	19.3	2.32	0.57	0.88	2.65
A7	703±73	125±1	16.6	1.58	0.55	0.85	1.87
A8	580±60	87±1	17.9	1.72	0.56	0.86	2.00
A9	65	64±1	20.3	1.63	0.60	0.85	1.76

which corresponds to a pressure drop of 0.71 psi at minimum fluidization of the total bed. After completion of the run, the bed was analyzed for size distribution. These results are given in part (b) of Table 20 and correspond to a mean particle diameter of 1122 μm. The other conditions relating to this experiment and the computed results are given in Table 21. In run A9, for which the operating conditions were approximately the same as in run 6, both u_{mf} and u'_{mf} were larger than were found for the latter run. This is attributed to the different particle size distributions for the two cases, a condition that may also be responsible for a smaller percentage of the bed being fluidized and a greater segregation of the bed material in run A9. Because about the same amount of material was fluidized in both cases, a larger flow rate, *i.e.*, a higher velocity, for run A9 should imply a greater value for voidage or L_{mf} since the effective cross-sectional area of the reactor was constant. This is confirmed by measurements of L_{mf}, which was about 10% larger for run A9 than for run A6.

The data of Table 21 indicate only to some extent the earlier observed[15] effects of temperature (70-800°F) and pressure (26-121 psia) on u_{mf}. It had been observed[15] and u_{mf} is probably almost constant in this temperature range at a constant pressure and that it decreases at constant temperature as the pressure increases. The three runs (A4-A6) at 65°F only weakly exhibit this trend, but runs A6′ through A8, with only slight variation in the ΔP and Q values, display this qualitative dependence more clearly. It should be noted that the trends of minimum fluidization velocity for the partial bed, u_{mf}, and the minimum fluidization velocity for the total bed, u'_{mf} with respect to T and P are the same. The method adopted here for the determination of u'_{mf} is regarded as valid when (1) the bed is composed of particles of relatively uniform size and (2) only a small amount of segregation takes place in the bed ($S \leq 0.3$).

The reactor was next charged with 11.970 kg of fresh dolomite of a wide size range having the distribution given in Table 22. After a series of eleven runs (B-1 through B-10) was completed, the dolomite recovered from the bed weighed 10.699 kg. The total loss in the bed was thus 10.9%. The values given in Table 23 for runs B-1 and B-1A were computed on the basis of the pressure drop, ΔP, 1.05 psi corresponding to the initial bed weight. For the remaining runs, values of Q were determined on the basis of the pressure drop 0.935 psi corresponding to the residual amount of dolomite in the bed. The operational conditions for the eleven runs are given in columns two and three of Table 23, while the computed values of L_{mf} (at ΔP of column six) are given in column four and the Q and u'_{mf} values are listed in columsn seven and eight, respectively. Some of the salient features of these data are discussed below.

In run B 1, fluidization of the partial bed was observed for ΔP = 0.88 psi, corresponding to u_{mf} of 1.88 ft/sec (Run B-1A). As the fluidizing air velocity was increased, the pressure drop exhibited a step increase, and fluidization of the total bed occured at u'_{mf} = 2.25 ft/sec for ΔP = 1.05 psi. Since particle size analysis revealed that the smaller particles had been elutriated during runs B-1 and B-1A, the bed for subsequent runs (B-2 through B-10) was regarded as constituted of particles of a relatively narrow size range. This is also the justification for using ΔP = 0.935 in computing the factor representing the degree of segregation in the fluidized bed. It should be noted that u_{mf} and u'_{mf} decrease in value as the pressure increases, in conformity with earlier

Table 22. Particle Size Distribution of Fresh Unsulfated Dolomite Before and After the Runs of Series B

US Sieve Series No.	Size Range (mm)	Weight Fraction in the Range	
		Before	After
+10	>2.00	0.0000	0.0025
- 10 + 12	2.00 - 1.68	0.0422	0.0329
- 12 + 14	1.68 - 1.41	0.1881	0.1859
- 14 + 16	1.41 - 1.19	0.2787	0.2945
- 16 + 18	1.19 - 1.00	0.1812	0.1923
- 18 + 20	1.00 - 0.84	0.0802	0.0913
- 20 + 30	0.84 - 0.59	-	0.1024
- 20 + 35	0.84 - 0.50	0.0602	-
- 30 + 35	0.59 - 0.50	-	0.0236
- 35 + 45	0.50 - 0.35	0.0242	0.0513
- 45 + 80	0.35 - 0.177	0.0173	0.0226
- 80 + 120	0.177 - 0.125	0.0657	-
- 80 + 170	0.177 - 0.088	-	0.0007
-120 + 170	0.125 - 0.088	0.0277	-
- 170	<0.088	-	0
-170 + 200	0.088 - 0.074	0.0035	-
-200 + 270	0.074 - 0.053	0.0000	-
-270 + 325	0.053 - 0.044	0.0069	-
-325	<0.044	0.0242	-
Average Particle Diameter, μm		444	963

Table 23. Series B: Experimental Values of u_{mf} and L_{mf} at Various Temperatures and Pressures

Equipment: ANL 6-in.-dia reactor
Bed Charge: Unsulfated fresh dolomite

Run No.	Temp (°F)	Pressure (psia)	L_{mf} (in.)	u_{mf} (ft/sec)	ΔP (psi)	Q	u'_{mf} (ft/sec)
B-1	65	23±2	21.0	2.25	1.05	1.00	2.25
B-1A	65	35±2	23.0	1.88	0.88	0.84	2.25
B-2	65	70±4	17.3	1.48	0.72	0.77	1.82
B-3	65	100±0	17.7	1.18	0.68	0.72	1.49
B-10	65	120±0	15.2	1.09	0.62	0.66	1.45
B-4	530±20	39±8	15.4	2.36	0.80	0.85	2.65
B-5	600±40	64±1	17.6	2.20	0.83	0.88	2.41
B-6	480±35	120±1	16.6	1.42	0.72	0.77	1.71
B-7	810±40	40±15	15.9	2.74	0.80	0.85	3.12
B-8	800±5	69±4	16.8	2.60	0.82	0.87	2.95
B-9	680±20	119±1	16.2	1.57	0.70	0.74	1.96

measurements. In contradiction to the earlier observations, however, results for these runs also indicate that u_{mf} increases with temperature at a fixed pressure. This related to the magnitude of the fluidization factor, Q, and such trends may be quite pronounced for beds where the factor is much smaller than unity. We thus infer that the temperature and pressure dependencies of u_{mf} also depend on the factor Q of segregated fluidized beds.

Quality of Fluidization of a Segregated Bed

Various criteria developed for testing the quality of fluidization will now be briefly referred to and examined in the context of our experimental data. It was pointed out in an earlier report[15] that the simple criteria developed on the concept of interparticle forces in the vicinity of bubbles in terms of dimensionless groups, such as the Froude number[16] and other groups,[17,18] are of only limited utility in their present form for predicting the quality of fluidization of systems composed of multisize nonspherical particles such as those studied here. Geldart[19] has reviewed some of the other criteria suggested to distinguish between bubbling (aggregative or heterogeneous) fluidization and nonbubbling (particulate or homogeneous) fluidization. Verloop and Heertjes[20] developed a criterion by considering bed elasticity and the occurrence of shock waves to distinguish between bubbling and nonbubbling fluidized beds. This has been commented upon further by Creasy[21] and Geldard.[19] Creasy[21] modified it for a particle Reynolds number of less than 2, but Geldart[19] found that the criterion is poor in making predictions for gas-solid fluidization. Rietema[22] suggests on the basis of measurements of the angle of repose that particles with a wide size distribution exhibit greater elasticity than do the systems of narrow particle size range. Verloop and Heertjes[23] have shown that if the experiments and their interpretation ar carried out with care, experimentally determined values of minimun fludization velocity by either the angle of repose or the pressure drop method are about the same. It has been pointed out that the pressure drop method needs special care if reliable data is to be obtained.[24,25]

Geldart's[19] criterion, developed for a large range of particles, is directly applicable to our data. He classified the behavior of solids fluidized by gases into four different groups characterized by density difference ($\rho_s - \rho_g$) and average particle size, d_p. Our experiments come close to his category B, which includes particles in the average size and density ranges: 40 μm < d_{sv} < 500 μm, 4 g/cm^3 > ρ_s > 1.4 g/cm^3. Here, d_{sv} is the surface/volume diameter of the particle. Such particle systems, when fluidized, start bubbling at or only slightly above minimum fluidization velocity. The following relationship is found on the basis of experimental data.[19]

$$U_{MB} = K_{MB} d_{sv} \tag{4}$$

Here the constant K_{MB} has the units of frequency (*e.g.*, sec^{-1}) and is equal to 100 when the superficial velocity of gas at minimum bubbling condition, U_{MB}, is in cm/sec and d_{sv} is in cm. Combining the above relation with the minimum fluidization velocity expression given by Davies and Richardson,[26] Geldart[19] established the lower limit for group B powders. As can be observed by referring to Fig. 3 of Geldart's paper[19] for $\rho_s - \rho_g \simeq 2.75$ g/cm^3, particle

systems having a mean particle size, d_{sv}, in the range 80-600 μm will lie in category B and will be homogeneously fluidized, with bubbles appearing at or near the minimum fluidization velocity. Particles of larger size fall in group D, and these can form stable spouted bed. It would appear that our first series of experiments (Runs 2 through 8) and those of Series A and B are in accord with the criterion of Geldart[19] for smooth (or total) fluidization. It may be recalled that in Series A and B experiments, because of segregation, the average diameters of the particles fluidized in partially fluidized beds are much smaller than those listed in Tables 20 and 22. Further, our particle diameters are based on screen analyses and, if converted to d_{sv}, are in the range 80 to 600 μm.

Rowe, Nienow, and Agbim[27] have experimentally examined the mechanism by which mixtures of small (and/or light) and large (and/or heavy) particles become segregated when fluidized in either a two-dimensional bed or a cylindrical bed. The systems examined consisted of binary combinations of near-spherical particles. The density differences induce segregation much more effectively than do the size differences. However, the different mechanisms that bring about particle mixing or segregation are all found to be associated with bubbles. These authors investigated the size effect in a two-dimensional bed with a 10% layer of large particles (642 μm) arranged on the top of small particles (96 μm). Such a bed was found to begin fluidization from the bottom, supporting a quasistable inert bed above it, which collasped; large particles then fell through bubbles at an air velocity well below their own fluidization velocity. The large particles thus became preferentially collected at the bottom and acted roughly as a porous distributor. A large proportion of the large particles was found to be distributed throughout the bed, even at a velocity only one-fourth of their minimum fluidization velocity.

In the light of the above comments and the results of the three series of experiments with dolomite particles of wide size ranges, some inferences may be drawn for systems composed of multisize particles. Good mixing and fluidization were found[15] in the first series of experiments (Runs 2 through 8), in which the particle size ranged mainly from 88 to 1410 μm, with one or two percent of the particles having sizes above 1410 μm (U.S. Sieve 14) and below 177 μm (U.S. Sieve 170). It thus appears that nonspherical dolomite particles of a wide size range, as employed in our experiments described here, mix and disperse well in the fluidized state. Probably, the continuous size distribution is a favorable feature in comparison to discrete distribution (even when the size may vary by an order of magnitude) to bring about fairly uniform mixing according to the mechanism observed by Rowe *et al.*[27] and referred to above. When size range is further increased as in the Series A (88-2000 μm) and Series B (44-2000 μm) experiments, relatively poor mixing is observed, and partial segregation occurs at air flow velocities where about 80-90% of the bed material is fluidized.

Fluidization of the partial bed was also observed by Knowlton[28] for several bed materials, primarily coal and coal-derived materials, having a wide particle-size distribution (74-2000 μm). These experiments were conducted in a cylindrical column (with a 11.5-in. internal diameter and about a 40-in. packed-bed height) at ambient temperature over a pressure range of 15-1000 psia. It was found that approximately one-third or less of the bed was fluidized at the minimum fluidization velocity for the partial bed while the remainder of the

bed was stagnant. At a higher gas velocity, the total bed was fluidized; this is referred to as the complete fluidization velocity by Knowlton.[28] The minimum fluidization velocity for the partial bed was about 67 to 75 percent of the minimum fluidization velocity for the total bed. No segregation details of the bed in relation to the particle sizes are given by Knowlton.[28]

Jolly and Doig[29] have examined the vast amount of published data on pressure drop in fluidized beds and have found that the fluidization factor, Q, varies between the limits 0.45 and 1.78. They have summarized reasons that can explain this large variation in the factor, which implies that the observed ΔP does not equal the buoyant weight of the entire bed per unit area. The maldistribution of bed material is primarily responsible for the factor Q being smaller than unity. They also found[29] that the diameter of the fluidized-bed reactor definitely influences the observed pressure drop values. Q is less than unity for bed diameters of 6 in. and larger. The influence of particle size on ΔP for such large-diameter beds is relatively insignificant. Our experiments were performed in the ANL 6-in.-dia fluidized-bed reactor, and the average particle diameter for the three series of experiments ranged from 444 to 1177 μm. Results of ANL work on a dolomite bed composed of particles of a wide size range suggest that the bed in a 6-in.-dia reactor can be entirely fluidized if the bed comprises particles within a range of about 88-1410 μm (average particle diameter, 704 μm), resulting in Q = 1. Only a limited number of the investigations critically examined by Jolly and Doig[29] indicate fluidization of the entire bed, and none of these studies has been performed with particles of mean size greater than about 600 μm. Thus, the present Argonne work further extends the range for the particle size in a 6-in.-dia combustor for which pressure drop data have been reported and demonstrates that in a carefully designed reactor, fluidization of the entire bed of larger particles than studied before is possible. The present experiments also suggest that particle size influences the detailed mechanism of fluidization, even in a 6-in.-dia reactor. For example, when a larger size range (44-2000 μm) was used for the particles, partial segregation of the bed occurred at low flow velocities, only a part of the bed was fluidized, and Q values ranged between 0.66 and 0.92.

Experiments of Rowe, Nienow, and Agbim[27] (referred to above) shed light on the mechanism of segregation in a fluidized bed of a wide range of particle sizes. These workers[30,31] have performed additional experiments and have presented[30] a simple quantitative theory for segregation of particles in a binary system in terms of a mixing index, M. It is defined such that its value is zero for a bed that is completely segregated about a horizontal plane and is unity for a completely mixed bed. They suggest that

$$x' = f[u - u_{mf(F)}] \, (d_B/d_S)^{-1/5} \qquad (5)$$

Here x' is the proportion of jetsam (the material that tends to sink, *i.e.*, larger particles) in the upper part of the bed, u is the superficial gas velocity, $u_{mf(F)}$ is the minimum fluidization velocity of the flotsam (the smaller particles that tend to float), and d_B and d_S are the diameters of the larger and smaller particles, respectively. They could not determine the nature of the function, f, in Eq. 5.

Two findings from the work of Rowe *et al.*[30,31] are of special importance in the fluidization of particles of varying sizes but having the same density. First, the velocity of the fluidizing gas is very important in mixing particles of different sizes in the fluidized bed; the extent of mixing depends on the excess of the fluidizing-gas velocity over the minimum fluidization velocity of the material forming the upper part of the bed. Secondly, they found that the presence of a small amount of fines in a bed of coarser particles lowers the u_{mf} very significantly, but that the addition of a large amount of coarse particles to a bed of fines produces very little effect. Thus, if the fines are elutriated during an experimental run, the fluidization characteristics may undergo severe changes in terms of u_{mf} and the segregation behavior of the bed.

Wen and Yu[32] found that in a bed of particles of two sizes and the same density, uniform fluidization takes place with very little particle stratification if the ratio of the particle diameters is less than 1.3. We have found in our experiments that in a multisize particle system (88-1410 μm) where the ratio of largest to smallest particles was about 16 or less, homogeneous single-layer fluidization occurred at minimum fluidization of the total bed. The presence of small particles in the bed probably contributed significantly to the observed uniform fluidization, according to the mechanism suggested by Rowe *et al.*[30] and referred to above. The conjecture concerning the role played by small particles during fluidization is backed by our experimentation inasmuch as about four to five times greater velocities than were actually used for multisize particle beds would be required for fluidization of a bed that consisted only of particles of the largest size of appreciable proportion in the bed (1410 μm).

Wen and Yu[32] found that if the particle diameter ratio is greater than 1.3 in a binary system, bed separation into two layers occurs. We have observed such a phenomenon in two multisize particle systems investigated by us and described above. The ratio of the smallest to the largest particle diameter was about 23 in series A experiments and about twice that in series B experiments. In our experiments, we observed partial fluidization of the bed, with about 10 to 15 percent of the bed remaining unfluidized in series A and a still larger proportion in series B experiments. Apparently, the behavior behavior of fluidized beds of multisize particles differs quantitatively from that observed[27,30-32] with simple, fluidized beds of spherical particles of two sizes. On the basis of the coal combustion experiments performed at ANL on this 6-in.dia fluidized-bed reactor with fluidizing-gas velocities of 2-3 ft/sec, it appears that a bed such as those employed in series A and B experiments will also be entirely fluidized at some higher flow rates. The prediction of minimum fluidizing velocities for such beds does not appear to be simple. At present, we propose the procedure based on Fig. 25 for its estimation. Useful information could be obtained by performing experiments in a fluidized bed which could be visually observed.

REFERENCES

1. G. J. Vogel *et al.*, A Development Program on Pressurized, Fluidized-Bed Combustion, Annual Report, July 1974-June 1975, ANL/ES-CEN-1011.

2. G. J. Vogel *et al.*, Reduction of Atmospheric Pollution by the Application of Fluidized-Bed Combustion and Regeneration of Sulfur-Containing Additives. Annual Report, Argonne National Laboratory, July 1971-June 1972. ANL/ES-CEN-1005 (1973).

3. T. D. Wheelock and D. R. Boylan, "Reduction Decomposition of Gypsum by Carbon Monoxide," Ind. Eng. Chem. 52, 217 (1960).

4. R. T. Yang, P. T. Cunningham, W. I. Wilson, and S. A. Johnson, "Sulfur Removal and Recovery from Industrial Processes," Advances in Chemistry Series 137, pp. 149-157 (1974).

5. R. B. Bird, W. E. Stewart, and E. N. Lightfoot, Transport Phenomona, New York, 1962, pp. 522-537.

6. G. J. Vogel *et al.*, A Development Program on Pressurized Fluidized-Bed Combustion. Quarterly Report, July 1-September 30, 1975, Argonne National Laboratory, ANL/ES-CEN-1013.

7. Mechanical and Physical Properties of the Austenitic Chromium-Nickel Stainless Steels at Elevated Temperatures, International Nickel Company, 1963.

8. ASME Boiler and Pressure Vessel Code, Section VIII-Rules for Construction of Pressure Vessels, Division 1 (1974).

9. R. R. Ruch, H. J. Gluskoter, and N. F. Shimp, "Occurrence and Distribution of Potentially Volatile Trace Elements in Coal," a Final Report, Environmental Geology Notes, No. 72, Illinois State Geological Survey (August 1974).

10. R. J. Guidoboni, "Determination of Trace Elements in Coal and Coal Ash by Spark Source Mass Spectrometry," Anal. Chem. 45, (7), 1275 (1973).

11. T. Y. Kometani, "Effect of Temperature on Volatilization of Alkali Salts During Drying Ashing of Tetrafluorethylene Fluorocarbon Resin," Anal. Chem. 38, (11), 1596 (1966).

12. W. T. Reid, External Corrosion and Deposits - Boilers and Gas Turbines, 3, p. 51, American Elsevier Publishing Company, Inc. New York, 1971.

13. H. D. Levene and J. W. Hand, "Sulfur Stays in the Ash When Lignite Burns," Coal Min. Process. 12(2), 46-48 (February 1975).

14. G. J. Vogel *et al.*, Reduction of Atmospheric Pollution by the Application of Fluidized-Bed Combustion and Regeneration of Sulfur-Containing Additives, Annual Report, July 1973 - June 1974, Argonne National Laboratory, ANL/ES-CEN-1007 (1974).

15. S. C. Saxena and G. J. Vogel, The Properties of a Dolomite Bed of a Range of Particle Sizes and Shapes at Minimum Fluidization, Argonne National Laboratory, ANL/ES-CEN-1012 (1975).

16. R. H. Wilhelm and M. Kwauk, Chem. Eng. Prog. 44, 201-218 (1948).

17. W. J. Rice and R. H. Wilhelm, Am. Inst. Chem. Eng. J. 4, 423-429 (1958).

18. J. B. Romero and L. N. Johanson, Chem. Eng. Prog. Sym. Series 58(38), 28-37 (1962).

19. D. Geldart, Powder Tech. 7, 285-282 (1973).

20. J. Verloop and P. M. Heertjes, Chem. Eng. Sci. 25, 825-832 (1970).

21. D. E. Creasy, Powder Tech. 7, 353-354 (1973).

22. K. Rietema, Chem. Eng. Sci. 28, 1493-1497 (1973).

23. J. Verloop and P. M. Heertjes, Powder Tech. 7, 161-168 (1973).

24. R. D. Toomey and H. F. Johnstone, Chem. Eng. Prog. 48(5), 220-226 (1952).

25. R. C. Trivedi and W. J. Rice, Chem. Eng. Prog. Sym. Series 62(67), 57-63 (1966).

26. L. Davies and J. F. Richardson, Trans. Inst. Chem. Eng. 44, T293-T305 (1966).

27. P. N. Rowe, A. W. Nienow, and A. J. Agbim, Trans. Inst. Chem. Eng. 50, 310-323 (1972).

28. T. M. Knowlton, High-Pressure Fluidization Characteristics of Several Particulate Solids: Primarily Coal and Coal-Derived Materials, Paper No. 9b, 67th Annual Meeting of the American Institute of Chemical Engineers held in Washington, D. C., during Dec. 1-5, 1974.

29. R. D. Jolly and I. D. Doig, Chem. Eng. Sci. 28, 971-973 (1973).

30. P. N. Rowe, A. W. Nienow, and A. J. Agbim, Trans. Inst. Chem. Eng. 50, 260-264 (1973).

31. A. W. Nienow, P. N. Rowe, and A. J. Agbim, Trans. Inst. Chem. Eng. 51, 260-264 (1973).

32. C. Y. Wen and Y. H. Yu, Chem. Eng. Prog. Sym. Series 62, No. 62., 100-111 (1966).